Thermoelectrochemical model for RFB with an application at a grid level for peak shaving to reduce cost of the total electricity

by

Laura Magallanes Ibarra

B.Eng, Western Institute of Technology and Higher Education, 2013

A Thesis Submitted in Partial Fulfillment of the
Requirements for the Degree of

Master of Applied Science

in the Department of Mechanical Engineering

Thermoelectrochemical model for RFB with an application at a grid level for peak shaving to reduce cost of the total electricity

by
Laura Magallanes Ibarra

B.Eng, Western Institute of Technology and Higher Education, 2013

Supervisory Committee

Dr. Andrew Rowe, Supervisor
(Department of Mechanical Engineering)

Dr. Heather Buckley, Co- Supervisor
(Department of Civil Engineering)

ABSTRACT

Reliable, low-cost energy storage solutions are needed to manage variability, provide reliability, and reduce grid-infrastructure costs. Redox flow batteries (RFB) are a grid-scale storage technology that has the potential to provide a range of services. Desirable characteristics are long cycle life, high efficiency, and high energy density. A key challenge for aqueous redox flow battery systems is thermal sensitivity. Operating temperature impacts electrolyte viscosity, species solubility, reaction kinetics, and efficiency. Systems that avoid the need for active thermal management while operating over a wide temperature range are needed. A promising RFB chemistry is iron-vanadium because of the use of low-cost iron. This is an analysis of the thermal response of on Iron-Vanadium (Fe/V) RFB using a zero-dimensional electrothermal model. The model accounts for the reversible entropic heat of the electrochemical reactions, irreversible heat due to overpotentials, and the heat transfer between the stack and environment. Performance is simulated using institutional load data for environmental conditions typical of Canadian jurisdictions.

Contents

List of Tables

List of Figures

ACKNOWLEDGEMENTS

This work would have not been possible without the support from some people in my life, first I will like to thank my life-partner Diego, thank you for giving up our life's in Mexico to follow my dream, thank you for the unconditional love and support during the moments that I needed the most.

My supervisor Dr. Andrew Rowe, I could not be more thankful for trusting me and all your continuous support during my whole program and the guidance.

Dr. Heather Buckley, your insightful feedback pushed me to sharpen my thinking, thank you for believing in me and always motivate me to keep working and encouraging me at all moments.

Pauline, you had the hardest work of all, review and edit my whole thesis, thank you for everything and the patience.

To all my graduate friends, I'm so thankful that I was not alone in this journey, thanks to everyone for sharing how we felt and supporting emotional and technical throughout my program, this chapter would have not been the same without any of you.

Last but not least, my family back home, for always believing in, for supporting me at all times without hesitating, and making me feel proud of myself no matter what.

Thank you
I love you
I forgive you
I am sorry

DEDICATION

I want to dedicate this work to all the women who work to purse their dreams, and no matter how big or small they are, they are your dreams. Keep working, trust and let go.

Nomenclature

Abbreviation

CE	Current efficiency
EE	Energy efficiency
ESS	Energy storage systems
Fe/V	Iron-Vanadium
OCV	Open-circuit voltage
$PNNL$	Pacific northwest national laboratory
RFB	Redox flow battery
SOC	State of charge
UPS	Unit power supply
UPS	Unit power supply
VER	Variable energy resources
VRB	Vanadium redox battery

Symbols

$(IR)_e$	Ohmic loss electrolyte	V
$(IR)_m$	Ohmic loss membrane	V
ϵ	Porosity of the electrode	
η	Activation overpotential	V

$\forall$	Volume of the reservoir	m^3
κ	Conductivity of the electrolyte	mS/cm
ρ	Density	Kg/m^3
σ_m	Conductivitiy of the membrane	S/m
A	Area	m^2
a	Specific surface area	$1/m$
C_i	Heat capacity	$J/(kgK)$
c_i	Molarity (or concentration of species i)	mol/m^3
D_i^{eff}	Diffusion coefficient	m/s
e	Elementary charge of the electron	
E°	Standard cell potential	V
E_{cell}	Cell voltage	V
E_{cell}^{rev}	Reversible open circuit voltage	V
I	current	A
i	current density	A/m^2
k	Reaction rate constant	m/s
L_c	Thickness of electrode	m
L_h	Height of electrode	m
L_h	Height of the cell	m
L_m	Thickness of membrane	m
L_w	Width of electrode	m
L_w	Width of the cell	m
n	electrons transferred per ion	

N_i	Molar flow of specie i	mol/m^3
Q	Heat	W
Q_c	Volumentric flow	m^3/s
S	Entropy	J/K
T	Temperature or K	$^\circ C$
z	Charge number	

Physics Constants

F	Farady's constant	$96485.3365\,C/mol$
N_A	Avogadro number	$6.023 \times 10^{23}/mol$
R	Gas constant	$8.3144\,J/molK$

Chapter 1

Introduction

This chapter will introduce the objective and the motivation of this work and the structure of the thesis, as well as a brief review of redox flow batteries.

1.1 Background

Electricity demand is increasing as a result of the growth of the global population and the desire to electrify and provide a substitute for fossil fuel use. It is estimated that global electricity generation will be 54 billion MWh by 2050 [1], compared to the 21.5 MWh registered in 2010[1]. Currently, electricity demand is being met largely by carbon-intensive fuels [2] and the emission of CO_2 during combustion makes this a major contributor to global warming. The actual electric grid consists of a near-instantaneous transmission of the power source and generation assets to the end-user with little or no storage. The grid often suffers fluctuations in supply and demand which requires that the grid be extremely flexible; this need makes fossil fuel generators with fast response attractive.

The growing demand for energy and the increasing attention to environmental problems, it requires not only the optimal use of the common resources but also needs to replace the existing technologies with environmentally- friendly sources.

Renewable sources, except for hydropower, currently provide 6% of the electricity production (mainly solar and wind energy.[3]) Variable energy resources (VERs) such as solar and wind are rapidly increasing and becoming more available. For example, photovoltaics and solar-energy implementation is wasted because of the inability to release solar energy when needed. The result of adding storage to the grid will have

a significant added value. Also with wind, which could have its it maximum energy generation during the night while customer demand is at its lowest.

The diurnal and intermittent nature and low energy density of VERs causes a lack of balance between electricity demand and availability. To meet demand and avoid curtailment or blackouts, grid-level storage must be integrated into the current system. The ability of grid-level storage to provide application-specific energy services allows for immediate response to fluctuations in demand[2]. Multiple energy storage systems (ESS) are currently being studied, such as flow batteries, pumped hydro, and compressed air.

Energy storage can also be useful in reducing electricity costs for distributors and consumers when electric companies employ hourly pricing policies. Additionally, the use of energy storage helps reduce the need for upgrading power plants on the basis of peak demand evolution, meaning that the energy storage would allow the current system to avoid an upgrade as the ESS could potentially absorb the peak demand. ESS can be distinguished by these two metrics:

- Power quality
- Energy management

Power quality refers to charge/discharge cycle on a short time scale (s-min) which includes power smoothing, grid stabilization, and frequency regulation.

Energy management refers to charge/discharge cycle on a long time scale(min-h), which it includes load leveling, power balancing, peak shaving, and time-shifting.

This can also work as a power supply. The operating time range, response time and services, and the range of kilowatt or gigawatt-scale will decide the appropriate ESS.

Figure 1.1 shows different storage options and what they are used for, it should be noted that batteries can vary significantly in terms of power rating. Each option has its advantages and disadvantages, for example, compressed air relies upon on caves with stable geologic structures; pumped hydro has geographic requirements but has a high capacity with a proven technology; Li-ion batteries have a high energy density and efficiency requires a protection circuit to maintain safe operation. The electrochemical reactions within a redox battery occur at the surface of the electrodes, and both oxidized and reduced species remain dissolved in the electrolyte, therefore no forces are exerted on the electrode. In the case of a lithium-ion battery, the lithium

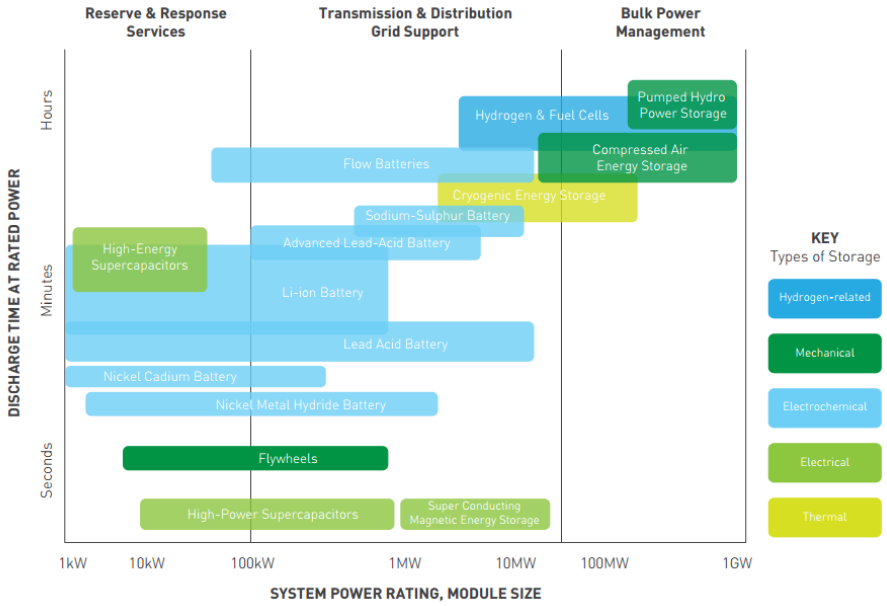

Figure 1.1: Energy Storage technologies comparison based on application adaptation from [4]

cation is inserted between planes of graphite creating stresses on the electrode as the charge/discharge cycles occur, reducing its lifetime. [5, 6].

To maintain a secure and reliable electricity grid, the operators must attempt to maintain a steady supply and demand for electricity in order to meet peak demand. The electricity grid is usually set up with different types of generators:

- Base-load Generators: are able to operate predictably for twenty-four hours a day at a high capacity factor, but if demand changes quickly they can't react at the same pace, This is why the grid includes intermediate generators and peakers.

- Intermediate Generators: typically come on line when daily electricity demand increases in the morning and then they shut down when the demand drops off in the evening.

- Peakers: Peaking power plants operate only during times of peak demand. In general the demand for electricity peaks around the start and end of the working day. Peakers are the most expensive and the highest emitters of CO2

The grid use peaker generators which can be a powered up or down as needed to meet the demand. However, it is important to mention that this way (ramping up

and down) is not ideal since these generators are more efficient when they run at full power. The use of peakers generators to smooth out the demand is contributing CO_2 emissions.

Therefore the current electric grid will not be sustainable since the peak demands will become greater and the generators will need to be more flexible, resulting in the constant use of peakers. Energy storage systems can be used to either replace the peakers or provide more flexibility to the electricity grid.

With the increased use renewable energy, and its intermittent nature results in an imbalance in supply and demand. To avoid blackouts or curtailment it is important to integrate energy storage at a grid level. In the case of failures in the systems it is completely necessary to have a power system supply connected to the network. In this way, it is possible to avoid breakdowns in systems and the resulting disruption to critical services.

The current grid system is oversized in order to handle demand peaks. Energy storage can save utilities and their users money by eliminating the need for expansion and the updating of transmission lines and infrastructure. Peak shaving can be referred to as leveling out the peak use of electricity by industrial and commercial power consumers. Peak shaving is the process of reducing the amount of energy purchased from the utility companies during peak hours of energy demand. Peak shaving isn't just beneficial by saving cost but can also potentially provide a benefit from Demand Response incentive programs, which are always looking to reduce regional energy demand during "peak load" periods (periods of the day that there is highest power demand). Energy storage can be used a "peak-shaver" and can provide a backup when the grid is down. The grid can thereby stare energy produced by both the traditional plants and renewable sources to use at times of greater demand.

1.2 Motivation

Among multiple ESS, the redox flow batteries(RFB) represent one of the most recent technologies with highly promising options for ESS.

Figure 1.2 shows a schematic of an aqueous RFB system. Energy is stored in liquid electrolytes that flow through a stack of electrochemical cells during charge and discharge. An ion-selective membrane or porous separator prevents the two electrolytes from mixing in a cell. The maximum voltage across the RFB stack is specific to the chemical species involved in the reaction and the number of cells

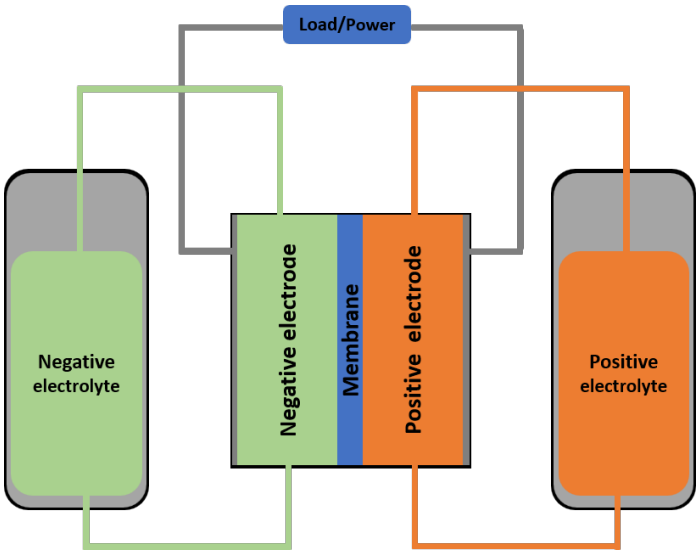

Figure 1.2: Schematic of a Redox Flow Battery

connected in series. The amount of energy that can be stored in an RFB is determined by the potential of redox couples, the concentration of active species, and the size of the tanks that contain the electrolytes (negative and positive). The power of an RFB system is determined by the size (active area) of the stack. Unlike more conventional solid-state secondary batteries, energy and power capacity are decoupled in a standard RFB.

Research on flow batteries or redox flow batteries (RFB) has been conducted since 1974 by NASA[7], the RFB used (Fe^{2+} /Fe^{3+}) in the positive cell and (Cr^{2+} /Cr^{3+}) in the negative cell (Fe/Cr). Today one of the most advanced systems is the all-vanadium (V/V) redox battery, which is being deployed by utilities for grid support. All-vanadium systems have demonstrated a long cycle life, good efficiency, and zero-flammability [8, 9]. RFB does not undergo physical and chemical changes during cycling, this attribute is free of structural or mechanical stress, thus extending their service life. This could result in a lower capital cost of the battery system since the investment can be spread over a longer period.

Researchers at the Pacific Northwest National Lab (PNNL) have developed a mixed chemistry, which aims to combine the advantages of the (Fe/Cr) and (V/V) systems (Fe/V) mixed-acid system.[10]

With the PNNL electrolyte, the species stability is increased by removing the energy losses caused by thermal management devices. Also, the electrolytes are less corrosive allowing a more affordable separator to be used. These changes alone may

reduce investment costs by 20% [11]. Using Fe in place of the higher potential V species avoids the limited upper-temperature stability problem and reduces cost as V is approximately 10x the cost of iron. This chemistry employs a mixed electrolyte system. If the electrolytes become unbalanced or if an osmotic solvent transfer occurs it is easily countered by remixing the electrolytes.[12] This mixed chemistry has the disadvantage of having a lower volumetric energy density compared with the all vanadium RFB [10].

Electro-thermal models can be important tools in the optimization of RFB, this work aims to create an electrothermal model for the new chemistry (Fe/V), which accounts for the reversible entropic heat of the electrochemical reactions, irreversible heat due to overpotentials, and the heat transfer between the stack and environment. These types of models can assist in scaling up as well as the optimization of the battery. There is a need for simple battery models that are detailed enough to capture the performance so that use-cases can be tested. This type of model will assist in define the battery size, operation, and design parameters.

1.3 Objective

The purpose of this work is to develop a full understanding of why energy storage is needed, to present the redox flow battery as most promising technology to meet this need and how RFB can be used as peak shaving tool to reduce cost of the total electricity. A simple thermo-electrochemical model was used, the chemistry of interest is the iron-vanadium which accounts for the reversible entropic heat of the electrochemical reactions, irreversible heat due to overpotentials and the heat transfer between the stack and environment. Followed by two simple dispatch strategy which aim to use the performance from the thermo-electrochemical model and integrate it into a dispatch strategy to obtain a new demand profile.

- Develop a thermo-electrochemical model of the Fe/V system.
- Dynamics of the model, obtain the current profile for a grid-size battery.
- Case study; implement the dynamics of the model for one type of scenario, UVic's demand profile and obtain the benefits of having an RFB

1.4 Thesis Structure

This section provides an outline of this work. Each chapter will contain a brief introduction. The document concludes with a summary of main results and recommendations for future work. The content of each chapter are as follows:

Chapter 1 Presents a general background on redox flow batteries. The motivation and objective of this work are also defined in Chapter 1.

Chapter 2 Describes what is a redox flow battery, it's structure, advantages and disadvantages as well as some modelling strategies found in the literature.

Chapter 3 Presents the electrochemical model of the chemistry Fe/V, describes the model assumptions.

Chapter 4 Presents the validation of the model.

Chapter 5 This chapter will be a case study for the RFB; it contains the system approach to a real scenario (UVic electricity demand) .

Chapter 6 Provides a restatement of the whole work and the results of the model. It also identifies avenues of future research and further development of the concept and its applications.

This chapter introduced the motivation, the objective, the structure of the thesis and a general background on energy storage in redox flow batteries. The upcoming chapter will go into detail of the structure of redox flow batteries as well as a literature review of the most common types of chemistries employed in the industry and in research.

Chapter 2

Electric Energy Storage Systems: Redox Flow Battery

This chapter will introduce what a redox flow battery is, explain three different types of chemisitries used in RFB as well as the structure of a cell in a RFB. Later on this chapter will discussed Energy store systems and a brief introduction to modelling RFB will be provided.

2.1 Introduction

Redox flow batteries have been researched since the 1970s [7]. Redox flow batteries can be categorized by phase:

1. All liquids phase
2. All solid phase
3. Hybrid redox flow battery

The most common type of RFB is the all liquid, in which the negative and positive active species are dissolved in electrolytes. The electrochemical reactions (reduction and oxidation) in this type of RFB usually requires a membrane, which is used as a separator between the positive electrolyte and the negative, and it prevents cross-contamination. Some of the all-solid RFB store energy uses electrodeposition (charge) at both electrodes, positive and negative. The energy is released when the deposit is dissolved (discharge). Finally a hybrid RFB is the combination of the previous two

where electroactive material is deposited on the surface of the electrode during the charge cycle and then dissolved back into the electrolyte solution during discharge.

The general reactions can be written as:

$$A + B \longrightarrow A^+ + B^- \tag{2.1}$$

$$A \longrightarrow A^+ + e^- \quad oxidized \tag{2.2}$$

$$B + e^- \longrightarrow B^- \quad reduced \tag{2.3}$$

Typically, the RFB electrolytes are solutions of water, stabilizing agent (an acid). The electrolyte has a significant impact in the reversibility of the RFBs, the pH is an important aspect in terms of the ion stability. Acid liberates ions and enhances the electrolyte conductivity [13, 14, 15] which shows how the electrolyte significantly impacts the reversibility in the redox reactions.

Multiple chemistries have been explored since the first redox flow battery invented by NASA[7] which used Fe^{2+} $/Fe^{3+}$ in the positive cell and Cr^{2+} $/Cr^{3+}$ in the negative cell, the Iron-Chromium (Fe/Cr). Today one of the most advanced systems is the All-vanadium (V/V) redox battery[16].

Since the reactive materials are stored separately, the RFBs are safer systems compared with other types of batteries. The flowing electrolytes function as a cooling system since it carries away the heat generated during operation.

2.2 Types of Redox Flow Batteries

Another way to classify Redox flow batteries is by their active species or solvent:

- All Vanadium Redox Flow Battery.
- Vanadium-bromine Redox System.
- Bromine/polysulphide Flow Battery.
- Zinc/bromine Redox Flow cells.
- Iron-chromium Redox System.
- Iron- Vanadium Redox System.

A review of the chemistry of each can be found in [17], this work will briefly discuss the All vanadium, Iron-Chromium, and the Iron-Vanadium.

2.2.1 Iron-Chromium

The development of energy-storage in an electrochemical dorm started in the 1970s at NASA, when it was demonstrated a 1kW/13kWh system for a photovoltaic array application [7]. This system is an aqueous solution of ferric/ferrous (Fe^{2+}/Fe^{3+}) redox couple in the positive electrode; at the negative electrode there is a mixture of chromic and chromous ions (Cr^{2+}/Cr^{3+}). The system is in a hydrochloric acid electrolyte. The cell voltage is 1.18 V . This system is an affordable stationary electrochemical energy store, it has simple electrode reactions and high exchange current density. The redox reaction are:

$$\mathrm{Fe^{3+} + e^- \xrightleftharpoons[\text{Charging}]{\text{Discharging}} Fe^{2+}} \qquad E^\circ = 0.77V \tag{2.4}$$

$$\mathrm{Cr^{2+} \xrightleftharpoons[\text{Charging}]{\text{Discharging}} Cr^{3+} + e^-} \qquad E^\circ = 0.41V \tag{2.5}$$

$$\mathrm{Fe^{3+} + Cr^{2+} \xrightleftharpoons[\text{Charging}]{\text{Discharging}} Fe^{2+} + Cr^{3+}} \qquad E^\circ = 1.18V \tag{2.6}$$

The system can operate with low-cost carbon felt electrodes. Both of the reactions require only a single electron and this simplifies the charge transfer. The iron side of the cell shows good reversibility and fast kinetics, the Cr side of the cell has slower kinetics so this side of the cell requires a catalyst [18]. Higher voltage redox couples can result in H_2 evolution in which hydrogen ions are more easily reduced than Cr^{3+} ions. Hydrogen evolution not only reduces the coulombic efficiency but also causes the state of charge (SOC) of positive and negative electrolytes to become imbalanced over prolonged cycles, eventually causing capacity decay. This hydrogen evolution represents a loss of protons from the electrolyte and it also leads to a chemical imbalance with each charge-discharge cycle. [19]. Other advantages of the (Fe/Cr) system is the low cost of each active species and the ability to operate at temperatures of 60-65°C [19, 18].

2.2.2 All vanadium

The All-vanadium (VRB) was first proposed in the 1980s by Skyllas-Kazacos [20] to address the loss in efficiency which results in cross-over contamination from the other species. The cross over contamination affects the efficiency and the degradation in the overall performance system, which could result in an expensive electrolyte separation reactant recovery. The VRB can solve this by using more than two oxidation states of

the same element where crossover only represents an efficiency loss because no species are irreversibly consumed or removed from their reactive electrolytic solution.

Although it seems to have advantages over other flow battery systems, such a low energy density makes it less attractive when compared to rivals, like a lithium-ion battery, this is also the main barrier to commercialization. The redox reaction are:

$$\mathrm{VO_2^+ + 2\,H^+ + e^-} \underset{\text{Charging}}{\overset{\text{Discharging}}{\rightleftharpoons}} \mathrm{VO^{2+} + 2\,H_2O} \qquad E^\circ = 1.0V \tag{2.7}$$

$$\mathrm{V^{2+}} \underset{\text{Charging}}{\overset{\text{Discharging}}{\rightleftharpoons}} \mathrm{V^{3+} + e^-} \qquad E^\circ = 0.26V \tag{2.8}$$

$$\mathrm{V^{2+} + VO^{2+}} \underset{\text{Charging}}{\overset{\text{Discharging}}{\rightleftharpoons}} \mathrm{V^{3+} + VO_2^{3+}} \qquad E^\circ = 1.26V \tag{2.9}$$

Energy efficiencies are high (85%) [21, 22]. While energy density is not necessarily a primary concern for RFB and grid applications, nonetheless, the VRB energy density is limited by the solubility of vanadium. All-vanadium systems require thermal management since the ion solubility and stability has a limited temperature range [23] (5 to $50°C$). Alternatively, the use of acid stabilizers can increase the temperature range but may require more expensive components. Furthermore VRBs require more costly membranes for ion transport. An advantage of the all-vanadium chemistry its the long cycle-life. This is partially due to the use of vanadium in both positive and negative electrolytes, decreasing the cross-contamination that may occur.

2.2.3 Iron-Vanadium

A mixed chemistry which aims to combine the advantages of the Fe/Cr and V/V systems Fe/V mixed-acid system has been described by researchers at PNNL [10, 24]. Since the Fe^{2+}/Fe^{3+} has a lower potential, this reduces the corrosive strength compared to the all vanadium battery.

One of the biggest challenges for this particular chemistries is the energy density as it is lower than both of the previously mentioned. However, this can be compensated by increasing the reactant concentration in both sides of the cell, which will translate into achieving a higher specific capacity and a higher energy density.

The cell reaction of the redox flow battery:

$$\mathrm{Fe^{3+} + e^{-} \underset{\text{Charging}}{\overset{\text{Discharging}}{\rightleftharpoons}} Fe^{2+}} \qquad E^{\circ} = 0.77V \tag{2.10}$$

$$\mathrm{V^{2+} \underset{\text{Charging}}{\overset{\text{Discharging}}{\rightleftharpoons}} V^{3+} + e^{-}} \qquad E^{\circ} = 0.26V \tag{2.11}$$

$$\mathrm{Fe^{3+} + V^{2+} \underset{\text{Charging}}{\overset{\text{Discharging}}{\rightleftharpoons}} Fe^{2+} + V^{3+}} \qquad E^{\circ} = 1.02V \tag{2.12}$$

In addition, the electrolytes are less corrosive allowing a more affordable separator to be used. These changes alone may reduce investment costs by 20% [11]. Using Fe in place of the higher potential V species avoids the limited upper temperature stability problem and reduces cost as V is approximately 10x the cost or iron. One paper [10] employs a chemistry with a mixed electrolyte system. If the electrolytes become unbalanced or if osmotic solvent transfer occurs it is easily countered by remixing the electrolytes. [12] more information can be found in the appendix A This mixed chemistry has the disadvantage of having a lower volumetric energy density compared with the all vanadium RFB [10]. However this works will based in a mixed- acid electrolyte not mixed electrolyte. In which a mixed-acid electrolyte employs sulfuric and hydrochloric acid to increase the concentration of the active species to increase the energy density.

2.3 General Structure RFB

All the Redox Flow batteries have generally the same structure. Figure 2.1 illustrates the components of a redox flow battery.

One of the particular qualities of an RFB is that the redox-active substances are always in flowing media (fluids, gases, suspensions, etc). This allows for the separation of the scaling of energy and power. RFB and fuel cells share this characteristic, although fuel cells utilize reactions that often are not electrochemically reversible. Thus both systems share a similar structure of the electrochemical cell and cell stacks. They vary when looked at in detail depending upon the redox couple utilized. In Figure 2.1 it can be seen that the cell is divided by a membrane into two half cells. The solutions are pumped through the cell, and the relevant solutions are pumped in circulation, using the battery convention where the positive electrode is always referred to as the cathode and the negative electrode as the anode.

Figure 2.1 represents the structure of a redox flow battery cell. The endplates

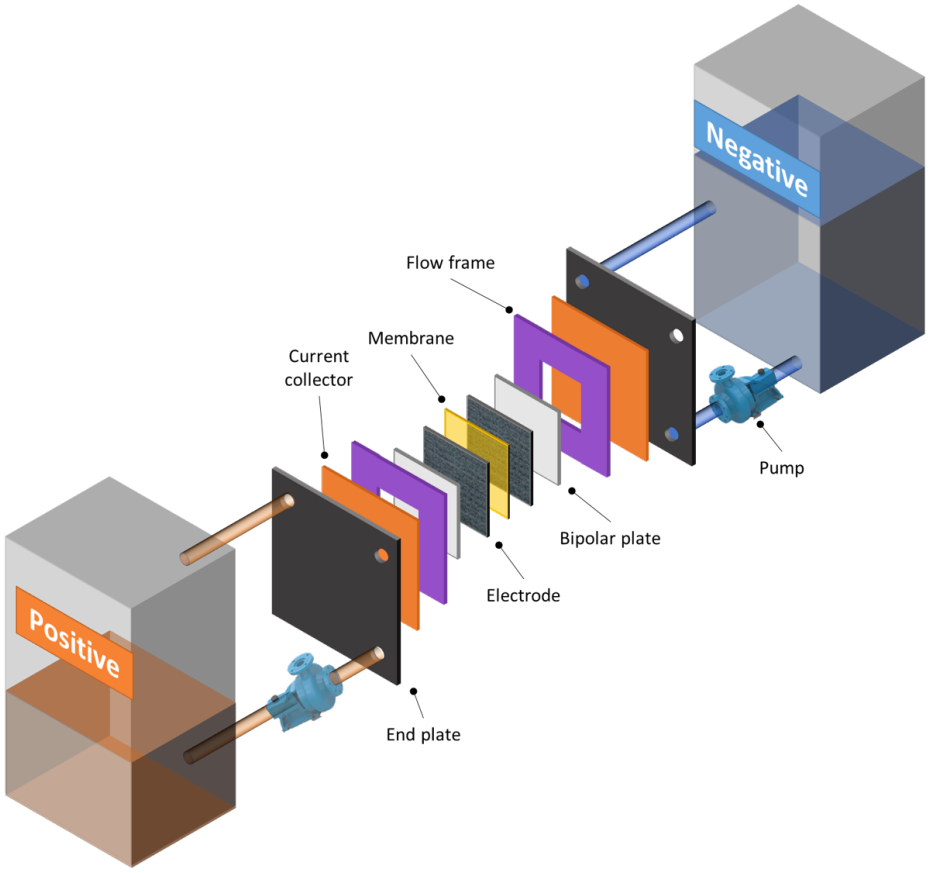

Figure 2.1: Exploded cell of common Redox flow battery

ensure the mechanical stability of the structure. The bipolar plate provides electrical isolation between both parts of the cell. The graphite felt act as the electrodes to ensure a large surface area. The flow frames ensure the distribution of the electrolyte through the felt and membrane. The membrane serves as physical separator and as an ion-exchange medium. Each part will be discussed later in this chapter.

To be a complete system these elements need to be taken into account: pumps, fluid technology, heat management (if needed), sensor, battery management, etc. It should be noted that the design of cells and cell stacks varies considerably depending on the chemistry used. Some of the parameters that have to be considered are:

- Energy Density: Is the capacity of the battery divided by the weight of the battery resulting in Wh/kg, gravimetric energy density.
- Energy Efficiency: Is the ratio of the energy extracted and introduced and can be differentiated according to the system boundary, for example, into half-cell,

cell, and battery efficiency. Often the energy efficiency of cells is given without any consideration of the peripherals.

- Voltage Efficiency: Is the ratio of the average discharge voltage to the average charge voltage.

- Current Efficiency: Is the ratio of the number of charges that enter the battery during charging compared to the number that can be extracted from the battery during discharging over a full cycle.

Energy density and power density, are two parameters that can be described as the amount of energy or power stored in a given system or region of space per unit volume. The difference between these two parameters is that energy is the amount of power consumed over time, and power is how much power can be quickly delivered to the system.

2.3.1 Mechanisms and losses

The polarization curve represents the behavior of an electrochemical reaction. It displays the output voltage of the cell at a given current density or state of charge (SOC). In a typical polarization curve there are three main regions in which it dominates a different kind of mechanism (although all the mechanisms are present at all time). Figure 2.2 shows the three main voltage losses:

- Activation loss: In the polarization curve dominates at low current density, and is the potential difference above the equilibrium potential required to overcome the activation energy of the cell reaction to produce a specified current. This loss is modeled by Butler-Volmer [17, 25] in chapter 3 the model is explained in detailed by equations (3.25- 3.29).

- Ohmic loss occurs at moderate current densities and represents the voltage drop due to the transfer of electrons in the electric circuit and the movement of ions through the electrolyte and membrane. These phenomena are determined on one hand by the electronic conductivity of the electrodes and the current collectors (usually copper and aluminum) and on the other by the ionic conductivity of the electrolyte and membrane which shows that the losses are primarily a lineal region, the ohmic loss uses Ohm's law, it has to be noted that the other losses are still present however the dominant loss is ohmic.

- Mass transport loss: at high current densities the cell potentials decrease due to more pronounced concentration polarization resulting in voltage loss. It also shows the limiting current, meaning the highest current which can be withdrawn from the system. Further explanation of the three main mechanisms are explained in chapter 3.

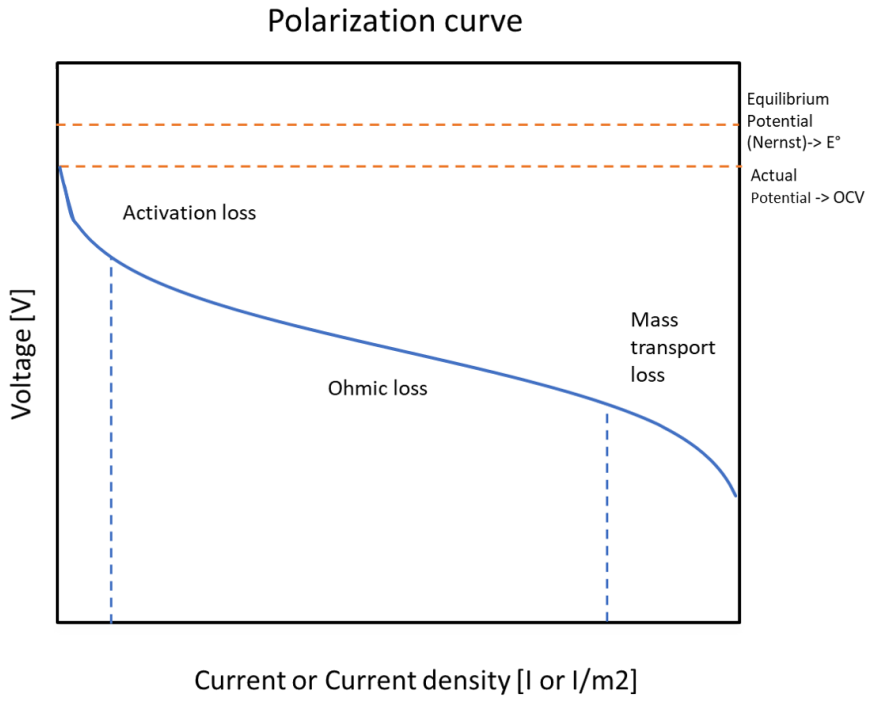

Figure 2.2: Typical Polarization curve

The main parts of the RFB contribute to the losses mentioned, understanding all the parts of the RFB can help design a battery to minimize the losses.

2.3.2 Membrane

An ion exchange membrane divides the two electrolytes within the cell, it works also as a physical barrier to avoid the mix of the electrolytes, this prevents a self-discharge while still allowing the flow of ion to complete the circuit, which provides proton conduction to maintain the electrical balance.

Nafion is the material most commonly used for proton exchange in RFB because of its high proton conductivity and good chemical stability in acid environments. Nafion sulfonated tetrafluoroethylene (Teflon) based fluoropolymer-copolymer was

discovered in the late 1960s by Walther Grot. It has unique ionic properties due to perfluorovinyl ether groups terminated with sulfonate groups onto a tetrafluoroethylene (PTFE) backbone. In recent years it has received attention as a proton conductor for RFB and fuel cells. Multiple works have tested and characterize this membrane [26, 27, 28]. However, it cannot prevent ion-crossover and this results in a decrease in coulombic efficiency, voltage efficiency, and energy efficiency.

Much research has attempted to reduce the permeation of the crossover ions and a handful of proposed methods have obtained satisfactory results.[29, 30, 31, 32]. The membrane contributes to the ohmic loss. Multiple studies have determined a model to predict the conductivity of the membrane at different temperatures and different degrees of saturation (of water).

2.3.3 Electrolyte

The electrolyte consist of mainly soluble salts. In an acid or base medium (liquid, gelled or dry forms), the electrolyte serves as a conductor for the ions from one electrode to the other. The electrolyte can be liquid or solid, and it works also as a catalyst making the battery more conductive. The electrolyte plays a huge roll in terms of designing the cell since one of the advantages of RFB is that the energy and power are separate parameters which can be modified to design the whole cell. The energy is contained in the tanks and the concentration of the soluble salt will determine the energy density of the cell.

However the electrolyte contributes largely to the ohmic loss. There have been multiple attempts to predict the conductivity of an electrolyte, and despite multiple theories being formulated the conductivity depends on multiple factors that it makes it difficult to use models only to recreate the conductivity of the electrolyte. What has been done is to use data from previous work or measured conductivity. [25, 33, 34, 35]. Chapter 4 will discuss how to adequate the conductivity of the electrolyte and a detailed explanation of why the current theories are not an accurate prediction of the conductivity, more information can be found in appendix B

2.3.4 Electrode

The electrodes in RFBs are responsible for providing active sites for redox reactions and facilitating the distribution of chemical species. Electrochemical reduction and oxidation of redox couples occur at the negative electrode and the positive electrode,

during charge, with the reverse processes occurring during discharge [36] Therefore, the performance of the RFB is dependent on the properties of the electrodes, in particular, their microstructure. The carbon presents some electric properties such as electrical conductivity and dielectric constant.

Although these materials are inert and durable, they also have some drawbacks including low surface area, poor wettability, and high-pressure drop [36, 37, 38]. To enhance the electrochemical activity and wettability of carbon-based materials in RFBs, there have been multiple attempts to change the surface of the carbon felts. Different methods such as coating with metals such as iridium,[39] doped with nitrogen [40] or applied nanomaterials such as graphene-nanowalls[41] or graphite carbon nanotubes have been tried.[42]

The main components of the RFB have been described, now it's possible to recreate a schematic of a cell and refer to the parameters that need to be monitored when designing RFB. The following figure 2.3 illustrates the cell and all its parts.

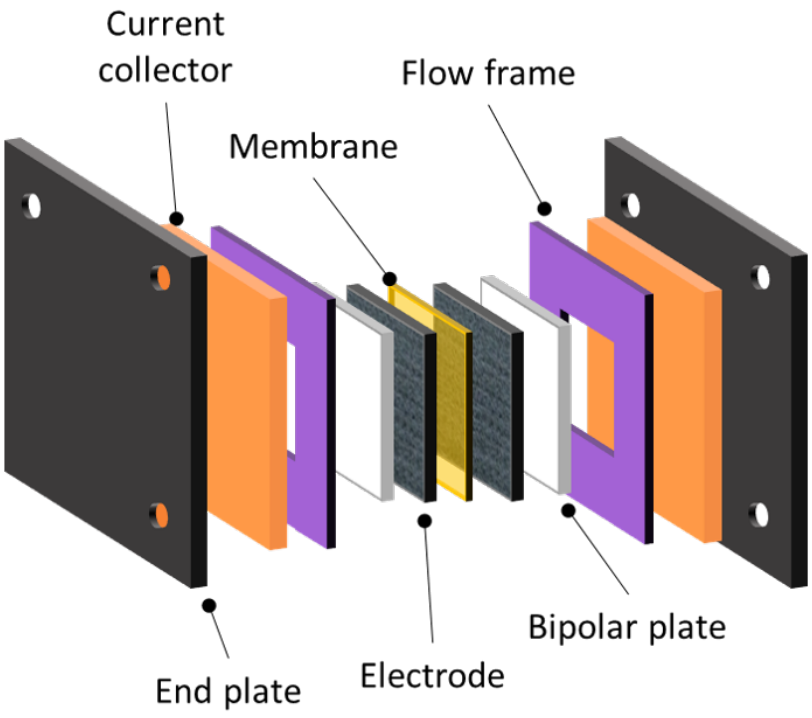

Figure 2.3: Exploded cell with all the common parts of a flow cell battery

2.4 Energy Storage Systems

When comparing an electric storage system with the conventional systems, such as petroleum or natural gas, the electricity in the conventional systems must be used when the energy is generated, but with an electric storage system it is possible to use the energy when it is needed. This is the reason stored energy can be more flexible and will have a wide range of applications due to this flexibility. For the supply power application it can be seen as an advantages when encountering problems in energy delivery on the part of the principal source. A good example would be a hospital, where a constant power supply is a necessity. Here the electrical storage system plays an crucial role.

In this case the electric storage system must have the requirements for partial load. Another advantage could be in the daily consumption of energy in the home. The electricity market purchases of cheaper electricity when domestic consumption is lower and the generation is greater and is resold when the demand is higher. In this way the company increases its profits. This happens because the market is always regulated by the supply and demand paradigm, where when the demand is lower and the supply is higher, the prices are lower and when the demand is higher than the supply the prices rise.

Similarly, for the consumer it is possible to take advantage of the variation of the price and consume "cheap" electricity during the night and use the energy storage during the day. For the infrastructure/transmission and distribution of energy, energy storage could be used to avoid oversizing the grid in order to satisfy the peak demands.

2.4.1 Modeling Redox flow batteries

Electro-thermal models can be important tools in the optimization of RFB. These models can be divided into two main groups: equivalent circuit models and numerical models.

The equivalent circuit models simulate the cell with resistors and capacitors able to capture the dynamics of the RFB while maintaining the simplicity and do not require significant computations. These type of models are often used in control-oriented systems. However, these type of models do not reflect internal processes within the cell, therefore they require much measured data to correlate the system with the model. The numerical models are more flexible since they are based on the physical process so they are able to adapt to any type of system, needing only to

change the coefficients related to the physical properties of the component.[43]

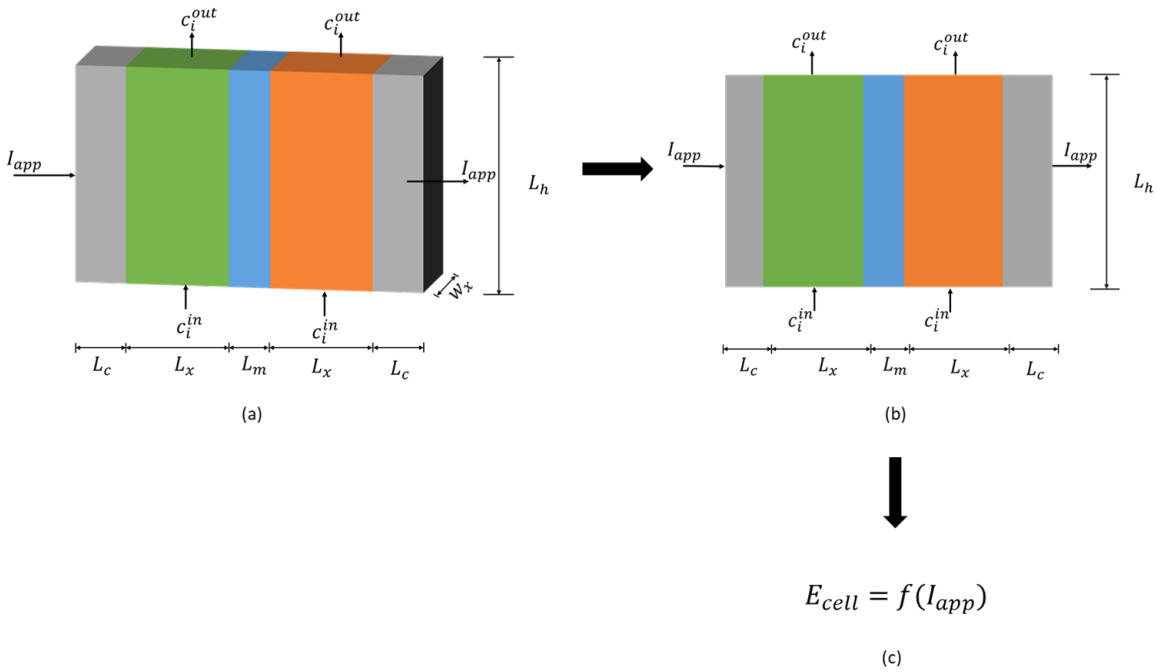

Figure 2.4: Schematic of a single cell RFB represented at different spatial dimensions (a) 3D model, (b) 2D model and (c) 0D model. Adaptation from [44]

For iron-vanadium chemistry there is an electrochemical model [45] which assumes an iso-thermal condition through the cell assuming a constant temperature throughout the whole cell, while in reality, the cell interacts with the environment and self-heating due to the redox reactions. Multiple models have been developed for the all-vanadium RFB [46, 47, 48, 49], You[50] as well as Stephenson [45] found a strong correlation using a simple model which ignored the effect of migration on the transport of ionic species. Stephenson suggests that a zero-dimensional electrochemical model could be appropriate for RFB modeling if the reacting species do not a create large concentration of gradients through the thickness and width of the electrodes.

The reduction from a 3D to a 2D model is straight forwards, since the membrane and electrode change in the dependent variable in the z-direction are negligible. It does not require detailed analysis, however the 0D model needs more analysis in order to account for the porous nature of the carbon felt and the membrane. Relative error of less than 1% was found. This suggests that the reduced model is able to reflect enough of the physics to reproduce the charge-discharge curve. Detailed explanation

on how to reduce from 2D to a 0D can be found in [44].

The zero-dimensional electrochemical model is illustrated in 2.4. It shows how the 0D model considers electrochemistry as a function of the current applied. The development of an effective control system for electrolytes re-balancing requires a dynamic model that can predict RFB behavior as a real-time operation so that the controllers can be able to schedule and re-balance the process. However, the microscopic models require significant computational time, and therefore, are not suitable for this purpose. On the contrary, 0-D models can fulfill this requirement, having briefer time complexity. Moreover, they require significantly less computational power which enables them to be implemented thorough on low-cost control hardware

A thermo-electrochemical model was be developed. An equivalent circuit model that describe the dynamics of the battery while the thermal model which considers he reversible entropic heat of the electrochemical reactions, irreversible heat due to overpotentials, and the heat transfer between the stack and environment. With the integration of models, performance, power and temperature can be obtained for a system, this was be coupled with a dispatch strategy that will be described in chapter 5. The University of Victoria was chosen as the study case, in which the goal is to reduce the total electricity bill of the university, increasing the energy demand and reducing the power demand by deploying the battery.

This chapter discussed some of the typical chemistries used in RFB as well as the structure of a cell in all RFB with a a brief introduction in how to model RFB. The following chapter will go into more detail and explain how RFB's are modeled, including the electrochemical and thermal part of the reaction.

Chapter 3

Thermo-Electrochemical Model Fe/V

This chapter describes a thermo-electrochemical model of an Fe-V redox flow battery. A lumped model of the stack and reservoirs is developed to capture stack voltage as a function of current density, state of charge, temperature and design parameters.

3.1 Electro-chemical Model

The electrochemical model follows that reported by Stephenson et al. [45]. The following section describes the main assumptions and resulting expressions. Subsequent sections describe the thermal model. In defining the electrochemical model, the following assumptions are made:

1. The state of charge (SOC) is assumed to be known at all times.
2. The fluid is assumed to be an incompressible flow.
3. The Nernst potentials relate to the electrolyte SOC.
4. The membrane, electrode and electrolyte physical properties are isotropic and homogeneous.
5. No cross-over contamination and no side reactions occur in the system, thus achieving 100% coloumbic efficiency.
6. Change in the electrolyte volume is negligible.

7. The Butler-Volmer kinetics is udes to describe the system reactions

8. Averaged current density is assumed.

9. The concentration of the redox species across the electrode is negligible.

At a high flow rate the variation in concentration of each active species through the thickness of the electrode will not affect the performance.

3.1.1 State-of-Charge (SOC)

The efficiency of the battery is determined by the relationship between current and voltage and parasitic losses such as pumping power. Over a cycle the concentration of active species in the power stack (the state of charge) is changing because of the relationship between species activity and voltage, the state of charge is a key parameter determining efficiency at any time. Figure 3.1 shows a schematic representing the two electrolyte tanks and the power conversion stack. The active vanadium species are in the left electrolyte tank and iron species are in the right tank. If the external circuit is closed as the electrolyte is pumped through the stack, discharge will occur until two half-cells come to equilibrium. The rate of discharge is proportional to the current, I.

As each redox reaction proceeds, the concentration of species in the tanks is changing. Assuming a well-mixed tank, the SOC is defined by the following,

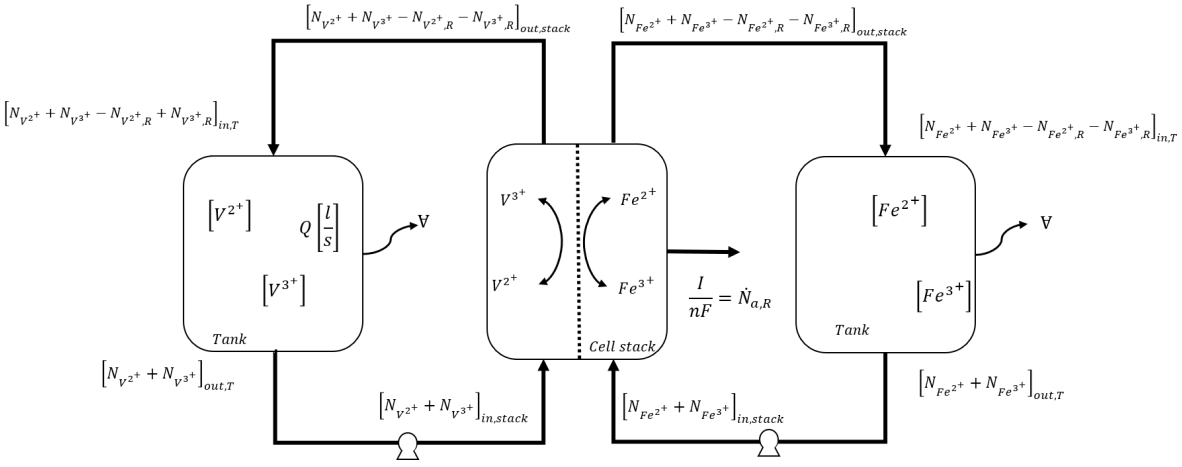

Figure 3.1: Diagram showing of the system

The varying concentrations in the stack and the tanks are coupled by current and electrolyte flow rates. Assuming no crossover of vanadium or iron in the stack, the

state of charge is given by the concentration of active species in each tank via,

$$\begin{aligned} SOC &\equiv \frac{c_{Fe^3+}}{c_{Fe^3+} + c_{Fe^2+}} \\ &\equiv \frac{c_{V^2+}}{c_{V^3+} + c_{V^2+}} \end{aligned} \tag{3.1}$$

The stack voltage is a function of SOC which varies in time. Therefore, to determine instantaneous voltage, the time dependent SOC must be determined.

Each redox half cell involves the conversion of one ion, a, to another b. Assuming no parasitic reactions, leaks, or crossover, the total concentration c° remains constant.

$$c^\circ = c_a + c_b \tag{3.2}$$

Thus, the concentration of each species can be expressed in terms of the SOC via equation 3.1:

$$\begin{aligned} c_a &= c^\circ * SOC \\ c_b &= c^\circ * (1 - SOC) \end{aligned} \tag{3.3}$$

The state of charge in a tank varies with average concentration of active species a, as given by a mass balance on a tank:

$$\begin{aligned} \dot{N}_{a,in,T} &= \dot{N}_{a,out,stack} \\ \frac{dN_{a,T}}{dt} &= \dot{N}_{a,in,T} - \dot{N}_{a,out,T} \\ \frac{dN_{a,T}}{dt} &= c_{a,in}Q - c_{a,out}Q \end{aligned} \tag{3.4}$$

Using $N_a = c_a \forall$ where the subscript T refers to the tank, $\forall$ is the volume of a tank and Q volumetric flow of electrolyte,

$$\forall \frac{dc_a}{dt} = -(c_{a,in} - c_{a,out})Q \tag{3.5}$$

Using the equation 3.3 to solve for SOC in the reservoir.

$$\begin{aligned} \forall c^\circ \frac{dSOR_R}{dt} &= (c_{a,out} - c_{a,in})Q \\ \frac{dSOR_R}{dt} &= \frac{(c_{a,out} - c_{a,in})}{\forall c^\circ} Q \end{aligned} \tag{3.6}$$

A mass balance on any active species, a, through the stack is:

$$\dot{N}_{a,out} = \dot{N}_{a,in} - \dot{N}_{a,R} \tag{3.7}$$

where $N_{a,in}$ is the molar flow rate in to the stack and $N_{a,R}$ is the reaction rate. From Faraday's law of electrolysis [51],

$$\dot{N}_R = \frac{I}{nF} \tag{3.8}$$

F is Faraday's constant and n is the number of electrons transfered per mole of active species. Current is assumed to be positive when discharging. Combining equation 3.5 and equation 3.8 and writing the molar flow rates in terms of concentration gives,:

$$(c_{a,in} - c_{a,out})Q = \frac{I}{nF} \tag{3.9}$$

Equation 3.9 can be used to rewrite equation 3.6 as,

$$\frac{dSOC_R}{dt} = \frac{-I}{c^\circ nF\forall} \tag{3.10}$$

Integrating to obtain the SOC as a function of time

$$\begin{aligned} SOC_R(t) &= SOC_R^\circ - \int \frac{I}{c^\circ nF\forall} dt \\ SOC_R(t) &= SOC_R^\circ - \frac{1}{c^\circ nF\forall} \int I dt \end{aligned} \tag{3.11}$$

Where SOC_R° is the initial state of charge of the battery.

The average concentration of reactants in the stack at any time can be determined by an arithmetic mean of SOC or concentration at inlet and exit. The difference in the state of charge across the stack can be expressed as:

$$\Delta SOC \equiv SOC_{exit} - SOC_{inlet} = -\frac{I}{Qc^\circ nF} \tag{3.12}$$

The average state of charge in the stack is then,

$$SOC_{avg}(t) = SOC_{inlet}(t) + \frac{\Delta SOC}{2}. \tag{3.13}$$

Assuming a well-mixed reservoir, the state of charge entering the stack is equal to

the reservoir, $SOC_{in}(t) = SOC_R(t)$, thus,

$$SOC_{avg}(t) = SOC_R^{\circ} - \frac{1}{c^{\circ}nF\forall}\int_o^t Idt - \frac{I}{2Qc^{\circ}nF} \tag{3.14}$$

3.1.2 Equivalent Circuit model

From Shah [52] the cell voltage, E_{cell}, can be calculated using the following equation:

$$E_{cell} = E_{cell}^{rev} - (IR)_m - (IR)_e - \eta \tag{3.15}$$

In which E_{cell}^{rev} is the reversible open-circuit cell voltage (OCV), η is the activation overpotential (with contributions from each electrode), $(IR)_m$ is the ohmic drop across the membrane, $(IR)_e$ is the ohmic drop associated with the electrolyte.

The OCV, E_{cell}^{rev} is determined using Nernst's equation and a correction, $E_{shift}(T)$:

$$E_{cell}^{rev}(T) = (E_p^{\circ} - E_n^{\circ}) + \frac{RT}{F} ln(\frac{c_{v2^+}^{avg} c_{Fe3^+}^{avg}}{c_{v3^+}^{avg} c_{Fe2^+}^{avg}}) - E_{shift}(T) \tag{3.16}$$

where E_n° and E_p° are the standard potentials for each half reaction from reactions 2.10, R is the molar gas constant, T is temperature, F is Faraday's constant and, c_i^{avg} is the average concentration of the active species, E_{shift} is an empirical correction of the Nernst equation given by Stephenson [45],

$$E_{shift}(T) = 0.00038T + 0.073 \tag{3.17}$$

E_{shift} is in Volts, T is in Kelvin.

3.1.3 Voltage losses

The reduction of cell potential relative to the open-circuit potential is due to losses arising from:

1. Electrolyte resistance
2. Membrane resistance
3. Kinetics.

Electrolyte

For the electrolyte, uniform reactions along the entire porous electrode (carbon felt) is assumed. The following equation describes the losses in the electrolyte:

$$IR_i = 2iA\frac{L_w}{\kappa(T)} \tag{3.18}$$

Where $\kappa(T)$ is the effective conductivity of the electrolyte which is dependant on the temperature, L_w is the width of the electrode, for each half cell. A is the area of the electrode and i is the current density. Experimental data from [45] is used for electrolyte conductivity as a function of temperature:

$$\kappa(T) = \kappa_{eff}[1 + 0.0171(T - 296)] \tag{3.19}$$

κ_{eff} is the conductivity at 296 K calculated using dilute solution theory:

$$\kappa_{eff} = \frac{F^2}{RT}\sum_i z_i^2 \times D_i^{eff} \times c_i^{avg} \tag{3.20}$$

Where the subscript i designates a species, z_i is the charge number, and D_i^{eff} is the effective diffusion coefficient calculated using the Bruggemann correction for porosity [53].

$$D_i^{eff} = \epsilon^{3/2} D_i \tag{3.21}$$

ϵ is the porosity of the electrode and D_i is the diffusion coefficient.

Membrane

The ohmic loss in the membrane is modeled as:

$$IR_m = iA\frac{L_m}{\sigma_m} \tag{3.22}$$

Where L_m is the membrane's thickness and σ_m is the conductivity. The conductivity of Nafion® is calculated using the empirical relationship [54, 55]:

$$\sigma_m = (0.5136\lambda - 0.0326)exp\big(1268[\frac{1}{303} - \frac{1}{T}]\big) \tag{3.23}$$

Where λ is the water content which is assumed to be saturated $\lambda = 22\frac{molH2O}{molSO3}$

Overpotential

The Butler-Volmer equation is used to describe the overpotential associated with the activation barrier of the electrode reactions. The total activation polarization is:

$$\eta = \eta_p - \eta_n \tag{3.24}$$

Assuming an equal charge transfer coefficient of 0.5 [52, 56]

$$\eta_n = \frac{-2RT}{F} asinh(\frac{i}{2Fk_n \epsilon a L_x \sqrt{c_{V^{2+}} c_{V^{3+}}}}) \tag{3.25}$$

and,

$$\eta_p = \frac{2RT}{F} asinh(\frac{i}{2Fk_p \epsilon a L_x \sqrt{c_{Fe^{2+}} c_{Fe^{3+}}}}) \tag{3.26}$$

Where k_p and k_n are the reaction rate constant associated with the reactions in the positive electrode and negative electrode, a is the specific surface area and L_x is the thickness of the electrode. The temperature dependence of the rate constants follows the Arrhenius law:

$$k_n = k_{n,ref} exp(\frac{-FE_n^\circ}{R}[\frac{1}{T_{ref}} - \frac{1}{T}]) \tag{3.27}$$

$$k_p = k_{p,ref} exp(\frac{FE_p^\circ}{R}[\frac{1}{T_{ref}} - \frac{1}{T}]) \tag{3.28}$$

3.2 Thermal model

The thermal model is based on energy and mass balance equations coupled with the equivalent circuit which computes the shunt current. The thermal model takes into consideration the reversible entropic heat of the main reactions and losses due to the overpotentials. Heat is generated in the stack and transferred into the environment by the flow of the electrolytes.

3.2.1 Energy Balance

The temperature of the stack is determined assuming a lumped mass approximation. The second law states:

$$\frac{dS}{dt} = -\frac{Q_{out}}{T} + \sum(\dot{N}s)_{in} - \sum(\dot{N}s)_{out} + \Sigma \tag{3.29}$$

Where Σ is the entropy generation. Using this result in the first law, gives the well-known result:

$$W = W_{rev} - T\Sigma \tag{3.30}$$

where W is the actual work and W_{rev} is the reversible work.

The difference between ideal and actual work is given by the deviation in cell potential and current:

$$W_{rev} - W = (E_{cell}^{rev} - E_{loss})I = T\Sigma \tag{3.31}$$

where E_{loss} is the voltage loss calculated in 3.18-3.28. Defining the reaction entropy as,

$$\Delta\dot{S} = \sum(\dot{N}s)_{in} \tag{3.32}$$

the internal heat generation can be written:

$$(E_{cell}^{rev} - E_{loss})I = Q_{out} + T\Delta\dot{S} \tag{3.33}$$

Relating the reaction rate to current and rewriting, the heat generated is,

$$Q_{out} = Q_{gen} = (E_{cell}^{rev} - E_{loss})I - T\Delta S \times \frac{I}{nF} \tag{3.34}$$

$(E_{cell}^{rev} - E_{loss})$ is the irreversible heat and $T\Delta S$ is the reversible heat generation.

Assuming the system has an effective specific heat, C_p

$$\rho_s C_{p,s} V \frac{dT_s}{dt} = Q_{gen} - Q_{ext} + \sum_{in} \dot{m}_i h_i(T) - \sum_{out} \dot{m}_i h_i(T) \tag{3.35}$$

Where Q_{ext} is heat transfer with the environment and is modeled using an overall transfer coefficient U:

$$Q_{ext} = UA_s(T_s - T_{\inf}) \tag{3.36}$$

T_s is the temperature of the cell stack and A_s is the assumed surface area of the stack and can be expressed as:

$$A_s = (2(2L_h)(2L_x)) + (4L_t N_{cells}) \tag{3.37}$$

where L_t is the cell thickness and N_{cell} is the number of cells. Figure 3.2 illustrates the dimensions of each cell.

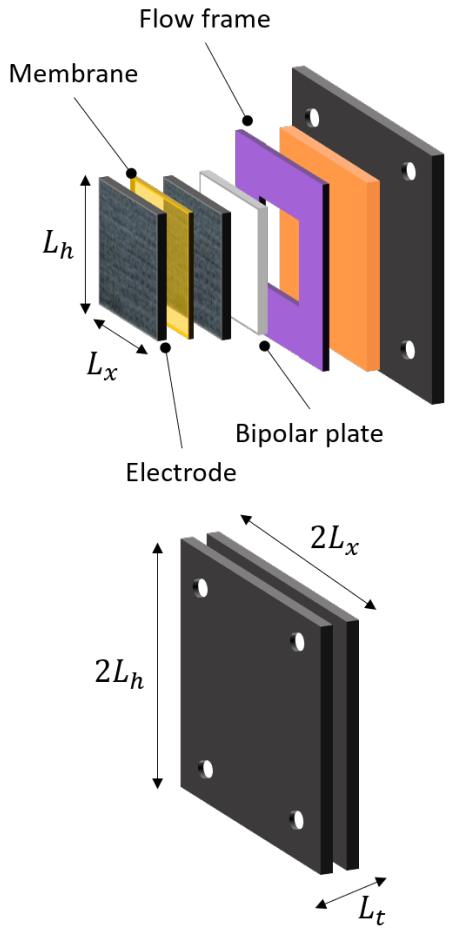

Figure 3.2: Cell dimensions for the stack and active area used for the model.

From equation 3.34 the energy balance will be adjusted to the system and illustrated in figure 3.3 . Where Q_{gen} is the heat generation and it is separated into:

$$Q_{gen} = Q_r + Q_s \tag{3.38}$$

Where Q_r is the irreversible heat from the ohmic loss and the reversible reaction

entropic heat is Q_s. Other internal sources of heat, like viscous dissipation are negligible for liquids and will not be considered. $C_{p,s}$ is considered to be the heat capacity

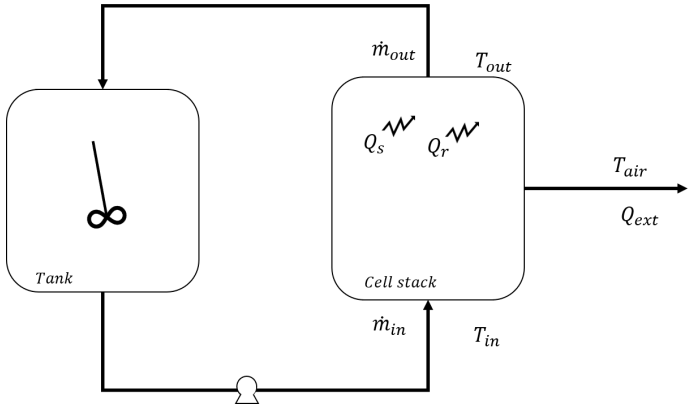

Figure 3.3: Energy balance of the whole system in which reversible entropic heat of the electrochemical reactions is considered, irreversible heat due to overpotentials and the heat transfer between the stack and also environment with a tank to mix inlet and outlet temperature.

of a mix of both electrolytes, ρ_s is the density of the mix electrolyte and V_c is cell electrolyte volume. The left hand side of the equation will be considered to be the cell stack properties, as the electrolyte makes up more than 80% of the system. For the flow mass rate of the species:

$$\sum_{in} \dot{m}_i h_i(T) - \sum_{out} \dot{m}_i h_i(T) = \rho_{FeCl_2} C_{p,FeCl_2} Q_{c,in}(T_{in} - T_{out}) + \rho_{VCl_3} C_{p,VCl_3} Q_{c,out}(T_{in} - T_{out}) \tag{3.39}$$

ρ_{FeCl_2} and ρ_{VCl_3} are the density flux of each electrolyte, $C_{p,i}$ is the heat capacity of each electrolyte, and Q_c is the flow rate of the electrolyte for input and ouput of the stack. The irreversible heat is caused by ohmic loss, ionic loss, and overpotential loss. The overpotential loss refers to the activation overpotential. The ionic loss and the ohmic loss are caused by the resistance that impedes the electrical flow. This term is the summation of the resistance calculated in 3.18 for the electrolyte, 3.22 for the membrane, and 3.24 for overpotential.

$$IR_{eq,d} = IR_m + IR_e + \eta \tag{3.40}$$

The following expression was used to represent them [48] [1]

$$\begin{aligned}(E_{cell}^{rev} - E_{loss})I &= IR_{eq,d} \\ Q_r &= IR_{eqd}\end{aligned} \tag{3.41}$$

The reversible entropic heat, which is positive during discharge and negative during charge. It is calculated using the following expression:

$$Q_s = IT_s\frac{\Delta S}{nF} \tag{3.42}$$

Where ΔS is the entropy change calculated

$$\Delta S_r = s^{\circ}[V^{2^+}] + s^{\circ}[Fe^{3^+}] - s^{\circ}[V^{3^+}] - s^{\circ}[Fe^{2^+}] \tag{3.43}$$

or

$$\Delta S_r = -130 + (-280.3) - (-230) - (-107.1) = -73.2\frac{J}{molK} \tag{3.44}$$

Where the values for s° (Standard molar entropy) of each species are taken from [57], the heat absorbed by the cell at $T = 25^{\circ}C$ is:

$$Q_{abs} = T_{\circ}\Delta S = -21.8\frac{kJ}{mol} \tag{3.45}$$

The negative sign indicates that it is generating heat at a rate of 21.8 kJ per mol. To incorporate the electrochemical model previously discussed with the thermal model, the equation 3.37 was integrated and solve for T_s which was assumed to be the same temperature as the outlet. This temperature was then placed in the electrochemical equations to capture the dynamics of the system 3.20,3.23-3.26. In this way the temperature increase will affect the chemical reactions.

3.2.2 Algorithm

To solve these thermal balance this algorithm was employed: Firstly, the thermal balance equation 3.35 was integrated and solved for the initial conditions, where the $T_{out,stack}$ =$T_{in,stack}$. Then it was assumed that $T_{out,stack} = T_s$. The following diagram 3.4 shows how the algorithm was solved until it converged into the T_{out} or T_{stack}. To solve the model Jupyter notebook [58] was used. The codes for the electrochemical model can be found in appendix C.1. To recreate a closed loop an average of the outlet

[1] Note that IR_{eq} is in Voltage

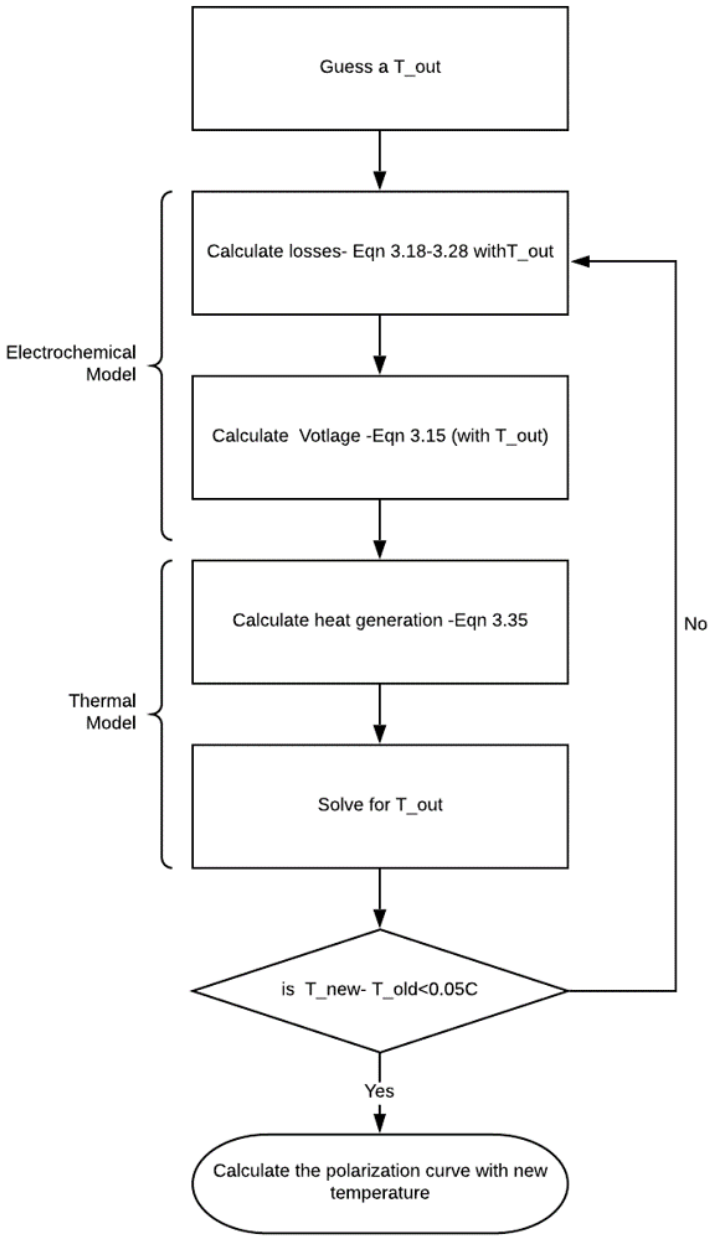

Figure 3.4: Flow chart to demonstrate how the thermal and electrochemical model coupled to capture the dynamics of the system.

temperature and the inlet temperature was taken resulting the new inlet temperature:

$$T_{in}(t) = \frac{T_{out}(t) + T_{in}(t-1)}{2} \tag{3.46}$$

This chapter explained the whole model used in this work, including the electrochemical model and the thermal model in which was included reversible entropic heat of the electrochemical reactions, irreversible heat due to overpotentials, and the heat transfer between the stack and environment. The following chapter will state how the model was in order to be used as a real application.

Chapter 4

Validation of the model

This chapter will validate the model presented. The validation of the model is needed to show its potential as an application for as optimization or sizing the battery. The present work does not include testing; therefore, literature data are used to validate model results. The electrochemical calculations are compared to data in [45], while the thermal results use multiple papers [59, 60].

4.1 Polarization and Electrochemical Validation

Parameters used for validation - The electrothermal model was compared to the paper which describes the electrochemical model of the Fe/V system [45] using the parameters listed in Table 4.1 taken from model[45]:

Table 4.1: Electrode Parameters

Symbol	Parameter	Value
L_w	Width of electrode [10]	0.02m
L_h	Height of electrode[10]	0.05m
L_x	Thickness of electrode[10]	0.0045m
L_m	Thickness of membrane[10]	5.08×10^{-5} m
ϵ	Porosity of the electrode[10]	0.929
a	Specific surface area[61]	$39000m^{-1}$

Table 4.2 shows the standard half-cell potentials and the kinetic parameters for each reaction. Because these parameters are inherent to the cell chemistry, these values do not change for the application results.

Table 4.2: Kinetic Parameters

Symbol	Parameter	Value
E_n°	Reference potential for negative electrode (298K)[10]	-0.255V
E_p°	Reference potential for positive electrode (298K)[10]	0.77V
$k_{n,ref}$	Reference rate constant for negative electrode (298K) [62]	$8.7 * 10^{-6}$ m/s
$k_{p,ref}$	Reference rate constant for positive electrode (298K)[24]	$1.6 * 10^{-6}$ m/s

Finally, the electrolyte properties are shown in table 4.3, these were used to validate the electrochemical model.

Table 4.3: Electrolyte Parameters

Symbol	Parameter	Value
i	Applied charge current density[10]	$-500 A/m^2$
i	Applied discharge current density[10]	$500 A/m^2$
$D_{v^{2+}}$	Diffusion coefficient V^{2+}(296K)[62]	$2.4 * 10^{-10} m^2/s$
$D_{v^{3+}}$	Diffusion coefficient V^{3+}(296K)[62]	$2.4 * 10^{-10} m^2/s$
$D_{Fe^{2+}}$	Diffusion coefficient Fe^{2+}(296K)[63]	$3.95 * 10^{-10} m^2/s$
$D_{Fe^{3+}}$	Diffusion coefficient Fe^{3+}(296K)[63]	$3.32 * 10^{-10} m^2/s$
$D_{HS0_4^-}$	Diffusion coefficient HSO_4^-(296K)[63]	$1.4 * 10^{-10} m^2/s$
D_H^+	Diffusion coefficient H^+(296K)[63]	$9.31 * 10^{-9} m^2/s$
c_v°	Initial vanadium concentration both electrodes[10]	1600 mol/m^3
c_{Fe}°	Initial iron concentration both electrodes[10]	1600 mol/m^3
c_{HCl}°	Initial HCl concentration both electrodes[10]	2300 mol/m^3
SOC_0	Beginning state of charge for charge	0.025
SOC_0	Beginning state of charge for discharge	0.975
$z_{V^{2+}}$	Charge number of V^{2+}	2
$z_{V^{3+}}$	Charge number of V^{3+}	3
$z_{Fe^{2+}}$	Charge number of Fe^{2+}	2
$z_{Fe^{3+}}$	Charge number of Fe^{3+} [10]	3
Q_c	Volumetric flow rate	20mL/min

The parameters described in the table 4.1 can be modified as they are the same size of the cell that was used to validate the thermal model in Stephenson's paper [45]. The Kinetic parameters presented in table 4.2 are inherent to the chemical species involved in the reaction. If the model plans are to be used for different chemistries the parameters will change according to the species involved. Finally the electrolyte parameters in table 4.3 are a combination of fixed parameters and values that can vary for different scenarios, such as i the current density can be modified for different runs,

as well as for the initial concentrations employed in the battery. The volumetric flow rate is an important parameter that has not been studied in this work, nevertheless, it is important to mention that this parameter can be modified and will directly impact the performance of the battery.

Conductivity of the electrolyte

The conductivity of the electrolyte is a parameter that is debated in the literature. Whether calculated or measured. The most common approach to calculate the conductivity of the electrolyte is to use dilute solution theory (equation 3.20). All ion species have the velocity of the bulk and no interaction between the species occurs. This assumption is questioned because the ion concentration is very high and therefore, at the upper boundary of the theory.

Stephenson [45] mentions that the measured intrinsic conductivity of the Fe/V compared to the results obtained by using the dilute solution theory (equation 3.22) gives an error of $\sim 600\%$. The calculated conductivity is several times higher than the measured conductivity, this finding is cited in multiple papers [25, 64]. Instead multiple studies [35, 34, 65] suggest using linearized functions based on measured conductivity as a function of the SOC.

For this work the conductivities were calculated using Corcuera's relationship between the SOC and the temperature of the electrolyte, because the concentrations used in this work are similar [35].

Equation 4.1 shows the relationship between the SOC and the temperature of the electrolyte stated by Corcuera and Skyllas-Kazacos [35] where T is the temperature in $Celsius$ and SOC is the state of charge and κ is the conductivity of the solution in mS/cm and the coefficients can be found in table 4.4. Further information can be found in appendix B.

$$\kappa = (A \times T + B) \times SOC + (C \times T + D) \tag{4.1}$$

4.2 Model Simulation and Validation

The first part of the model was validated by the data obtained from Stephenson's paper [45]. Once the conductivity of the electrolyte from Corcuera and kyllas-Kazacos (equation 4.1) was implemented, the electrochemical model was coupled with the

Table 4.4: Coefficient for relation of the conductivity of the electrolyte

Coefficient	Positive half cell	Negative half cell
A	1.8	0.7050
B	93.5030	55.0420
C	4.6713	2.6176
D	172.07	122.37

thermal model. Figure 4.1 shows the experimental data obtained from [45] and the model explained in chapter 3. [1]

Figure 4.1

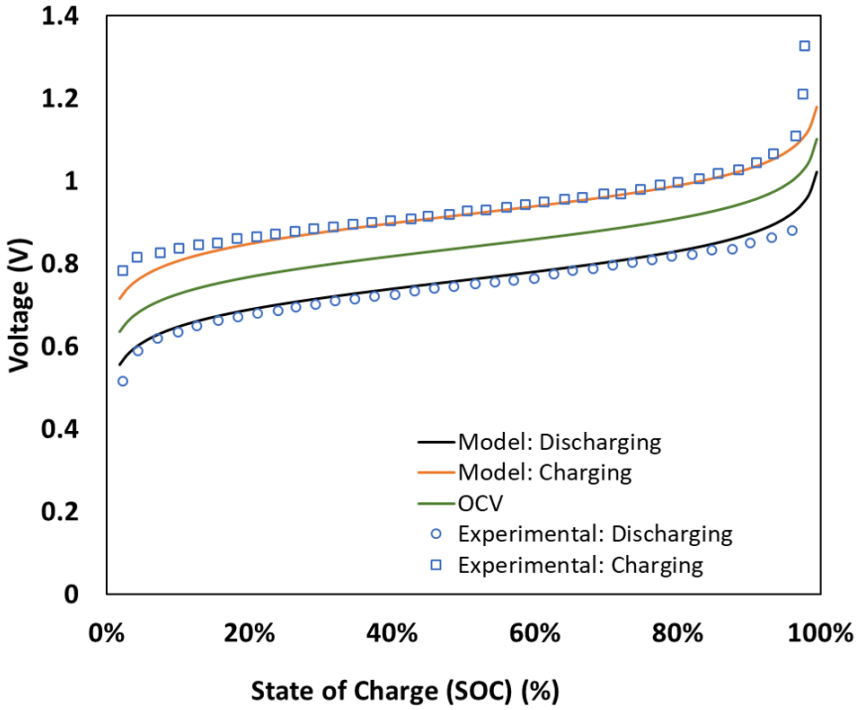

Figure 4.1: Iron vanadium system at $23°C$. Open circuit voltage is calculated by equation 3.17. Model results correlate with experimental data from paper[45]

.

Since the cell size in paper [45] used is too small, a number of cells were combined to create a stack model. Further results are described in the next section.

[1]Note that the temperature employed was 23° C in [45] so the same temperature was used for comparison.

4.3 Sizing

To obtain a scalable model the thermo-electrochemical model previously discussed, will account for a battery that could potentially be used at the University of Victoria. A 500 kW/2MWh battery was chosen to be used. As this could reduce the cost of the electricity. In chapter 5 the dispatch strategies used to deploy the battery to reduce the electricity cost will be discussed. The current density used in the system was set up to be $500A/m^2$ or $50mA/cm^2$. Since the chemical reactions in both sizes of the electrode only exchange one electron, the calculations to obtain the tank size of the electrolyte, as well as the cell area, are simplified.

For a stack made of m cells, the stack power P is $P(t) = V(t)I(t)$, the energy produced will be the area under the curve:

$$E = \int_0^t P(t)dt = \int_0^t V(t)I(t)dt \tag{4.2}$$

where the Voltage $V(t)$ is the stack voltage, in terms of m cells:

$$V(t) = mv(t) \tag{4.3}$$

Where $v(t)$ is the cell voltage and m is the number of cells in the stack, assuming a constant discharge current density.

$$E_s(t) = mA_{cell}i \int v(t)dt \tag{4.4}$$

Where $E_s(t)$ is the energy of the stack, A_{cell} is the area of the cell and i is the current density.

$$\triangle SOC_R(t) = \frac{iA_{cell}}{c^{\circ}\forall nF}t \tag{4.5}$$

The maximum change in SOC is 1, hence, the the maximum discharge time with fixed current density is:

$$t^{max} = \frac{c^{\circ}\forall nF}{iA_{cell}} \tag{4.6}$$

The maximum theoretical energy derived would be when the cell voltage is the open circuit potential. Assuming that $v_{cell}^{max} = E_p^{\circ} - E_p^{\circ} \cong 1Volt$, the maximum energy stored in the battery is given by,

$$\begin{aligned} E_s^{max} &= mA_{cell} i v_{cell}^{max} \frac{c^{\circ} V_r nF}{iA_{cell}} \\ &= mc^{\circ} \forall nF v_{cell}^{max} \end{aligned} \tag{4.7}$$

Using equation 4.2 and equation 4.7:

$$\begin{aligned} P_s^{max} &= \frac{E_s^{max}}{t^{max}} = \frac{mc^{\circ} \forall nF v_{cell}}{c^{\circ} \forall nF} \\ &= m v_{cell} i A_{cell} \end{aligned} \tag{4.8}$$

Equations 4.2 to 4.8 were used to calculate the area needed for a battery that could dispatch 500 kW and the volume of the tank to store 2MWh of energy of the electrolyte used in the system. The volume of the tank and the size of the cell are summarized in table 4.5.

Table 4.5: System Parameters and Cell Area

Parameter	Value
Voltage	48 [V]
Current density	500 $[A/m^2]$
Power	500 [kW]
Time	4 [hours]
Tank Volume	0.975 $[m^3]$
Area needed	20.2 $[m^2]$
Number of cells	48
Cell area	0.42$[m^2]$
L_x	0.65 [m]
L_h	0.65 [m]
Cell thickness	20 [mm]
Overall transfer coefficient	10 $[W/(m^{2\circ}C)]$
Flow rate	30 [L/min]

The flow rate used in the simulation was taken from a previous work as a 30 L/min [66]. This parameter can have significant impacts on the system performance; nevertheless, for this work, flow rate for each electrolyte is fixed. The model was run at different ambient temperatures: $5^{\circ}C, 20^{\circ}C$ and $50^{\circ}C$

Figure 4.2 illustrates the transient temperature increase when the cell is operated with a current density of $500 mA/cm^2$ for a charge and discharge cycle. From figure 4.2 it can be noted that there is a slight cooling at the beginning of the reaction over

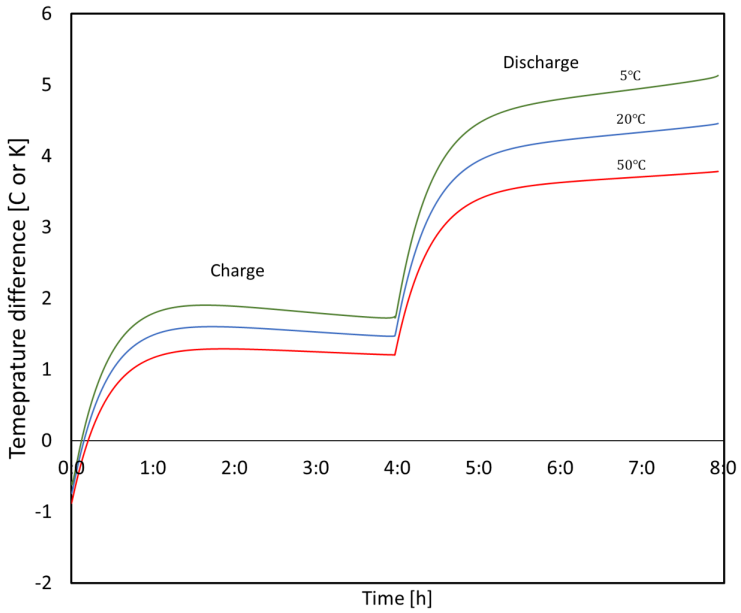

Figure 4.2: Temperature increase for $5°, 20°$ and $50°$ Charging and Discharging.

a few minutes. This can be associated with the entropy as the charging reactions are endothermic, however the battery start to self heat due to ohmic losses of the reaction. At higher ambient temperatures the temperature increase is less compared to a lower ambient temperature, this is associated with the overpotential as at higher temperature the energy required to overcome the potential is reduced as we as the ohmic losses decrease, since the conductivity is highly correlated with the temperature.

It should be noted that the discharging was done immediately after the charging. In reality the discharging might take place a few hours later and this result in the tank returning to the ambient temperature.

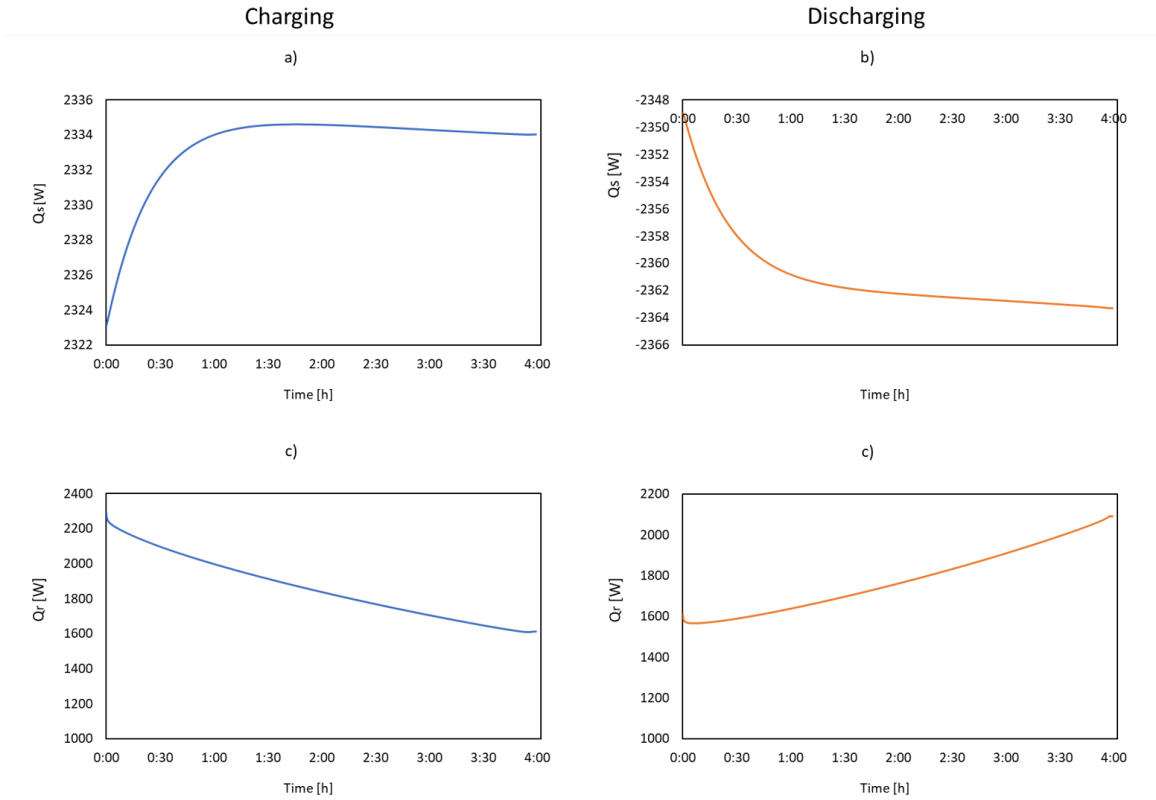

Figure 4.3: Simulation results at $500 A/m^2$ for 8 hours (a-b) reversible entropic heat rate (c-d) Irreversible heat rate at 20° C

At $20°C$ figure 4.3 a) and b) show the stack reversible entropic heat rate Q_s in load operations. It is positive since the reactions are exothermic during discharge and negative (endothermic reaction) during charge. In both operations the Q_r values are almost constant and the very small variations shown in the figures are due to a secondary effect. As the system has no active cooling implemented, it can be seen that the entropic heat has the same shape as the temperature increase. However the irreversible heat is practically linear as it is represented by the ohmic losses.

4.4 Limitations of the model

This model only accounts for this type of chemistry, however, the model can be modified to modeled different chemistry by modifying the properties of the electrolyte. It has to be mention that the reaction should be similar and no secondary reactions will be taken into account, such as hydrogen evolution. Being a 0D model, it is heavily based on the correlations obtained from experimental data, however, this work does not include any experimental part. As such, the correlations were obtained from previous works such as [45, 67, 20]. The electrolyte conductivity being an important factor in terms of losses, can not be modeled with precision and require data to correlate the model further explanation can be found at appendix B.

The model is based on the assumptions discussed in chapter 3 The battery operated from 10% to 85% of SOC per Souentie's findings [59]. The model is set up so that the current density is always constant. It ca be modified to keep the power constant and change the current density. In the current model the voltage and the power varies as the SOC is decreased or increased.

The model does not account for any degradation of any kind. This is a major limitation but it was decided to leave the degradation model out.

This chapter validates the model and calculated the cell size, the tank and the number of cells needed for a particular case. The next chapter will use the validated model and the size of the system into the electrical system of the University of Victoria using the output power to deploy the battery at different dispatch strategies.

Chapter 5

Study Case

This chapter will use the validated model and the size of cell stack and integrate into the electrical system of the University of Victoria using the output power to deploy the battery at different dispatch strategies.

The University of Victoria's electrical system consists of four transformers in where one is used as a backup for the other three. Each transformer connects the electricity grid of BC Hydro to specific university buildings.

The university's electricity bill consists of four distinct fees determined by monthly peak demand (power), energy use, a fixed charge, and a peak-season demand charge [68]:

- Demand Charge
  - $12.34 per kW per month
  - Peak demand is the highest rate of electricity use over 15 minutes each month.
- Energy Charge
  - $0.0606 per kWh.
- Basic Charge
  - $0.2673 per day.
  - Daily amount which partially recovers fixed customer-related costs, including customer service channels, metering, billing, payment processing, collections, and distribution system costs that are customer-related (electrical lines and transformers).

- Minimum Charge
  - Equal to 50% of the highest demand charge during the previous November 1 to March 31 period.
  - A charge that covers the costs of maintaining the equipment year-round for customers with high electricity usage in the winter but low electricity usage in the summer.

An example of the demand profile for a sub-set of buildings at UVic during a winter day is shown in figure 5.1. Demand ramps up and down throughout the day. One application of energy storage could be to reduce the peak demand by charging a battery during low demand periods and using the stored energy during times of high demand. This strategy of load shifting increases energy use due to inefficiencies of the storage system, but with sufficient cost savings from the reduction in peak-demand, the cost of additional energy is offset and a net-benefit is realized.

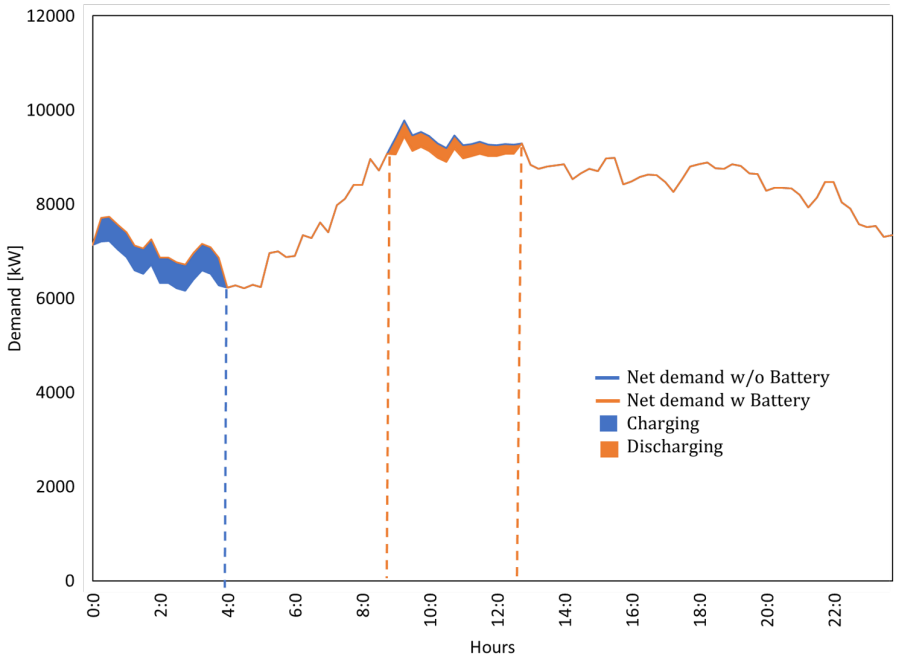

Figure 5.1: Demand profile for a sub-set of buildings at UVic during a winter day with and without a battery. A reduction in net peak load is obtained by charging the battery during low-demand hours and discharging during high-demand hours.

The model described in the previous chapter will be coupled with the dispatch strategies described in this section. The thermo-electrochemical model describes the

dynamics of the battery. This will provide the output power of the battery behaviour under the conditions of operation described. The dispatch model will use the power as an input for the dispatch strategy selected and will create a new demand, profile with and without the battery. After the new profile is obtained, the cost of the electricity can be calculated with and without the battery.

5.1 System Model

The following section describes dispatch the logic for a battery used to reduce peak demands. This type of use effects the UVic electricity bill through power demand and energy consumed. The demand charge is determined by the highest sustained peak of the month. While the energy charge is for total electricity delivered for an entire month. The battery will increase energy demand, but it can also reduce the peak power demand.

A simple schematic of the UVic connection to the grid and the deployment of a battery on the campus-side of the meter is shown in figure 5.2. There are four transformers (three used daily while the fourth is a backup) and the aggregated campus load at any instant in time is labeled, P_{ld}. The nomenclature for parameters defining the dispatch algorithm is summarized in Table 5.1.

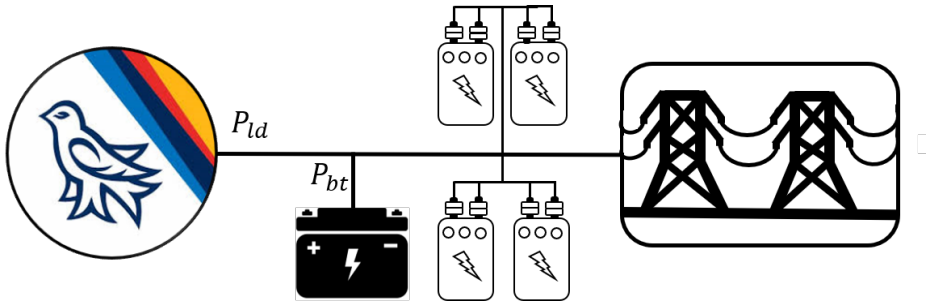

Figure 5.2: A schematic of the UVic electricity system with four transformers and a battery deployed on the campus-side of the meter.

The battery size considered:

- 500 kW/2 MWh

To meet instantaneous electrical demand, P_{ld}, the system will try to use power from the battery P_{bt-ld} or it will take if from the grid P_{g-ld},

Table 5.1: Nomenclature used

Variable	Description	Unit
P_{ld}	Actual demand (data)	kW
P_{g-ld}	Power taken from the grid to the load	kW
P_{bt-ld}	Power taken from the battery to the load	kW
P_{g-bt}	Charging power to the battery	kW
P_{max}	Maximum power drawn from the grid	kW
P_{bt}	Power flow to the battery	kW
$P_{bt,max}$	Maximum power flow	kW

$$P_{ld}(kW) = P_{bt-ld} + P_{g-ld} \tag{5.1}$$

The power from the grid is constrained to be less than or equal to a maximum, P_{max}, whereby total demand is due to the campus load and the battery combined:

$$P_{g-ld} + P_{g-bt} \leq P_{max} \tag{5.2}$$

The battery demand is positive when charging and is determined by battery control logic (to charge, discharge, or float = 0). At the connection to the campus, the power flow to the battery, P_{bt} is then,

$$P_{bt} = P_{g-bt} - P_{bt-ld} \tag{5.3}$$

where only one state is possible at each instant i.e. either charging (g–bt), discharging, (bt–ld), or idle.

Because of inefficiencies, not all power drawn for battery charging results in charge replenishment; likewise, not all stored energy is delivered during discharge. The dynamics of the battery were obtained from the model described in chapter 3, with a fixed current density the efficiencies were taken into account for charging and discharging. The efficiency varies depending on what associated the conditions were. The table 5.2 shows all the scenarios that were chosen. The scenarios showing the "Area calculated" refers to the battery size that was calculated with the equations 4.2 - 4.8 while the scenarios that shows "Number % more of the area calculated" refers that the area obtained from equations 4.1 - 4.7 the area was incremented by % indicated. The temperatures of the scenarios reflects all the possibilities of where the battery will be placed. $20°C$ is the ambient temperature if the battery was placed

inside a facility and no further thermal management is needed, $5°C$ the temperature if the battery is placed outside of the facilities and representing the coldest ambient temperature in Victoria BC, [69] while $50°C$ in the unlikely scenario, that the battery could be placed somewhere that the ambient temperature could reach $50°C$.

Table 5.2: Scenarios chosen

Current density	Temperature	Area
$400A/m^2$	$20°C$	Area calculated
$600A/m^2$	$20°C$	Area calculated
$350A/m^2$	$20°C$	Area calculated
$350A/m^2$	$20°C$	20 % more of the area calculated
$350A/m^2$	$20°C$	40 % more of the area calculated
$350A/m^2$	$50°C$	Area calculated
$350A/m^2$	$5°C$	Area calculated

5.2 Data

Load data with a 15-minute resolution for April 2018-March 2019 is used for the simulations.[1] Figure 5.3 shows the probability of the peak load for each month occurring on a given day. Wednesday is the most likely day to find the peak load and a monthly peak never occurs on a weekend.

Figure 5.4 shows the probability of the peak demand occurring at selected times of the day. 93% of the time the peak falls between 09:00 and 13:00 and has nearly a 70% probability of occurring between 11:00-13:00.

5.3 Dispatch Strategies

There are numerous ways to determine when charging and discharging events, - and the magnitude of associated power flow, - should occur to provide the desired effect. Based on the data analysis above, two simple modes of battery dispatch are tested to demonstrate system benefit: (1) scheduled dispatch, and (2) dispatch on peak demand [2].

[1]The data provided by UVic is for a single transformer. The total load is determined by assuming the other two transformers have the same demand.

[2]The preferred method to predict demand and schedule battery operations is still to be determined. The two test cases are for illustrative purposes.

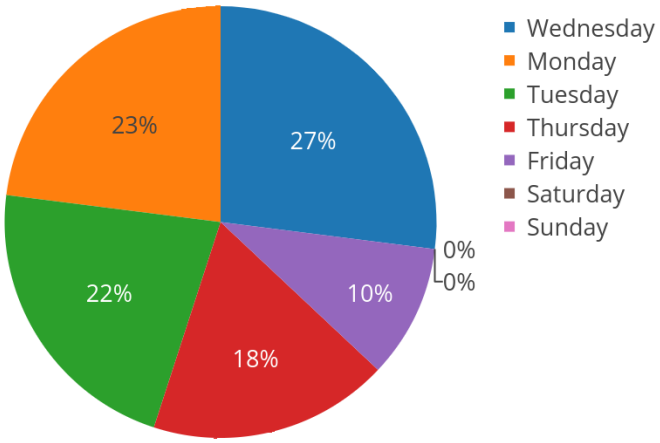

Figure 5.3: Probability of the peak demand in a month occurring on a given day of the week. The peaks never occur on weekend days.

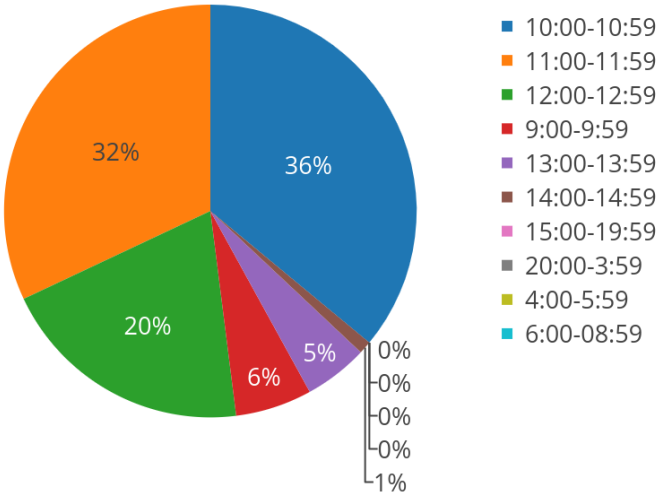

Figure 5.4: Probability of the peak demand occurring in a given time period within a day.

5.3.1 Strategy 1: Scheduled Dispatch

Scheduled dispatch specifies the times of day the battery will discharge and recharge. Because monthly peak demand always occurs on a weekday, the batteries are only operated Monday-Friday.

- For the 500 kW/2 MWh system, four hours of discharge at a different current densities. This battery is discharged at rated current density, which will vary the power from 9:15-13:00 where peak demand is most probable.

The battery is recharged every night at rated power to ensure the state of charge is at 85% before 9:15 the next day. The battery was run from 10% to 85%. Two months where chosen for studying the battery the month of July (which accounts for the lowest demand) and the month of February since its statistically the coldest month in Victoria BC [69]. The model was run at different temperatures where there is temperature control available. Assuming the university has an average temperature of 20°C inside the building, at 5°C which would be the coldest average temperature for Victoria and an extreme scenario in which the temperature would reach 50°C.

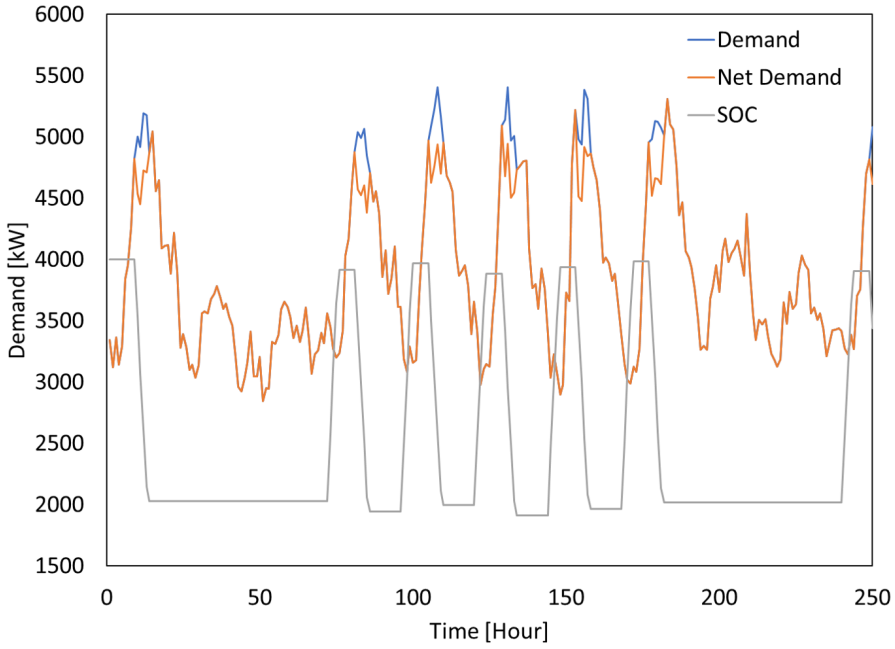

Figure 5.5: One week of the "Scheduled dispatch" strategy for the month of March .

5.3.2 Strategy 2: Dispatch on Peak Demands

Dispatch on peak demands assumes perfect foresight in each month and discharges the battery to smooth out a select number of peaks. Two sub-cases are tested; one where the 20 highest peaks are targeted, and a second where the 40 highest peaks are reduced. The battery is discharged at a rated capacity for the 15-minute duration of

each peak (and consecutive periods if they are also a peak.) Likewise, the battery is recharged during periods of lowest demand.

Figure 5.6 shows how the net load is impacted using a load duration curve where the load for each 15-minute period is ordered from highest to lowest for the entire month. The top 20 or 40 points in the demand are reduced and the energy demand will increase in the lowest demand when the battery is being charged.

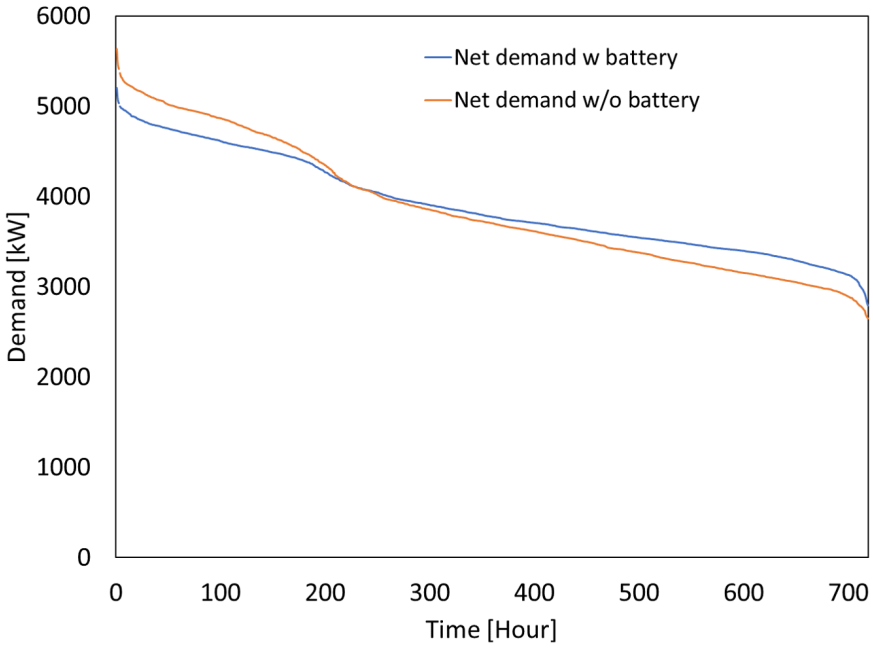

Figure 5.6: Gross demand and net demand for the month of February using dispatch strategy 2 where the top 20 peak loads are reduced with 500kW battery at a constant current density

5.4 Results

After running all the scenarios figure 5.7 illustrates the energy efficiencies of all them. The highest energy efficiency was achieved at $350A/m^2$ at $50°C$. However, to to provide a more realistic scenario for all the runs, the temperature chosen was 20° C instead of $50°C$ and the current density was lowered from $500A/m^2$ to $350A/m^2$. Stephenson used $500A/m^2$ [45] however they were using a small cell 2cm by 5 cm. The monthly savings which accrue due to demand charge reduction are partially offset by additional energy consumed by the battery. Given the impact of efficiency

on benefit, a sensitivity analysis was performed by varying the current density and the temperature. The monthly reduction in electricity bill was determined for each battery size, efficiency and dispatch strategy.

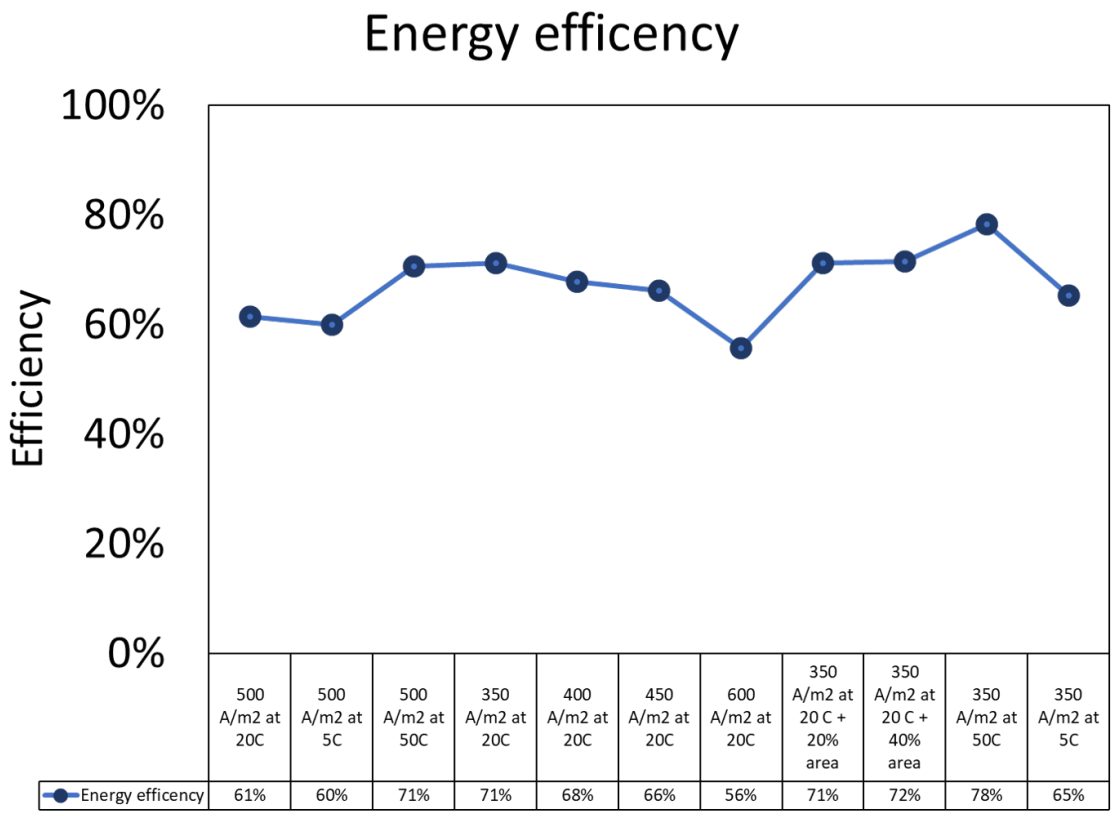

Figure 5.7: Comparison of energy efficiency the 500kW and 1MW battery at different temperatures and current densities

5.4.1 Scheduled Dispatch

For the scheduled dispatch strategy the results are presented below:

Figure 5.8 shows expected monthly bill reductions for some scenarios. In some months the battery reduces the monthly bill. However, the scheduled dispatch can lead to small or even negative benefits in other months. This occurs because either the peak demand was missed or the peak demand saved by using the battery was not sufficient compared to the increase in energy demand. For this strategy, the 500 kW/2 MWh battery running at \$350 A/m^2 at $50°C$ was the scenario that the battery will save the most in a month, \$5,345 in February. Nevertheless, to maintain

a temperature of $50°C$ there will be a cost associated with thermal management, which is something that this chemistry claims is not needed. Therefore, looking at the same current density but with an ambient temperature, the savings for February are $3,050 giving an average saving of $22,000 per year, which includes the losses in March, November, and December.

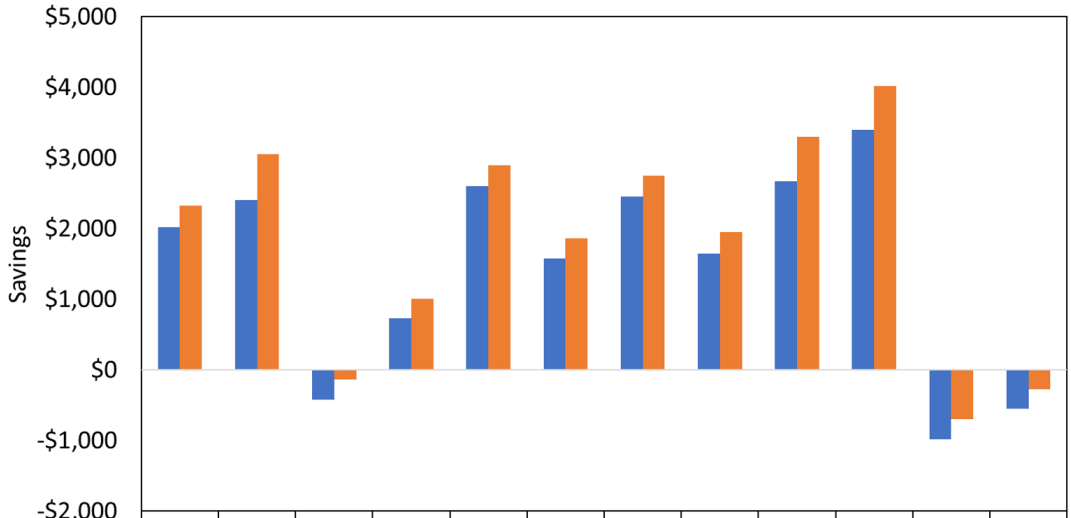

	Jan	Feb	Mar	April	May	June	July	Aug	Sept	Oct	Nov	Dec
500 A/m2 at 20C	$2,023	$2,400	-$416	$729	$2,597	$1,581	$2,455	$1,649	$2,665	$3,401	-$983	-$552
350 A/m2 at 20C	$2,326	$3,050	-$139	$1,006	$2,900	$1,858	$2,745	$1,953	$3,299	$4,022	-$693	-$275

Figure 5.8: Comparison of different current densities, different temperatures and area need using scheduled dispatch at the 500 kW and 1 MW.

5.4.2 Dispatch on peak demands

Using the same current density ranges as before, the 500 kW/2MWh battery is dispatched assuming perfect foresight for monthly demand so that a desired number of peaks can be reduced. Scenarios for top 20 and 40 monthly peak demands are here examined.

20 Peaks

For the dispatch strategy the highest 20 peaks of the month were selected and the results are presented below:

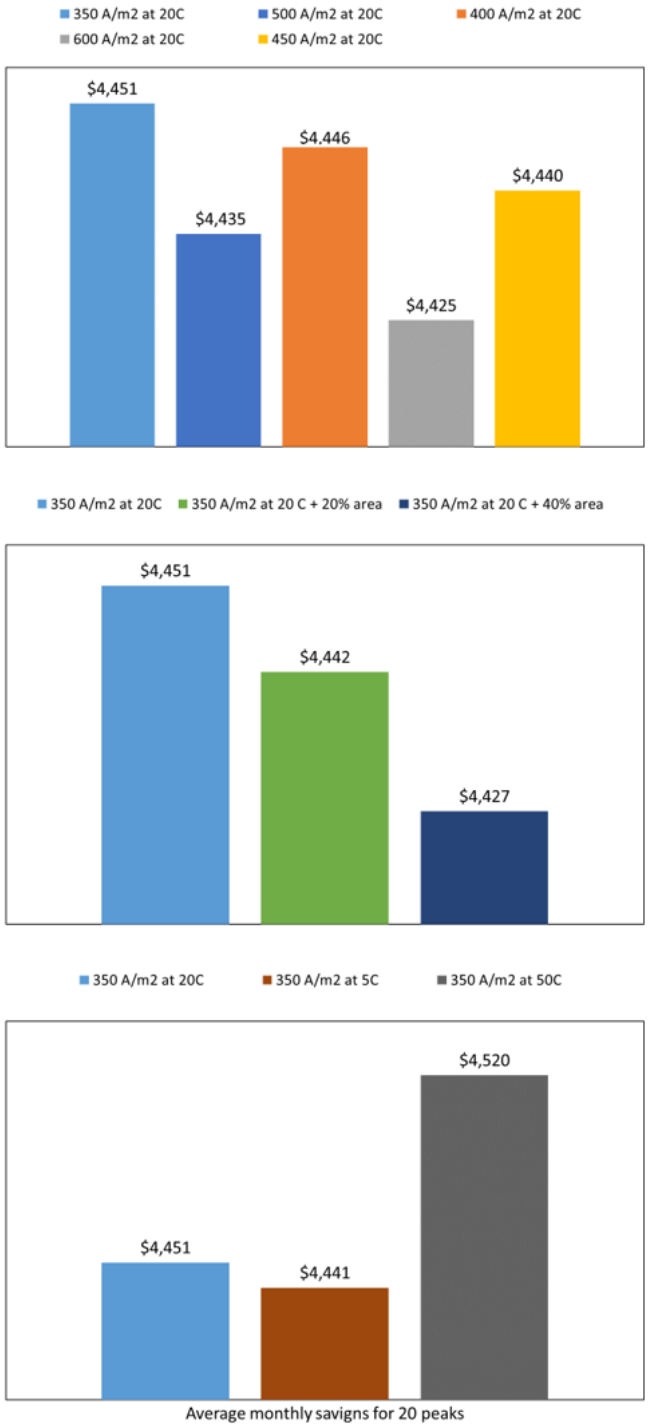

Figure 5.9: Average savings of the 500kW shaving the 20 highest peaks of each month, first plot have at different current densities, second plot different areas and third plot at different ambient temperatures

Figure 5.9 shows the average monthly bill reductions for the scenario system where the top 20 monthly peaks are reduced. With 500 kW/ 2 MWh, looking at the figure for the same scenario as the previous dispatch strategy it appears to be the best scenario . With $350A/m^2$ at $20°C$ in which there is no temperature control assuming that the battery will be placed indoors, the average saving per year is around $57,200.

The battery was run at multiple scenarios as figure 5.9 shows. In the first plot shows different current densities from $350A/m^2$ to $600A/m^2$ the second plot shows different areas in which the area calculated for the 500 kW/4MWh was increased by 20% or by 40% and the third plot different ambient temperatures.

40 Peaks

For the dispatch strategy in which the highest 40 peaks of the month the results are presented below:

Figure 5.10 shows the average monthly reductions for each battery system where the top 40 monthly peaks are reduced. With 500 kW/ 2 MWh with this strategy, the best scenario is $350A/m^2$ at $20°C$ in which there is no temperature control assuming that the battery will be placed indoors here the average saving per year is around $60,800.

Similar to 20 peaks, figure 5.10 shows in the first plot different current densities from $350A/m^2$ to $600A/m^2$, the second plot shows different areas in which the area calculated for the 500 kW/4MWh was increased by 20% or by 40% and the third plot different ambient temperatures of $5°C$.

5.4.3 Dispatch Summary

The savings per year for each dispatch strategy and battery capacity are summarized in Table 5.3. Dispatch strategies using knowledge of load dynamics outperform simply scheduled dispatch by up to three times.

Table 5.3: Saving summary table of different dispatch strategies

Dispatch Strategy	Battery size	Savings(per year)
Scheduled Dispatch	500kW/2MWh	$ 22,000
Peak on demands (20)	500kW/2MWh	$ 57,200
Peak on demands (40)	500kW/2MWh	$ 60,800

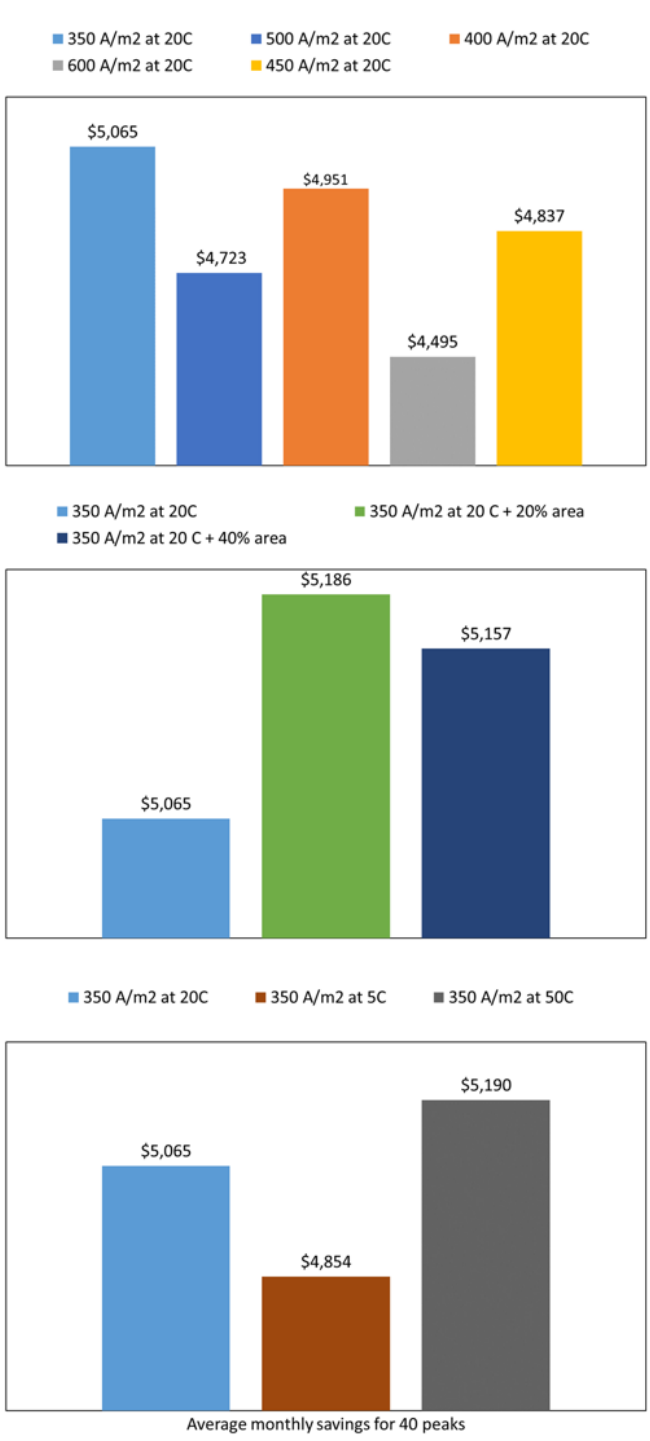

Figure 5.10: Average savings of the 500kW shaving the 40 highest peaks of each month, first plot have at different current densities, second plot different areas and third plot at different ambient temperatures

Crawford [70] determined the total energy storage system cost with a robust performance-based cost model for multiple RFB chemistries. The Fe/V system indicates that costs $ 600 kW/h while the All-vanadium is $ 350 kW/h. This means that a Fe/V battery of 2MWh result into a capital cost of around $ 1,200,000. A RFB is estimated to have from 10,000 - 14,000 cycles [71, 72]. For the scheduled dispatch 260 cycles per year are used, this translates into 38 years of life span. If the battery is used with the scheduled dispatch it will require 55 years to have profits and this assumed a 2% of degradation each year. If the 20 highest peaks are shaved it would require 20 years to recover the capital cost but the system will be in the first half of its life span. To be a profitable investment the cost per kW/h for the Fe/V has to be 200 $ kW/h, using the scheduled dispatch strategy, while if it implemented the 20 highest peaks the battery cost could increase to $350 kW/h. Figure 5.11 shows the savings per year per dispatch and current density used vs the saving and on the right axis the cost of kW/h of the battery.

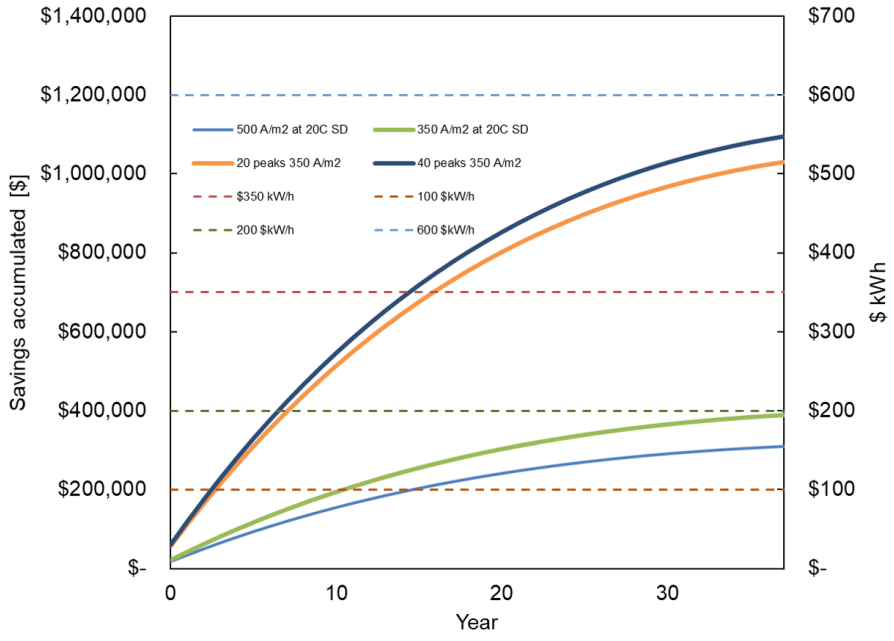

Figure 5.11: Savings per year with 2% degradation for every year. The cost of kW/h is the right axis

In figure 5.11 it is shown the two dispatch strategies at $500 A/m^2$ at $20°C$ with SD (Schedule Dispatch) and $350 A/m^2$ at $20°C$ with SD, as well as the dispatch of the highest 20 and 40 peaks with a current density of $350 A/m^2$ at $20°C$. On the right axis the cost per kW/h of the battery is shown while on the left axis is shown the

cumulative savings per technology used, and on the x axis it is shown the years of use of the battery. Sample of the code for both dispatch strategies can be found in the appendix C.2 and C.3.

5.5 Limitations

The scheduled dispatch strategy was chosen because there is an 87% probability that the peak demand will occur between 9:00 am to 1:00pm. However, while this was the case for the years of 2018-2019, it doesn't take into consideration any variations, such as vacations of the university, statutory holidays or if there is a pandemic. The only factor considered was whether it is a weekday or the weekend. This illustrates a big limitation of this dispatch strategy as the human factor plays a big role as to when the peak demand will occur. As a the result there is a possibility that the peak will not occur during the established hours and the electricity bill will be greater than if no battery was installed.

For the 20th and 40th highest peaks, the 20 highest peaks of 5 hours of continuous dispatch were chosen and that all peak occurred simultaneously. However historical data shows, the highest peaks of the month are not likely to be sustained for more than 2 hours. Nevertheless this strategy assumes that a perfect prediction of the demand is as important as understanding the performance of the battery.

5.6 Forecasting

Optimizing the preferred storage system capacity and energy requires some defined dispatch logic. Likewise, the effective use of storage implies knowledge of the dynamics of demand. In an ideal situation, the demand profile is known exactly in advance (i.e. with perfect foresight) and the storage system is optimally sized and operated to maximize benefits. With a demand pattern that has variability and uncertainty, rarely does this perfect foresight exist. Instead, some form of forecasting is used to predict the future at a particular time. Two methods of forecasting are considered here: linear regression (LR) and auto-regressive integrated moving average (ARIMA).

- Linear Regression: The linear regression approach correlates changes in specified independent variables to a linear change in a dependent variable. The

following parameters are considered to explain independent variables correlated to changes in electricity demand:

  - Time
  - Day of the week
  - Previous hour temperature deviation from 20 C
  - Month

- ARIMA: Auto-Regression-Integrated-Moving-Average takes into account the previous values in a time-series. Therefore, only the demand profile is needed to fit an ARIMA model. ARIMA is a light machine learning method in which changing parameters define the number of lagged observations, the amount of averaging. The size of the moving average window will determine the model predictions. 20% of the demand data was used to train the model with the remaining 80% used to test it.

Figure 5.12 shows the LR and ARIMA model predictions compared to the actual demand for a single day in September. For this day, the ARIMA model appears to better predict the actual demand. This result was obtained using p=2, d=1, and q=1 where p is the number of autoregressive terms, d is the number of nonseasonal differences, and q is the number of lagged forecast errors in the prediction equation. Although it is used in the literature, ARIMA is not considered the best forecasting method for electricity demand [73].

Sample of the Lineal and ARIMA code can be found in appendixC.4

5.7 Discussion

Dispatch using a predefined schedule could save $22,000 per year with the 500kW / 2MWh battery. This benefit is reduced relative to optimal dispatch due to the demand peak being missed, or because the additional energy for charging surpasses the savings in demand. Assuming demand can be predicted, dispatch strategy 2 targets the 20 or 40 highest peaks and is a more effective method to reduce the monthly electricity bill. Savings of up to $ 60,000 per year are realized with the 500kW/2MWh battery. However, demand can not be predicted with 100% accuracy using typical methods such as linear regression (76% accuracy).

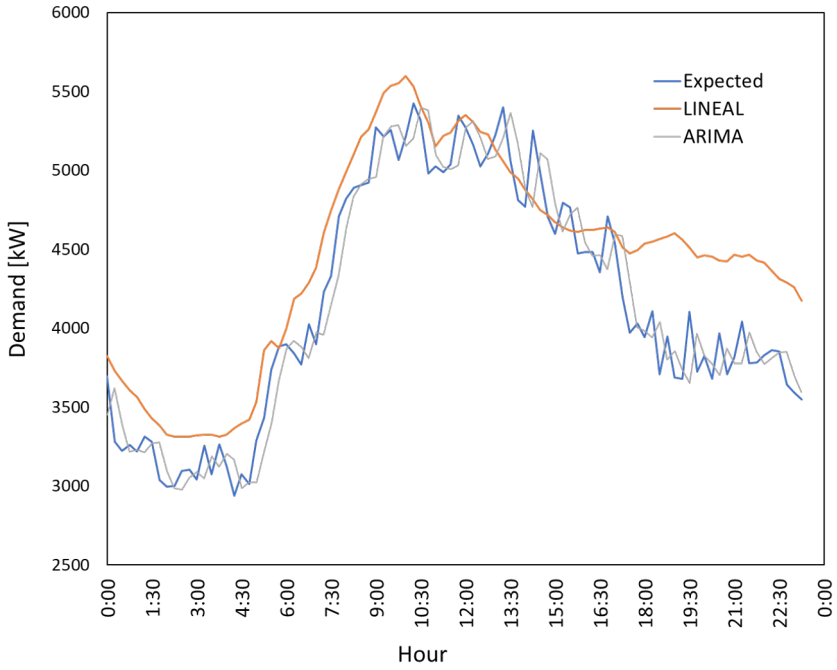

Figure 5.12: Comparison for forecasting using the methods OLS (linear regression) vs ARIMA

Further methods are being explored to predict the demand of the university. The advantages of the LR is that it takes into consideration multiple factors such as the temperature outside, the day of the week, the month, and the hour, giving it more flexibility to predict the demand for an isolated point, unlike the ARIMA which requires previous data to predict the next point.

As was mentioned, institutional demand data comes from one transformer only. It is assumed that the battery can mitigate demand on all three transformers but this may not be possible. To accurately size, dispatch, and locate storage, data for the other two transformers are needed. It may be that three smaller batteries located on each transformer are the preferred configuration. Further work is needed to develop forecasting algorithms and optimize dispatch, power capacity, and energy stored.

In this chapter previously discussed model was analysed and implemented into the electrical system of the University of Victoria using the output power to deploy the battery using different dispatch strategies, comparing different scenarios and obtaining the potential savings of each dispatch strategy. The next chapter will have a summary of the whole work and the results of the model. It will also discuss avenues of future research for the further development of the concept.

Chapter 6

Conclusions

This chapter will include a summary of the whole work and suggestions for the research. Summarizes the key findings of the study and provides recommendations for both experimental and theoretical studies to be conducted in future.

6.1 Summary

Since the electricity demand is increasing due to a rising global population, there is a need to generate more electricity. However, there is a desire to substitute our heavy fossil fuel grid, with different types of renewable energy. These new and emerging sources are being installed in the current electrical grids.Despite their advantages, renewable energy has a major drawback, all renewable energy (except for nuclear) with its intermittent nature creates an imbalance in supply and demand. Energy Storage is a much-needed technology for our current electrical grid, and offers many other advantages. Multiple chemistries have been explored through the years but the All-Vanadium is the most popular among the industry and in the research.

In an attempt to overcome the limitations that the All-Vanadium RFB, (explained in chapter 2), PNNL developed the Fe/V chemistry to address some of its limitations[10, 39]. This work presented a 0D model for the Fe/V chemistry similar to [45], as well as the thermal factor which is known to be a limitation to multiple RFBs [48, 66, 67] when it was coupled to simple dispatch strategies where the intention was to obtain the economical benefit of adding an RFB to the current electrical arrange of the University of Victoria. Also discussing the sizing of the battery and suggesting some optimal conditions for the battery. When modeling the electrochemical part of

the RFB, one of the major roadblocks is the conductivity of the electrolyte since the conductivity has multiple factors which need to be considered and the dilute solution theory does not provide them. Further discussion can be found at appendix B

6.2 Results and Findings

Sizing the battery was one of the expected results, however the optimal size was not modeled. The size was chosen arbitrarily to provide a clear idea of the potential savings if an RFB was installed at the university facilities.By having a fixed current density through charging and discharging, the optimal operation range of SOC was from 10% - 85%(as per suggested in the literature [59, 39, 10, 35]). Also when charging the battery the efficiencies are around 71% which is slightly lower than reported in [10, 39], nonetheless, discharging with a fixed current density varied from 78% to 60% in some cases. These are significantly different results from the literature and it's presumed that by including the thermal model discharging efficiencies were affected. A bigger cell, in terms of the area used for the reaction, does not necessarily benefit or reduce the electricity cost which is one of the objectives of installing an RFB at the University facilities

Previous research [39, 45, 67] suggest running the system at $500 A/m^2$. However, the results show that the system works better at lower current at $350 A/m^2$. The efficiency is 71 % by implementing the simple dispatch strategy (explained in chapter 5) suggests that there could be up to $ 22,000 dollars per year saved.

With the prices from Crawford [70] \$600 kW/h from 2015 and the scheduled dispatch strategy, the 500kW/ 2MWh will not be good investment as it requires over 50 years to be profitable. However, the prices of RFB have significantly dropped since 2015. There is no current price as in $\$kW/h$ for the Fe/V chemistry. Nevertheless, the analysis showed that to be profitable the cost of kW/h should be less than $\$200 kW/h$. If the battery could reduce their cost to \$350 kW/h and if the strategy used to reduce the electricity is smooth the 20 highest peaks, the battery will be profitable after 15 years, with a battery life span of 38 years.

6.3 Recommendation and Future work

The battery size was not optimized as it was not part of the scope of this work, this could be a major work that could have more significant work, as the battery can

be either increase the power capacity or energy capacity. Looking at the university forecast from 2018- 2019 (as 2019-2020 had different power and energy needs due to the global pandemic). A battery with a power capacity between 500 kW to 1MW and a energy capacity between 2MWh to 3MWh should be sufficient to capture the highest peak of the month without increasing significantly the capital cost.

The flow rate of the cell stack has a fixed value, but it has been seen that hat the capacity increase, but the system efficiency decreases with increase of electrolyte flow rate at a constant current density [74]. With a flow control implemented in the system it has been reported an increase in efficiency from 3.5%[75] to 8%[74]. The geometry of the cell stack is another parameter that can be optimized as geometry impact the performance of the system [76, 77]. Further work is requires as 0D models requires data to be correlated to be considered accurate. The present work was based on data measured by [45] and [66].

Lastly, develop better tools to predict the demand of the university need to be carried out to increase the accuracy of the simulations. A coupled model could be implemented in which one model predicts the demand with a model that controls the battery to peak shave the demand of the university.

Appendix A

Standard potentials

The following table shows the standard potentials for each Red-Ox reaction described in this work.

Reaction	Potential	Reference
$Cr_2O_7^{2-} + 14H^+ + 6e^- \rightleftharpoons 2Cr^{3+} + 7H_2O$	$E^\circ = 1.33V$	[78]
$O_2 + 4e^- + 4H^+ \rightleftharpoons 2H_2O$	$E^\circ = 1.23V$	[79]
$[VO_2]^+ + 2H^+ + e^- \rightleftharpoons [VO]^{2+} + H_2O$	$E^\circ = 1.0V$	[20]
$Fe^{3+} + e^- \rightleftharpoons Fe^{2+}$	$E^\circ = 0.77V$	[7]
$O_2 + 4e^- + 2H_2O \rightleftharpoons 4OH^-$	$E^\circ = 0.40V$	[79]
$[VO]^{2+} + 2H^+ + e^- \rightleftharpoons V^{3+} + H_2O$	$E^\circ = 0.34V$	[20]
$2H^+ + 2e^- \rightleftharpoons 2H_2$	$E^\circ = 0.0V$	[80]
$Fe^{3+} + 3e^- \rightleftharpoons Fe$	$E^\circ = -0.04V$	[7]
$V^{3+} + e^- \rightleftharpoons V^{2+}$	$E^\circ = -0.26V$	[20]
$Cr^{3+} + e^- \rightleftharpoons Cr^{2+}$	$E^\circ = -0.41V$	[7]
$Cr^{3+} + 3e^- \rightleftharpoons Cr$	$E^\circ = -0.74V$	[78]
$Zn^{2+} + 2e^- \rightleftharpoons Zn$	$E^\circ = -0.76V$	[81]
$Cr^{2+} + 2e^- \rightleftharpoons Cr$	$E^\circ = -0.91V$	[78]
$V^{2+} + 2e^- \rightleftharpoons V$	$E^\circ = -1.13V$	[78]

Table A.1: Standard potentials Red-Ox

A mixed electrolyte system was used by [21] in which states that if the electrolytes become unbalanced or if the osmotic solvent transfer occurs it is easily countered by remixing the electrolytes. Operating the cell with mixed electrolyte, however, leads to a reduction in open circuit voltage, increased electrolyte costs, and possible complications over a large number of charge-discharge cycles which may limit its commercial viability and industrial applicability.

Using Fe in place of the higher potential V species avoids the limited upper-temperature stability problem and reduces cost as V is approximately 10x the cost of iron. One paper [10] employs chemistry with a mixed electrolyte system, if the electrolytes become unbalanced or if the osmotic solvent transfer occurs it is easily countered by remixing the electrolytes [12]. In the mixed electrolyte patent in which Vanadium is present in both electrolytes, positive and negative, the hydrogen evolution is claimed to be neglected, however as both reactants could potentially develop hydrogen gas one possibility in the mechanism is that the hydrogen evolution has higher potential thus the energy required to produced hydrogen is higher and having the Fe in place with a lower potential the energy will go into Fe^{2+} instead to produce hydrogen. The V^{4+} and V^{5+} works as a catalyst for the Fe side.

Appendix B

Electrolyte conductivity

The dilute-solution approximation is used as the bulk of the electrolyte is water. All ion species have the velocity of the bulk and no interaction between the species occurs. This assumption is to be questioned because the ion concentration is very high and therefore at the upper boundary of the theory.

The use of activities would be the more correct method, but they were unavailable for the considered electrolyte and are not used in this study[33]. The conductivity of the electrolyte is commonly calculated with the Nernst-Planck equations with Faraday's law derivation [25]

$$\kappa = \frac{F^2}{RT} \sum_i z_i^2 \times D_i^{eff} \times c_i \tag{B.1}$$

The calculated conductivity is several times higher than the measured conductivity's found in multiple papers [25, 64]. The Nernst-Planck equation is no suitable to describe the ionic conductivity of the electrolyte, thus this parameter is assumed to be a limiting factor, the divergence so high is not acceptable for any simulation as this would underestimate the influence of the electrolyte conductivity on the cell performance. Instead multiple studies [11, 35] suggest using linearized functions based on measured conductivity as a function of the SOC.

Stephenson[45] found that the intrinsic diluted theory overestimates the conductivity roughly 6.5 times compare to experimental data, however using the Bruggeman relationship reduces the effective conductivity and results in good agreement, between the model and data. Although the resulting average conductivity needed in the model to match the electrolyte losses of the electrode was three times higher than experimental, physically the conductivity of the electrolyte is analogous to the movement of the proton since this type of chemistry is moving a proton compared to an electron,

the proton movement is too slow (compared with an electron). It is believed that the entire electrode thickness is not utilized, most of the electrochemical reaction is believed to take place within one-half of the tested electrode thickness, it is also believed that the electrodes are thicker than electrochemical needed.

Viswanatha [11] found the conductivity of the electrolyte as a function of the concentration of reactant species and proton concentration was determined by semi-empirical principles using relationships from dilute solution theory but ultimately matching electrolyte ohmic losses at high flow rates (2.0 mL min/cm^2 or greater) by varying the electrolyte conductivity in the model. Model conductivities needed to match electrolyte ohmic losses were compared with measured conductivity and found to be 4 times larger.

To accommodate this discrepancy it is believed that not all the electrode is reacting and as such a thinner electrode volume is being utilized, which is expected to be the case when the felt electronic conductivity is much higher than the electrolyte conductivity and has been verified experimentally [45, 11].

One of the linearized relations is described in [34]. The way the conductivity of the electrolyte is being calculated of a two-dimensional model is :

$$\sigma_e = 17.69 + 7.50 \times SOC(negative) \tag{B.2}$$

$$\sigma_e = 27.67 + 13.36 \times SOC(positive \tag{B.3}$$

These equations were developed by creating an empirical model based on experimental conductivity data that has been shown to provide accurate predictions, with an average error of 0.77%, of the conductivity of the positive half-cell electrolyte as a potential state-of-charge detection too.

Corcuera and Skyllas-Kazacos derived another linearized relation that involves the temperature as well as the SOC of the electrolyte.

Coefficient	Positive half cell	Negative half cell
A	1.8	0.7050
B	93.5030	55.0420
C	4.6713	2.6176
D	172.07	122.37

$$\kappa = (A \times T + B) \times SOC + (C \times T + D) \tag{B.4}$$

Where T is the temperature in $Celsius$ and SOC is the state of charge and κ is the conductivity of the solution in $mS/cm^{-}1$

The conditions of the electrolyte is 1.5 M in the positive side and negative (All vanadium), the initial proton concentration on the positive is 6M and 4.5M in the negative [65]

$$\sigma_e = 35.716 + 7.699 \times SOC(negative) \tag{B.5}$$

$$\sigma_e = 43.763 + 12.251 \times SOC(positive) \tag{B.6}$$

It was performed a small sensitivity analysis on the conductivity of the electrolyte in which the conductivity of the electrolytes was varied from -20% to 20% because the conductivity of the electrolyte is a linear equation the variation is linear at an ambient temperature of $20°C$.

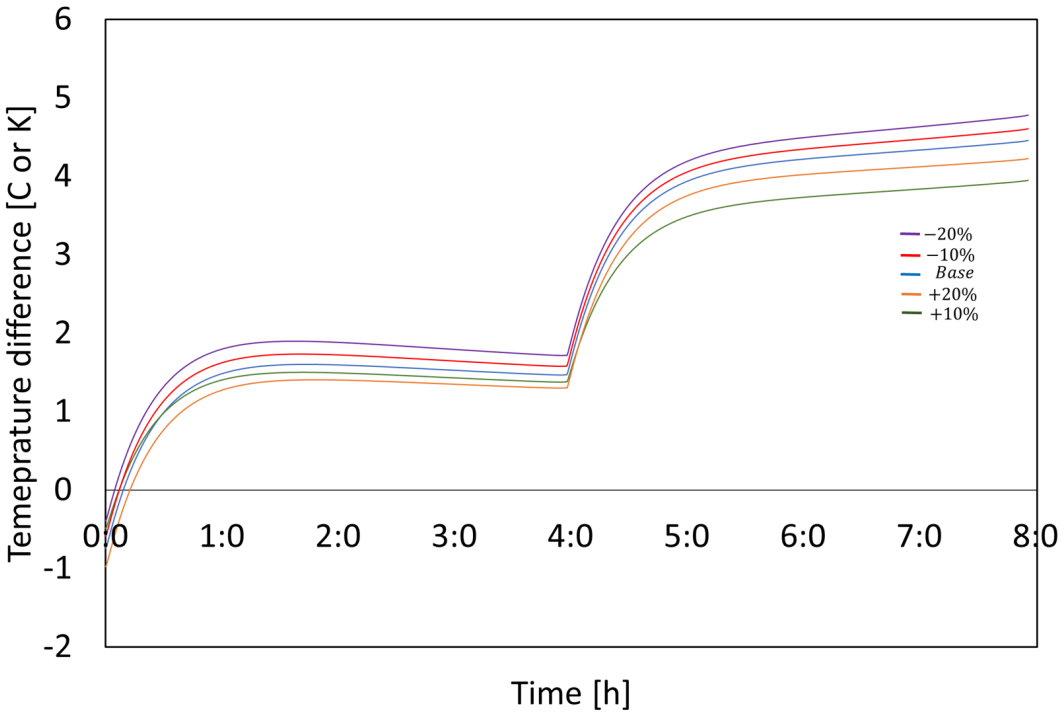

Figure B.1: Sensibility analysis; conductivity of the electrolyte varying from -20% to +20%.

Appendix C

Python codes

C.1 Thermo-electrochemical model

```
#Libraries needed
import math
import numpy as np
import matplotlib.pyplot as plt
import plotly.express as px
import plotly.graph_objects as go
import pandas as pd

##Inputs##
s=0#Area increased in %
t=4 *3600 #4 hours
v=48 # 48 volts
P_max=500000/(1-(s/100)) # 500kW
E_max=2000000/(1-(s/100))  #2MWh
N=48
rhof=1182 #Kg/m3-FeCl2
rhov=1158 #Kg/m3 VCl3
FM=126.751 #g/mol
VM=157.3# g/mol

Eo_p=0.77 #Fe Reference potential for positive electrode [V]
```

```
Eo_n=-0.255#V Reference potential for negative electrode [V]
Eo=Eo_p-Eo_n # [V]
L_m=5.08E-5 #Thickness of membrane [m]
eps=0.929 #Porosity of the electrode
a=39000 #Specific surface are [1/m]
kn_r=8.7E-6 #Reference rate constant for negative electrode [m/s]
kp_r=1.6E-5 #Reference rate constant for positive electrode [m/s]
Id=500 #Applied charge current density [A/m2]
Ic=-Id #Applied discharge current density [A/m2]
Dv2=2.4E-10 #Diffusion coefficient V2+ [m2/s]
Dv3=2.4E-10 #Diffusion coefficient V3+ [m2/s]
Df2=3.95E-10 #Diffusion coefficient Fe2+ [m2/s]
Df3=3.32E-10 #Diffusion coefficient Fe3+ [m2/s]
Dhso=1.4E-10 #Diffusion coefficient HSO4- [m2/s]
Dh=9.31E-9 #Diffusion coefficient H+ [m2/s]
cv_0=1600 #Intial vanadium concentration both electrodes [mol/m3]
cf_0=1600 #Initial iron concentration bothelectrodes [mol/m3]
chcl_0=2300 #Initial HCL concentration both electrodes [m/m3]
SOC_c0=0.025 #Beginning state of charge for charge
SOC_d0=0.975 #Beginning state of charge for discharge
zv2=2 #Charge number for V2+
zv3=3 #Charge number for V3+
zf2=2 #Charge number for Fe2+
zf3=3 #Charge number for FE3+
Qc=20000 #Volumetric flow rate [mL/min]
Q=Qc*1.666667*(10**-8) #m3/s
gamma=2 #Pre Bruggeman factor
theta=2 #Non-ideal reactor factor
alpha=1.5 #Bruggeman exponent
lam=22
s_e=370 #Conductivity of electrolyte
F=96485.3365 #Faraday's constant [C/mol]
R=8.314 #Constant Gas [J/(K mol)]
#### Thermal variables needed####
S_v2=-130 #J/molK
```

```
S_v3=-230 #J/molK
S_f2=-107.1 #J/molK
S_f3=-280.3 #J/molK
H_v2=-226000#J/mol
H_v3=-259000#J/mol
H_f3=-50200#J/mol
H_f2=-92500#J/mol
G_v2=-218 #J/mol
G_v3=-251.3 #J/mol
G_f3=-16.7 #J/mol
G_f2=-91.5#J/mol
cpf=3498 #J/kgK- VANADIUM
rhof=1182 #Kg/m3-FeCl2
cpv=3200 #J/kgK - VANADIUM
rhov=1158 #Kg/m3 VCl3
#A= L_w*L_h*10 # Area of the Electrode
N=48 # Number of cells
h=5 # Natural convections W/(m2K)
l=22 #Lamda , water content assumed to be saturated
T_ref=295
CP=3200 #Data from paper (the whole system)
RHO=1354 # Data from paper (The whole system)
n=1 #Number of electrons per mol

#Volume calculation#
Vc=(E_max*3600)/(N*n*cv_0*F*Eo)

#Area needed##
A_tot=P_max/(N*Eo*Id)
cell=A_tot/N

L_w=cell**0.5 # Width of electrode [m]
L_h=cell**0.5 # Height of electrode [m]
L_x=0.00425 #Thickness of electrode [m]
```

```
SOC_0=1
t=4*3600
SOC_=[]
cf2=[]
cf3=[]
cv3=[]
cv2=[]
for t in range(0,t,900):
    SOC_in=SOC_0-(t*A_tot*Id)/(cv_0*F*Vc)
    dSOC=Id*cell/(cv_0*Vc*n*F)
    SOC_avg=SOC_in-dSOC/2
    SOC_.append(SOC_avg)
    cf2_avg=cf_0*(1-SOC_avg)
    cf3_avg=cf_0*SOC_avg
    cv2_avg=cv_0*SOC_avg
    cv3_avg=cv_0*(1-SOC_avg)
    cf2.append(cf2_avg)
    cf3.append(cf3_avg)
    cv2.append(cv2_avg)
    cv3.append(cv3_avg)


P_p=0 #Pump power taken from SANSO PMD-641 where 12 Watts are with
↪  a flux of ~3.33x10^-4 m3/s

#coefficients condcutivity electrolyte from Sankyzos pape
A_e=0.705
B_e=55.042
C_e=2.6176
D_e=122.37

Tc=20*N/1000 #m of thickness
As=cell*2+Tc*((cell)**0.5)*4

S=S_f3+S_v2-S_v3-S_f2
```

```
# ## SOC  time dependent
# # Battery 500kW 4MWh

ta=20
Ac=A_tot
a=4*3600
Rc=[]
h=10
SOC_c=[]
T_in=[]
Ec_cell=[]
Ed_cell=[]
Ed_cell_rev=[]
Ec_cell_rev=[]
time=[]
cnt=[]
T_c=[]
ct=[]
per_c=[]
pentro_c=[]
ele=[]
err=0.0001
SOC_0=0.0
l=22 #Lamda , water content assumed to be saturated
#T_in2=ta+273 #[K] inlet temperature
T_air=ta+273
f=rhof*cpf*Q
v=rhov*cpv*Q
w=Vc*cpf*rhof
H=h*As
T_ref=295
count=0
count2=0
```

```
#obtaining constant c1#
#At t=0 T_stack_c=T_out1_c=T_in_c=T_ambient
#Remember T_stack is assumed to be the same at the outlet of the
↪  tanks thus
#stack temperature and outlet temperature are the same
cond=0
kn=kn_r*math.exp((-F*Eo_n/R)*((1/T_ref)-(1/T_air)))
kp=kp_r*math.exp((F*Eo_p/R)*((1/T_ref)-(1/T_air)))
E_shift=0.00038*T_air+0.073

l=22 #Lamda , water content assumed to be saturated
s_m=(0.5136*l-0.326)*math.exp(1268*((1/303)-1/T_air))
#s_e=F**2/(R*T_stack_c[t])* sum([zi[i]**2*(Di[i]*eps**(3/2))*ci[i]
↪  for i in range(len(zi))])
#k=s_e*(1+(0.0171*(T_stack_c[t]-296)))*1.2#4.12
↪  #s_e*(1+(0.0171*(T_stack_c[t]-296)))*1.2
k=((A_e*(T_air-273)+B_e)*SOC_avg+C_e*(T_air-273)+D_e)/10

            ###CHARGING###
IRm_c=Ic*L_m/s_m  ## LOSSES IN THE MEMRANE
IRi_c=2*Ic*(L_x/(k*(1+cond/100))) ## LOSSES IN THE ELECTROLYTE
nc_n=-2*R*T_air/F*math.asinh(Ic/(2*F*eps*a*L_x*kn*
math.sqrt(cv2_avg*cv3_avg)))
nc_p=2*R*T_air/F*math.asinh(Ic/(2*F*eps*a*L_x*kp*
math.sqrt(cf2_avg*cf3_avg)))
nc=nc_p-nc_n  ## LOSSES KINETIC OVERPOTENTIALS
Ec_cell_rev1=(Eo)+(R*T_air)/F*math.log((cv2_avg*cf3_avg)/
(cv3_avg*cf2_avg))-E_shift
Ec_cell1=Ec_cell_rev1-IRi_c-IRm_c-nc

           ##### Thermal model ####
S=S_f3+S_v2-S_v3-S_f2
P_entro=Ic*Ac*T_air*S/(F)# Watts
R1=IRi_c # Volts
R2=IRm_c# Volts
```

```
R_eq=R1+R2+nc# Volts
P_r= Ic*Ac*R_eq# Volts*Amps/m2*m2 = V*A = Watts
c1=T_air-(P_entro/(f+H+v)+(f*T_air)/
(f+H+v)+(T_air*v)/(f+H+v)+P_p/(f+H+v)+P_r/(f+H+v))-
((T_air*H)/(f+H+v))

###CHARGE###

T_out1_c=[ta+273+2]*a
T_out2_c=[ta+273]*a
T_stack_c=[ta+273]*a
T_in_c=[ta+273]*(a) #[K] inlet temperature

#-4.624052328915854
for t in range(10,a-100):
    SOC_in=SOC_0-(t*Ic*L_h*L_w*N)/(cv_0*F*Vc)
    dSOC=Ic*cell/(cv_0*Vc*n*F)
    SOC_avg=SOC_in-dSOC/2
    cf2_avg=cf_0*(1-SOC_avg)
    cf3_avg=cf_0*SOC_avg
    cv2_avg=cv_0*SOC_avg
    cv3_avg=cv_0*(1-SOC_avg)
    ci=[cf2_avg,cf3_avg,cv2_avg,cv3_avg]
    Di=[Df2,Df3,Dv2,Dv3]
    zi=[zf2,zf3,zv2,zv3]
    count=0

    while abs(T_out1_c[t]-T_stack_c[t])>err:# This while is used to
    ↪  converge , since it was guessed the inside temperature of
    ↪  the stack
        T_stack_c[t]=T_out1_c[t]
        kn=kn_r*math.exp((-F*Eo_n/R)*((1/T_ref)-(1/T_stack_c[t])))
        kp=kp_r*math.exp((F*Eo_p/R)*((1/T_ref)-(1/T_stack_c[t])))
        E_shift=0.00038*T_stack_c[t]+0.073
```

```
        s_m=(0.5136*l-0.326)*math.exp(1268*((1/303)-1/T_stack_c[t]))
        #s_e=F**2/(R*T_stack_c[t])*
        ↪  sum([zi[i]**2*(Di[i]*eps**(3/2))*ci[i] for i in
        ↪  range(len(zi))])
        #k=s_e*(1+(0.0171*(T_stack_c[t]-296)))*1.2#4.12
        ↪  #s_e*(1+(0.0171*(T_stack_c[t]-296)))*1.2
        k=((A_e*(T_out1_c[t]-273)+B_e)*SOC_avg+C_e*
        (T_out1_c[t]-273)+D_e)/10

            ###CHARGING###
        IRm_c=Ic*L_m/s_m  ## LOSSES IN THE MEMRANE
        IRi_c=2*Ic*(L_x/(k*0.8)) ## LOSSES IN THE ELECTROLYTE
        nc_n=-2*R*T_stack_c[t]/F*math.asinh
        (Ic/(2*F*eps*a*L_x*kn*math.sqrt(cv2_avg*cv3_avg)))
        nc_p=2*R*T_stack_c[t]/F*math.asinh
        (Ic/(2*F*eps*a*L_x*kp*math.sqrt(cf2_avg*cf3_avg)))
        nc=nc_p-nc_n  ## LOSSES KINETIC OVERPOTENTIALS
        Ec_cell_rev1=(Eo)+(R*T_stack_c[t])/
        F*math.log((cv2_avg*cf3_avg)/(cv3_avg*cf2_avg))-E_shift
        Ec_cell1=Ec_cell_rev1-IRi_c-IRm_c-nc

           ##### Thermal model ####
        S=S_f3+S_v2-S_v3-S_f2
        P_entro=-Ic*Ac*T_stack_c[t]*S/(F)# Watts
        R1=IRi_c # Volts
        R2=IRm_c# Volts
        R_eq=R1+R2+nc# Volts
        P_r= Ic*Ac*R_eq# Volts*Amps/m2*m2 = V*A = Watts
        T_out1_c[t]=((T_air*H)/(f+H+v))+c1*math.exp(((-f*t)/w)-
        ((h*t)/w)-((v*t)/w))+P_entro/(f+H+v)+(f*T_in_c[t])/
        (f+H+v)+(T_in_c[t]*v)/(f+H+v)+P_p/(f+H+v)+P_r/(f+H+v)
        count=count+1 #simple counter so wee how many iterations it
        ↪  took to converge

##ACTUAL MODEL##
```

```
 #once it caluclated a temperature that temperature will be used
 ↪  for that step time to calcualte all the losses#
 T_in2_c=(T_stack_c[t]+T_in_c[t])/2 #Mix temperaute of the tank
 T_in_c[t]=T_in2_c

 kn=kn_r*math.exp((-F*Eo_n/R)*((1/T_ref)-(1/T_stack_c[t])))
 kp=kp_r*math.exp((F*Eo_p/R)*((1/T_ref)-(1/T_stack_c[t])))
 E_shift=0.00038*T_stack_c[t]+0.073
 cf2_avg=cf_0*(1-SOC_avg)
 cf3_avg=cf_0*SOC_avg
 cv2_avg=cv_0*SOC_avg
 cv3_avg=cv_0*(1-SOC_avg)
l=22 #Lamda , water content assumed to be saturated
 s_m=(0.5136*l-0.326)*math.exp(1268*((1/303)-1/T_stack_c[t]))
 k=((A_e*(T_stack_c[t]-273)+B_e)*SOC_avg+C_e*
 (T_stack_c[t]-273)+D_e)/10

     ###CHARGING###
 IRm_c=Ic*L_m/s_m  ## LOSSES IN THE MEMRANE
 IRi_c=2*Ic*(L_x/(k*0.8)) ## LOSSES IN THE ELECTROLYTE
 nc_n=-2*R*T_stack_c[t]/F*math.asinh
 (Ic/(2*F*eps*a*L_x*kn*math.sqrt(cv2_avg*cv3_avg)))
 nc_p=2*R*T_stack_c[t]/F*math.asinh
 (Ic/(2*F*eps*a*L_x*kp*math.sqrt(cf2_avg*cf3_avg)))
 nc=nc_p-nc_n  ## LOSSES KINETIC OVERPOTENTIALS
 Ec_cell_rev1=(Eo)+(R*T_stack_c[t])/
 F*math.log((cv2_avg*cf3_avg)/(cv3_avg*cf2_avg))-E_shift
 Ec_cell1=Ec_cell_rev1-IRi_c-IRm_c-nc
 count2=count2+1
   ##### Thermal model ####
 S=S_f3+S_v2-S_v3-S_f2
 P_entro=Ic*Ac*T_stack_c[t]*S/(F)# Watts
 R1=IRi_c  # Volts
 R2=IRm_c# Volts
 R_eq=R1+R2+nc# Volts
```

```
    P_r= Ic*Ac*R_eq# Volts*Amps/m2*m2 = V*A = Watts
    R_c=(IRm_c+IRi_c+nc)/Ic*N
    T_out3_c=((T_air*H)/(f+H+v))+c1*math.exp(((-f*t)/w)-
    ((h*t)/w)-((v*t)/w))+P_entro/(f+H+v)+(f*T_in2_c)/
    (f+H+v)+(T_in2_c*v)/(f+H+v)+P_p/(f+H+v)+P_r/(f+H+v)
    T_out2_c[t]=T_stack_c[t]

    Rc.append(R_c)
    SOC_c.append(SOC_avg)
    cnt.append(count)
    #Ed_cell.append(Ed_cell1)
    Ec_cell.append(Ec_cell1)
    Ec_cell_rev.append(Ec_cell_rev1)
    time.append(t)
    T_in.append(T_in2_c)
    T_c.append(T_out3_c)
    pentro_c.append(P_entro)
    per_c.append(P_r)
    ele.append(k)


### DISCHARGE###

a=4*3600
Rd=[]
T_out1_d=[T_c[-1]]*a
SOC_d=[]
Ed_cell=[]
Ed_cell_rev=[]
time=[]
cnt=[]
T_d=[]
T_out2_d=[T_c[-1]]*a
ct=[]
per_d=[]
```

```
pentro_d=[]
err=0.0001
SOC_0=1
T_stack_d=[T_c[-1]+1]*a
T_in_d=[T_in[-1]+2]*(a) #[K] inlet temperature
T_in2=[T_in[-1]+2]*(a) #[K] inlet temperature
T_air=ta+273
f=rhof*cpf*Q
v=rhov*cpv*Q
w=Vc*cpf*rhof
H=h*As
T_ref=295
count=0
count2=0

for t in range(10,a-100):
    SOC_in=SOC_0-(t*Id*L_h*L_w*N)/(cv_0*F*Vc)
    dSOC=Id*cell/(cv_0*Vc*n*F)
    SOC_avg=SOC_in-dSOC/2
    cf2_avg=cf_0*(1-SOC_avg)
    cf3_avg=cf_0*SOC_avg
    cv2_avg=cv_0*SOC_avg
    cv3_avg=cv_0*(1-SOC_avg)
    ci=[cf2_avg,cf3_avg,cv2_avg,cv3_avg]
    Di=[Df2,Df3,Dv2,Dv3]
    zi=[zf2,zf3,zv2,zv3]
    count=0

    while abs(T_out1_d[t]-T_stack_d[t])>err:
        T_stack_d[t]=T_out1_d[t]
        kn=kn_r*math.exp((-F*Eo_n/R)*((1/T_ref)-(1/T_stack_d[t])))
        kp=kp_r*math.exp((F*Eo_p/R)*((1/T_ref)-(1/T_stack_d[t])))
        E_shift=0.00038*T_stack_d[t]+0.073

            ###DISCHARGING###
```

```
    l=22 #Lamda , water content assumed to be saturated
    s_m=(0.5136*l-0.326)*math.exp(1268*((1/303)-1/T_stack_d[t]))
    IRm_d=Id*L_m/s_m ## LOSSES IN THE MEMRANE

    #k=s_e*(1+(0.0171*(T_stack_d[t]-296)))*1.2
    k=((A_e*(T_stack_d[t]-273)+B_e)*SOC_avg+C_e*
    (T_stack_d[t]-273)+D_e)/10
    #IRi_d=Id*(L_x/(eps**(3/2)*k)) ## LOSSES IN THE ELECTROLYTE
    IRi_d=2*Id*(L_x/(k*0.8))
    nd_n=-2*R*T_stack_d[t]/F*math.asinh
    (Id/(2*F*eps*a*L_x*kn*math.sqrt(cv2_avg*cv3_avg)))
    nd_p=2*R*T_stack_d[t]/F*math.asinh
    (Id/(2*F*eps*a*L_x*kp*math.sqrt(cf2_avg*cf3_avg)))
    nd=nd_p-nd_n ## LOSSES KINETIC OVERPOTENTIALS
    Ed_cell_rev=(Eo)+(R*T_stack_d[t])/
    F*math.log((cv2_avg*cf3_avg)/(cv3_avg*cf2_avg))-E_shift
    Ed_cell1=Ed_cell_rev-IRi_d-IRm_d-nd

       ##### Thermal model ####
    S=-S_f3-S_v2+S_v3+S_f2
    P_entro=Id*Ac*T_stack_d[t]*S/(n*F)# Watts
    R1=IRi_d # Volts
    R2=IRm_d# Volts
    R_eq=R1+R2+nd# Volts
    P_r= Id*Ac*R_eq# Volts*Amps/m2*m2 = V*A = Watts
    T_out1_d[t]=((T_air*H)/(f+H+v))+c1*(math.exp(((-f*t)/w)-
    ((h*t)/w)-((v*t)/w)))+P_entro/(f+H+v)+(f*T_in_d[t])/
    (f+H+v)+(T_in_d[t]*v)/(f+H+v)+P_p/(f+H+v)+P_r/(f+H+v)
    count=count+1

T_in_d[t]=(T_out1_d[t]+T_in_d[t])/2
kn=kn_r*math.exp((-F*Eo_n/R)*((1/T_ref)-(1/T_stack_d[t])))
kp=kp_r*math.exp((F*Eo_p/R)*((1/T_ref)-(1/T_stack_d[t])))
E_shift=0.00038*T_stack_d[t]+0.073
cf2_avg=cf_0*(1-SOC_avg)
```

```
cf3_avg=cf_0*SOC_avg
cv2_avg=cv_0*SOC_avg
cv3_avg=cv_0*(1-SOC_avg)
ci=[cf2_avg,cf3_avg,cv2_avg,cv3_avg]
Di=[Df2,Df3,Dv2,Dv3]
zi=[zf2,zf3,zv2,zv3]
        ###DISCHARGING###
l=22 #Lamda , water content assumed to be saturated
s_m=(0.5136*l-0.326)*math.exp(1268*((1/303)-1/T_stack_d[t]))
IRm_d=Id*L_m/s_m ## LOSSES IN THE MEMRANE
#s_e=F**2/(R*T_stack_d[t])*
↪  sum([zi[i]**2*(Di[i]*eps**(3/2))*ci[i] for i in
↪  range(len(zi))])
#k=s_e*(1+(0.0171*(T_stack_d[t]-296)))*1.2
IRi_d=2*Id*(L_x/(k*0.8))## LOSSES IN THE ELECTROLYTE
nd_n=-2*R*T_stack_d[t]/F*math.asinh
(Id/(2*F*eps*a*L_x*kn*math.sqrt(cv2_avg*cv3_avg)))
nd_p=2*R*T_stack_d[t]/F*math.asinh
(Id/(2*F*eps*a*L_x*kp*math.sqrt(cf2_avg*cf3_avg)))
nd=nd_p-nd_n ## LOSSES KINETIC OVERPOTENTIALS
Ed_cell_rev=(Eo)+(R*T_stack_d[t])/F*math.log((cv2_avg*cf3_avg)
/(cv3_avg*cf2_avg))-E_shift
Ed_cell1=Ed_cell_rev-IRi_d-IRm_d-nd

  ##### Thermal model ####
S=-S_f3-S_v2+S_v3+S_f2
P_entro=-Id*Ac*T_stack_d[t]*S/(F)# Watts
R1=IRi_d  # Volts
R2=IRm_d# Volts
R_eq=R1+R2+nd# Volts
P_r= Id*Ac*R_eq# Volts*Amps/m2*m2 = V*A = Watts
R_d=(IRm_d+IRi_d+nd)/Id*N
T_out3_d=((T_air*H)/(f+H+v))+c1*math.exp(((-f*t)/w)-
((h*t)/w)-((v*t)/w))+P_entro/(f+H+v)+(f*T_in_d[t])/
(f+H+v)+(T_in_d[t]*v)/(f+H+v)+P_p/(f+H+v)+P_r/(f+H+v)
```

```
    T_out2_d[t]=T_stack_d[t]

    #ct.append(c1)
    Rd.append(R_d)
    SOC_d.append(SOC_avg)
    cnt.append(count)
    Ed_cell.append(Ed_cell1)
    #Ec_cell.append(Ec_cell1)
    Ec_cell_rev.append(Ec_cell_rev1)
    time.append(t)
    T_d.append(T_out3_d)
    pentro_d.append(P_entro)
    per_d.append(P_r)

#Comand to save a CSV file
df=pd.DataFrame(list(zip(T_c,T_d,Ec_cell,Ed_cell,SOC_c,SOC_d)),
                columns=['Temperature_c','Temperature_d',
                'Voltage_c','Voltage_d','SOC_c','SOC_d'])
df.to_csv('Temp20_-20%con.csv')
df=pd.DataFrame(list(zip(pentro_c,pentro_d,per_c,per_d)))
df.to_csv('powers20_-20%con.csv')
```

C.2 Scheduled Dispatch model

```
import pandas as pd
import numpy as np
import math
data1 = pd.read_csv('data_lau/Alldata_1.csv')
from datetime import date
import calendar
#Battery
cosP = 12.34
cosE=0.0606
cosF=0.02673
```

```
data1['Day_of_the_week']=pd.to_datetime(data1["Date"])
data1['Day_of_the_week']=data1.Day_of_the_week.dt.dayofweek #obtain
↪  the date format
data1['SOC']=4000
months=[1,2,3,4,5,6,7,8,9,10,11,12]
data1
Nobat=[]
Bat=[]
Sav=[]

for e in eff:
    #Discharge
    dis=cap*math.sqrt(e)
    #Increment in the Energy demand.
    cha=cap/math.sqrt(e)
    print("Efficency of %s " %e)
    for m in months:
        hour=[]
        demand=[]
        dema1=[]
        date=[]
        day=[]
        SOC=[]
        data=data1[data1['Month'] == m]
        v=data.loc[data['Month']==m,'Count'].iloc[0]
        for i in range(v,(len(data.Count)+v)):
            tempq=data.loc[data['Count']==i,'Time2'].iloc[0]
            dta=data.loc[data['Count']==i,'Date2'].iloc[0]
            dem=data.loc[data['Count']==i,'dem'].iloc[0]
            day1=data.loc[data['Count']==i,'Day_of_the_week'].iloc[0]
            soc=data.loc[data['Count']==i,'SOC'].iloc[0]
            hour.append(tempq)
            demand.append(dem)
            date.append(dta)
            day.append(day1)
```

```
    SOC.append(soc)

#SOC[0]=4000
char=0
for a in range(0,len(hour)):
    SOC[a]=SOC[a-1]
    if day[a]<5:
        ##DISCHARGE##
        if SOC[a]>=500/4: #if the battery has some SOC it
        ↪  can deploy
            if hour[a]>= '09:00':
                if hour[a]<='13:00':
                    char=char+1
                    SOC[a]=SOC[a-1]-dis/4
                    demand[a]=demand[a]-dis
        ##CHARGE##
        if SOC[a]<=3875:
            if hour[a]>= '00:00':
                if hour[a]<='04:00':
                    SOC[a]=SOC[a-1]+cha/4
   # MAINTAIN THE SAME SOC IF ITS NOT USING
    if hour[a]> '04:00':
         if hour[a]<'09:00':
                SOC[a]=SOC[a-1]


    if hour[a]> '13:01':
        if hour[a]<'23:59':
                SOC[a]=SOC[a-1]
    #else:

    #if SOC[a]>=4000:
     #   SOC[a]=4000
    #if SOC[a]<=0:
     #   SOC[a]=0
```

```
e_bat=char*cha
di={'Demand':demand,'Date':date,'Hour':hour,
↪  'Dw':day,'SOC':SOC}
df4=pd.DataFrame(di)


#Cost of the increment

cc_e=round(e_bat/4*cosE ,2)#divided by for due to the 15 min
↪  resolution

if m ==1:
    month='January'
elif m==2:
    month='February'
elif m==3:
    month='March'
elif m==4:
    month='April'
elif m==5:
    month='May'
elif m==6:
    month='June'
elif m==7:
    month='July'
elif m==8:
    month='August'
elif m==9:
    month='September'
elif m==10:
    month='October'
elif m==11:
    month='November'
elif m==12:
    month='December'
```

```
        bat=round(df4.Demand.max()*cosP+ (df4.Demand.sum()) /4 * cosE
        ↪  +cosF*(len(data.dem)/96)+cc_e,2)
        nobat=round(data.dem.max()*cosP+ data.dem.sum()/4 * cosE
        ↪  +cosF*(len(data.dem)/96),2)
        sav=round(nobat-bat,2)
        #Cost of charging the battery
        print(  month + "  " + 'No Battery=%f , Battery=%f ,
        ↪  Savings=%f  , Cost of charging Batery=%f' % (nobat, bat,
        ↪  sav,cc_e))
        Nobat.append(nobat)
        Bat.append(bat)
        Sav.append(sav)

mon=[]
for i in range(0,12):
    m=Sav[i],Sav[12+i],Sav[12*2+i],Sav[12*3+i],Sav[12*4+i],
    Sav[12*5+i],Sav[12*6+i],Sav[12*7+i],Sav[12*8+i],Sav[12*9+i]
    mon.append(m)
mon


Jan=mon[0]
Feb=mon[1]
Mar=mon[2]
Apr=mon[3]
May=mon[4]
Jun=mon[5]
Jul=mon[6]
Aug=mon[7]
Sep=mon[8]
Oct=mon[9]
Nov=mon[10]
Dec=mon[11]
```

```
import plotly.plotly as py
import plotly.graph_objs as go
x=['January', 'February','March',
↪  'April','May','June','July','August','September','October',
'November','December']
data=[]
fig = go.Figure()
for i in range(0,len(eff)):
    p=eff[i]*100
    p=' %s '%p+ '% Efficency'
    a=go.Scatter(x=x, y=Sav[(12*i):(12*(i+1))],
                    mode='lines+markers',
                    name= p )
    data.append(a)

layout = dict(title="Savings ",
              showlegend=True,
              xaxis=dict(title="Month"),
              yaxis=dict(title="$"))
data=data
# Create fig
fig = dict(data=data, layout=layout)
py.iplot(fig)

import plotly.plotly as py
import plotly.graph_objs as go
fig = go.Figure()
fig.add_trace(go.Box(y=Jan, name='January'))
fig.add_trace(go.Box(y=Feb, name = 'February'))
fig.add_trace(go.Box(y=Mar, name = 'March'))
fig.add_trace(go.Box(y=Apr, name = 'April'))
fig.add_trace(go.Box(y=May, name = 'May'))
fig.add_trace(go.Box(y=Jun, name = 'June'))
fig.add_trace(go.Box(y=Jul, name = 'July'))
fig.add_trace(go.Box(y=Aug, name = 'August'))
```

```
fig.add_trace(go.Box(y=Sep, name = 'September'))
fig.add_trace(go.Box(y=Oct, name = 'October'))
fig.add_trace(go.Box(y=Nov, name = 'Novemeber'))
fig.add_trace(go.Box(y=Dec, name = 'December'))

py.iplot(fig)

Jan2
j=['January','January','January','January','January',
'January','January','January','January','January']
b1=['500kW/1MWh','500kW/1MWh','500kW/1MWh','500kW/1MWh',
'500kW/1MWh','500kW/1MWh','500kW/1MWh','500kW/1MWh',
'500kW/1MWh','500kW/1MWh',]

# Import pandas library
import pandas as pd

# initialize list of lists
data = [[Jan1[0], 'January','500kW/1MWh'], [Jan1[1],
↪  'January','500kW/1MWh'], [Jan1[2], 'January','500kW/1MWh']]

# Create the pandas DataFrame
df = pd.DataFrame(data, columns = ['Saving', 'Month','Battery'])

# print dataframe.
df

# Import pandas library
import pandas as pd

# initialize list of lists
for i in range(0,len())
data = [[Jan1[0], 'January','500kW/1MWh'], [Jan1[1],
↪  'January','500kW/1MWh'], [Jan1[2], 'January','500kW/1MWh']]
```

```
# Create the pandas DataFrame
df = pd.DataFrame(data, columns = ['Saving', 'Month','Battery'])

# print dataframe.
df
```

C.3 Highest peaks dispatch model

```
import pandas as pd
import numpy as np
import math
data1 = pd.read_csv('data_lau/Alldata_1.csv')
from datetime import date
import calendar
#Battery
cap=500
e=0.8
cosP = 12.34
cosE=0.0606
cosF=0.02673
#Discharge
dis=cap*math.sqrt(e)
#Increment in the Energy demand.
cha=cap/math.sqrt(e)

data1['Day_of_the_week']=pd.to_datetime(data1["Date"])
data1['Day_of_the_week']=data1.Day_of_the_week.dt.dayofweek #obtain
↪  the date format
data1['SOC']=4000

data1.head()

Nobat=[]
Bat=[]
```

```
Sav=[]
ca=[]
co=[]
SOC=[]
demand=[]
months=[1,2,3,4,5,6,7,8,9,10,11,12]
for e in eff:
    #Discharge
    dis=cap*math.sqrt(e)
    #Increment in the Energy demand.
    cha=cap/math.sqrt(e)
    print("Efficency of %s " %e)
    for m in months:
        dem=[]
        temp=data1[data1['Month'] == m]
        md=temp.dem.nlargest(40)
        v=temp.loc[temp['Month']==m,'Count'].iloc[0]
        for i in range(v,(len(temp.Count)+v)):
            dem1=temp.loc[temp['Count']==i,'dem'].iloc[0]
            soc=temp.loc[temp['Count']==i,'SOC'].iloc[0]

            for a in md:
                if dem1==a:
                    dem1=dem1-dis
                #else:
                 #   dem1=dem1
                    #SOC[i]=SOC[i]-cha
            dem.append(dem1)
            SOC.append(soc)
        e_bat=52*cha
        di={'Demand':dem}
        df4=pd.DataFrame(di)
            #Cost of the increment
```

```
cc_e=e_bat/4*cosE #divided by for due to the 15 min
↪  resolution

if m ==1:
    month='January'
elif m==2:
    month='February'
elif m==3:
    month='March'
elif m==4:
    month='April'
elif m==5:
    month='May'
elif m==6:
    month='June'
elif m==7:
    month='July'
elif m==8:
    month='August'
elif m==9:
    month='September'
elif m==10:
    month='October'
elif m==11:
    month='November'
elif m==12:
    month='December'

bat=round(df4.Demand.max()*cosP+ (df4.Demand.sum()) /4 * cosE
↪  +cosF*(len(temp.dem)/96)+cc_e,2)
nobat=round(temp.dem.max()*cosP+ temp.dem.sum()/4 * cosE
↪  +cosF*(len(temp.dem)/96),2)
sav=round(nobat-bat,2)
#Cost of charging the battery
```

```
        print(  month + "   " + 'No Battery=%f , Battery=%f ,
        ↪  Savings=%f' % (nobat, bat, sav))
        Nobat.append(nobat)
        Bat.append(bat)
        Sav.append(sav)


import plotly.plotly as py
import plotly.graph_objs as go
x=['January', 'February','March',
↪  'April','May','June','July','August','September','October',
'November','December']
data=[]
fig = go.Figure()
for i in range(0,len(eff)):
    p=eff[i]*100
    p=' %s '%p+ '% Efficency'
    a=go.Scatter(x=x, y=Sav[(12*i):(12*(i+1))],
                    mode='lines+markers',
                    name= p )
    data.append(a)

layout = dict(title="Savings ",
              showlegend=True,
              xaxis=dict(title="Month"),
              yaxis=dict(title="$"))
data=data
# Create fig
fig = dict(data=data, layout=layout)
py.iplot(fig)

df = pd.DataFrame(list(zip(mo, b,ef,Sav1)),
               columns =['Month', 'Battery','Efficency','Savings'])
df.to_csv('deploy 20 peaks')
df
```

```
import plotly.express as px
tips = px.data.tips()
fig = px.box(df, x="Month", y="Savings", color="Battery",
             notched=True, # used notched shape
             title="Box plot of total bill",
             #hover_data=["day"] # add day column to hover data
            )
fig.show()

Nobat1=[]
Bat1=[]
Sav1=[]
months=[1,3,4,5,6,7,8,9,10,11,12]
b=[]
ef=[]
mo=[]
for c in cap:
    print("Cappacity of %s " %c)
    for e in eff:
        #Discharge
        dis=c*math.sqrt(e)
        #Increment in the Energy demand.
        cha=c/math.sqrt(e)
        print("Efficency of %s " %e)
        for m in months:
            dem=[]
            temp=data1[data1['Month'] == m]
            md=temp.dem.nlargest(20)
            v=temp.loc[temp['Month']==m,'Count'].iloc[0]
            for i in range(v,(len(temp.Count)+v)):
                dem1=temp.loc[temp['Count']==i,'dem'].iloc[0]
                for a in md:
                    if dem1==a:
                        dem1=dem1-dis
```

```
    dem.append(dem1)
e_bat=20*cha
di={'Demand':dem}
df4=pd.DataFrame(di)
    #Cost of the increment

cc_e=e_bat/4*cosE #divided by for due to the 15 min
↪  resolution

if m ==1:
    month='January'
elif m==2:
    month='February'
elif m==3:
    month='March'
elif m==4:
    month='April'
elif m==5:
    month='May'
elif m==6:
    month='June'
elif m==7:
    month='July'
elif m==8:
    month='August'
elif m==9:
    month='September'
elif m==10:
    month='October'
elif m==11:
    month='November'
elif m==12:
    month='December'
```

```
            bat=round(df4.Demand.max()*cosP+ (df4.Demand.sum()) /4 *
            ↪  cosE +cosF*(len(temp.dem)/96)+cc_e,2)
            nobat=round(temp.dem.max()*cosP+ temp.dem.sum()/4 * cosE
            ↪  +cosF*(len(temp.dem)/96),2)
            sav=round(nobat-bat,2)
            #Cost of charging the battery

            print(  month + "  " + 'No Battery=%f , Battery=%f ,
            ↪  Savings=%f' % (nobat, bat, sav))
            Nobat1.append(nobat)
            Bat1.append(bat)
            Sav1.append(sav)
            ef.append(e)
            b.append(c)
            mo.append(month)

df1 = pd.DataFrame(list(zip(mo, b,ef,Sav1)),
               columns =['Month', 'Battery','Efficency','Savings'])
df1.to_csv('deploy 20 peaks')

import plotly.express as px
tips = px.data.tips()
fig = px.box(df1, x="Month", y="Savings", color="Battery",
             notched=True, # used notched shape
            # title="Box plot of total bill",
             #hover_data=["day"] # add day column to hover data
            )
fig.show()


Sav500=Sav1[:120]
Sav1000=Sav1[120:]

import plotly.plotly as py
import plotly.graph_objs as go
```

```
x=['January', 'February','March',
↪  'April','May','June','July','August','September','October',
'November','December']
dat1=[]
dat2=[]
d=[]
fig = go.Figure()
for i in range(0,len(eff)):
    p=eff[i]*100
    p1=eff[i]*100
    p=' %s '%p+ '% Efficency 500kW Capacity'
    a=go.Scatter(x=x, y=Sav500[(12*i):(12*(i+1))],
                    mode='lines+markers',
                    name= p )

    p1=' %s '%p1+ '% Efficency 1000kW Capacity'
    b=go.Scatter(x=x, y=Sav1000[(12*i):(12*(i+1))],
                     mode='lines+markers',
                     name= p1 )
    dat1.append(a)
    dat2.append(b)
    d=dat1+dat2

layout = dict(title="Savings 20 max per month ",
              showlegend=True,
              xaxis=dict(title="Month"),
              yaxis=dict(title="$"))
data=d
# Create fig
fig = dict(data=data, layout=layout)
py.iplot(fig)

Nobat2=[]
Bat2=[]
Sav2=[]
```

```
b2=[]
ef2=[]
mo2=[]
months=[1,2,3,4,5,6,7,8,9,10,11,12]
for c in cap:
    #print("Cappacity of %s " %c)
    for e in eff:
        #Discharge
        dis=c*math.sqrt(e)
        #Increment in the Energy demand.
        cha=c/math.sqrt(e)
        #print("Effficency of %s " %e)
        for m in months:
            dem=[]
            temp=data1[data1['Month'] == m]
            md=temp.dem.nlargest(40)
            v=temp.loc[temp['Month']==m,'Count'].iloc[0]
            for i in range(v,(len(temp.Count)+v)):
                dem1=temp.loc[temp['Count']==i,'dem'].iloc[0]
                for a in md:
                    if dem1==a:
                        dem1=dem1-dis
                dem.append(dem1)
            e_bat=28*2*cha
            di={'Demand':dem}
            df4=pd.DataFrame(di)
                #Cost of the increment

            cc_e=e_bat/4*cosE #divided by for due to the 15 min
            ↪ resolution

            if m ==1:
                month='January'
            elif m==2:
                month='February'
```

```
elif m==3:
    month='March'
elif m==4:
    month='April'
elif m==5:
    month='May'
elif m==6:
    month='June'
elif m==7:
    month='July'
elif m==8:
    month='August'
elif m==9:
    month='September'
elif m==10:
    month='October'
elif m==11:
    month='November'
elif m==12:
    month='December'

bat=round(df4.Demand.max()*cosP+ (df4.Demand.sum()) /4 *
↪  cosE +cosF*(len(temp.dem)/96)+cc_e,2)
nobat=round(temp.dem.max()*cosP+ temp.dem.sum()/4 * cosE
↪  +cosF*(len(temp.dem)/96),2)
sav=round(nobat-bat,2)
#Cost of charging the battery

#print(  month + "  " + 'No Battery=%f , Battery=%f ,
↪  Savings=%f' % (nobat, bat, sav))
Nobat2.append(nobat)
Bat2.append(bat)
Sav2.append(sav)
ef2.append(e)
b2.append(c)
```

```
            mo2.append(month)

df2 = pd.DataFrame(list(zip(mo2, b2,ef2,Sav2)),
               columns =['Month', 'Battery','Efficency','Savings'])
df2.to_csv('deploy 40 peaks 2')
df2

import plotly.express as px
#data_canada = px.data.gapminder().query("Battery == '500'")
fig = px.bar(df2, x='Month', y='Savings')
fig.show()

import plotly.express as px
tips = px.data.tips()
fig = px.box(df2, x="Month", y="Savings", color="Battery",
             notched=True, # used notched shape
            # title="Box plot of total bill",
             #hover_data=["day"] # add day column to hover data
            )
fig.show()

Sav500=Sav2[:132]
Sav1000=Sav2[132:]

import plotly.graph_objs as go
x=['January', 'February','March',
 ↪  'April','May','June','July','August','September','October',
'November','December']
dat1=[]
dat2=[]
d=[]
fig = go.Figure()
for i in range(0,len(eff)):
    p=eff[i]*100
    p1=eff[i]*100
```

```
    p=' %s '%p+ '% Efficency 500kW Capacity'
    a=go.Bar(x=x, y=Sav500[(12*i):(12*(i+1))],
                    mode='lines+markers',
                    name= p )

    p1=' %s '%p1+ '% Efficency 1000kW Capacity'
    b=go.Bar(x=x, y=Sav1000[(12*i):(12*(i+1))],
                     mode='lines+markers',
                     name= p1 )
    dat1.append(a)
    dat2.append(b)
    d=dat1+dat2

layout = dict(title="Savings 40 max per month ",
              showlegend=True,
              xaxis=dict(title="Month"),
              yaxis=dict(title="$"))
data=d
# Create fig
fig = dict(data=data, layout=layout)
fig.show()
```

C.4 Lineal and ARIMA model

```
# # ARIMA

import pandas as pd
import numpy as np
Rdata = pd.read_csv('data_lau/Alldata_1.csv')
from datetime import date
import calendar
series=Rdata.dem
Rdata.head()
series=Rdata.filter(["Date", "dem"])
```

```
series['Date']=pd.to_datetime(series['Date'])
series.head()
series.set_index('Date',inplace=True)
series.head()
series.index
series.describe().transpose()
series.plot()
time_series=series['dem']
type(time_series)
time_series.plot()
time_series.rolling(2880).mean().plot(label='Montly')

import numpy as np
import pandas as pd
from pandas.plotting import autocorrelation_plot
import matplotlib.pyplot as plt
autocorrelation_plot(series)

from pandas import Series
from matplotlib import pyplot
from statsmodels.graphics.tsaplots import plot_acf

plot_acf(time_series)
pyplot.show()

from statsmodels.tsa.seasonal import seasonal_decompose
time_series=time_series[:96]
result = seasonal_decompose(time_series, model='multiplicative',
 ↪  freq=1)
result.plot()
pyplot.show()

from statsmodels.tsa.seasonal import seasonal_decompose
result = seasonal_decompose(time_series,
 ↪  model='multiplicative',freq=1)
```

```
print(result.trend)
print(result.seasonal)
print(result.resid)
print(result.observed)

import statsmodels.api as sm
decomposition = sm.tsa.seasonal_decompose(time_series,
↪  model='multiplicative')
decomposition.plot()

from pandas import read_csv
from pandas import datetime
from pandas import DataFrame
from statsmodels.tsa.arima_model import ARIMA
from matplotlib import pyplot

# fit model
model = ARIMA(time_series, order=(5,2,1))
model_fit = model.fit(disp=0)
print(model_fit.summary())
# plot residual errors
residuals = DataFrame(model_fit.resid)
residuals.plot()
pyplot.show()
residuals.plot(kind='kde')
pyplot.show()
print(residuals.describe())

from pandas import datetime
from matplotlib import pyplot
from statsmodels.tsa.arima_model import ARIMA
from sklearn.metrics import mean_squared_error

Xt = time_series
sizet = int(len(Xt) * 0.2)
```

```
traint, testt = Xt[0:sizet], Xt[sizet:len(Xt)]
history = [x for x in traint]
predictionst = list()
for t in range(len(testt)):
        model = ARIMA(history, order=(2,1,1))
        model_fit = model.fit(disp=0)
        outputt = model_fit.forecast()
        yhatt = outputt[0]
        predictionst.append(yhatt)
        obst = testt[t]
        history.append(obst)
        print('predicted=%f, expected=%f' % (yhatt, obst))
errort = mean_squared_error(testt, predictionst)
#print('Test MSE: %.3f' % errotr)
# plot
pyplot.plot(testt)
pyplot.plot(predictionst, color='red')
pyplot.show()

import matplotlib
import matplotlib.pyplot as plt
import matplotlib.cm as cm
import matplotlib.mlab as mlab
from matplotlib.ticker import LinearLocator, FormatStrFormatter,
↪  FuncFormatter, MaxNLocator
from pandas import datetime
from matplotlib import pyplot
from statsmodels.tsa.arima_model import ARIMA
from sklearn.metrics import mean_squared_error
len(predictionst)

len(testt)

# plot
plt.figure(1,figsize=(20,10))
```

```
#plt.plot(testt, label='Data',color='blue')
plt.plot(predictionst, label = 'Predictions',color='red')
plt.legend()
plt.xlabel('Time ')
plt.ylabel('Demand')

# plot
plt.figure(1,figsize=(20,10))
plt.plot(testt, label='Data',color='blue')
#plt.plot(predictionst, label = 'Predictions',color='red')
plt.legend()
plt.xlabel('Time ')
plt.ylabel('Demand')
x=predictionst[29377:32064]
y=testt[29377:32064]
a=y.reset_index()
index=a['Date']
a.dem
# plot
plt.figure(1,figsize=(20,10))
plt.plot(x, label='Data',color='blue')
plt.plot(a.dem, label = 'Predictions',color='red')
plt.legend()
plt.xlabel('Time ')
plt.ylabel('Demand')

# # Lineal Regression

import numpy as np
from numpy.random import randn
import math
get_ipython().run_line_magic('matplotlib', 'inline')
import plotly.graph_objs as go
import math
import numpy as np
```

```
import pandas as pd
import numpy as np
import matplotlib
import matplotlib.pyplot as plt
import matplotlib.cm as cm
import matplotlib.mlab as mlab
from matplotlib.ticker import LinearLocator, FormatStrFormatter,
↪  FuncFormatter, MaxNLocator

import pandas as pd
import numpy as np
Series =pd.read_csv('data_lau/Data3.csv', header=0, parse_dates=[0],
↪  index_col=0, squeeze=True)
Series.head()

X = Series[['t1','t2','t3','t4','t5','t6','t7','t8','t9','t10','t11',
't12','t13','t14','t15','t16','t17','t18','t19','t20','t21','t22',
't23','t24','t25','t26','t27','t28','t29','t30','t31','t32','t33',
't34','t35','t36','t37','t38','t39','t40','t41','t42','t43','t44'
,'t45','t46','t47','t48','t49','t50','t51','t52','t53','t54','t55',
't56','t57','t58','t59','t60','t61','t62','t63','t64','t65','t66',
't67','t68','t69','t70','t71','t72','t73','t74','t75','t76','t77',
't78','t79','t80','t81','t82','t83','t84','t85','t86','t87','t88',
't89','t90','t91','t92','t93','t94','t95','t-18','t(t-1)','BD',
'Month']]
Y = Series[['dem']]

# Note that there is a temperature that is being taken into account
↪  at t-18 since the temperature of the building to be at 18 C

from pandas import DataFrame
from sklearn import linear_model
import statsmodels.api as sm
# with sklearn
regr = linear_model.LinearRegression()
```

```
regr.fit(X, Y)
print('Intercept: \n', regr.intercept_)
print('Coefficients: \n', regr.coef_)

# with statsmodels
X = sm.add_constant(X) # adding a constant
model = sm.OLS(Y, X).fit()
predictions = model.predict(X)
print_model = model.summary()
print(print_model)
Feb_pred=predictions[29377:32064]
from sklearn import metrics
print(metrics.mean_absolute_error(Series.dem,predictions))
print(metrics.mean_squared_error(Series.dem,predictions))
print(np.sqrt(metrics.mean_absolute_error(Series.dem,predictions)))

type(predictions)
Series.dem.to_csv("series")

# plot
from matplotlib import pyplot
plt.figure(1,figsize=(20,10))
plt.plot(predictions, label='Data',color='blue')
plt.plot(Series.dem, label = 'Predictions',color='red')
plt.legend()
plt.xlabel('Time ')
plt.ylabel('Demand')
pyplot.show()

coef=regr.coef_
inter=regr.intercept_
temp=coef[0,95]
BD=coef[0,96]
mon=coef[0,97]
```

```
# # Gui
#
# This Gui takes the values from temperature and hour and can
↪  calculate point demand


from pandas import DataFrame
from sklearn import linear_model
import tkinter as tk
import matplotlib.pyplot as plt
from matplotlib.backends.backend_tkagg import FigureCanvasTkAgg
root= tk.Tk()

canvas1 = tk.Canvas(root, width = 1200, height = 450)
canvas1.pack()

# Temperature
label1 = tk.Label(root, text='Temperature ')
canvas1.create_window(100, 40, window=label1)

entry1 = tk.Entry (root) # create 1st entry box
canvas1.create_window(230, 40, window=entry1)

# Busisness Day
label2 = tk.Label(root, text=' BD (0= no 1= yes)')
canvas1.create_window(100, 60, window=label2)

entry2 = tk.Entry (root) # create 2nd entry box
canvas1.create_window(230, 60, window=entry2)

#Time
label31 = tk.Label(root, text=' Time (hhmm)')
canvas1.create_window(100, 80, window=label31)
```

```
entry31 = tk.Entry (root) # create 2nd entry box
canvas1.create_window(230, 80, window=entry31)

#Month
label4 = tk.Label(root, text='Month')
canvas1.create_window(100, 100, window=label4)

entry4 = tk.Entry (root) # create 2nd entry box
canvas1.create_window(230, 100, window=entry4)


def values():
    global Temperature #our 1st input variable
    Temperature = float(entry1.get())
    global BD #our 2nd input variable
    bd = float(entry2.get())
    global Month #our 1st input variable
    Month = float(entry4.get())
    global Time
    entry3=str(entry31.get())
    if entry3=="0000":
        a=coef[0,0]
    elif entry3=="0015":
        a=coef[0,1]
    elif entry3=="0030":
        a=coef[0,2]
    elif entry3=="0045":
        a=coef[0,3]
    elif entry3=="0100":
        a=coef[0,4]
    elif entry3=="0115":
        a=coef[0,5]
    elif entry3=="0130":
        a=coef[0,6]
    elif entry3=="0145":
```

```
        a=coef[0,7]
    elif entry3=="0200":
        a=coef[0,8]
    elif entry3=="0215":
        a=coef[0,9]
    elif entry3=="0230":
        a=coef[0,10]
    elif entry3=="0245":
        a=coef[0,11]
    elif entry3=="0300":
        a=coef[0,12]
    elif entry3=="0315":
        a=coef[0,13]
    elif entry3=="0330":
        a=coef[0,14]
    elif entry3=="0345":
        a=coef[0,15]
    elif entry3=="0400":
        a=coef[0,16]
    elif entry3=="0415":
        a=coef[0,17]
    elif entry3=="0430":
        a=coef[0,18]
    elif entry3=="0445":
        a=coef[0,19]
    elif entry3=="0500":
        a=coef[0,20]
    elif entry3=="0515":
        a=coef[0,21]
    elif entry3=="0530":
        a=coef[0,22]
    elif entry3=="0545":
        a=coef[0,23]
    elif entry3=="0600":
        a=coef[0,24]
```

```
    elif entry3=="0615":
        a=coef[0,25]
    elif entry3=="0630":
        a=coef[0,26]
    elif entry3=="0645":
        a=coef[0,27]
    elif entry3=="0700":
        a=coef[0,28]
    elif entry3=="0715":
        a=coef[0,29]
    elif entry3=="0730":
        a=coef[0,30]
    elif entry3=="0745":
        a=coef[0,31]
    elif entry3=="0800":
        a=coef[0,32]
    elif entry3=="0815":
        a=coef[0,33]
    elif entry3=="0830":
        a=coef[0,34]
    elif entry3=="0845":
        a=coef[0,35]
    elif entry3=="0900":
        a=coef[0,36]
    elif entry3=="0915":
        a=coef[0,37]
    elif entry3=="0930":
        a=coef[0,38]
    elif entry3=="0945":
        a=coef[0,39]
    elif entry3=="1000":
        a=coef[0,40]
    elif entry3=="1015":
        a=coef[0,41]
    elif entry3=="1030":
```

```
        a=coef[0,42]
    elif entry3=="1045":
        a=coef[0,43]
    elif entry3=="1100":
        a=coef[0,44]
    elif entry3=="1115":
        a=coef[0,45]
    elif entry3=="1130":
        a=coef[0,46]
    elif entry3=="1145":
        a=coef[0,47]
    elif entry3=="1200":
        a=coef[0,48]
    elif entry3=="1215":
        a=coef[0,49]
    elif entry3=="1230":
        a=coef[0,50]
    elif entry3=="1245":
        a=coef[0,51]
    elif entry3=="1300":
        a=coef[0,52]
    elif entry3=="1315":
        a=coef[0,53]
    elif entry3=="1330":
        a=coef[0,54]
    elif entry3=="1345":
        a=coef[0,55]
    elif entry3=="1400":
        a=coef[0,56]
    elif entry3=="1415":
        a=coef[0,57]
    elif entry3=="1430":
        a=coef[0,58]
    elif entry3=="1445":
        a=coef[0,59]
```

```
    elif entry3=="1500":
        a=coef[0,60]
    elif entry3=="1515":
        a=coef[0,61]
    elif entry3=="1530":
        a=coef[0,62]
    elif entry3=="1545":
        a=coef[0,63]
    elif entry3=="1600":
        a=coef[0,64]
    elif entry3=="1615":
        a=coef[0,65]
    elif entry3=="1630":
        a=coef[0,66]
    elif entry3=="1645":
        a=coef[0,67]
    elif entry3=="1700":
        a=coef[0,68]
    elif entry3=="1715":
        a=coef[0,69]
    elif entry3=="1730":
        a=coef[0,70]
    elif entry3=="1745":
        a=coef[0,71]
    elif entry3=="1800":
        a=coef[0,72]
    elif entry3=="1815":
        a=coef[0,73]
    elif entry3=="1830":
        a=coef[0,74]
    elif entry3=="1845":
        a=coef[0,75]
    elif entry3=="1900":
        a=coef[0,76]
    elif entry3=="1915":
```

```
        a=coef[0,77]
    elif entry3=="1930":
        a=coef[0,78]
    elif entry3=="1945":
        a=coef[0,79]
    elif entry3=="2000":
        a=coef[0,80]
    elif entry3=="2015":
        a=coef[0,81]
    elif entry3=="2030":
        a=coef[0,82]
    elif entry3=="2045":
        a=coef[0,83]
    elif entry3=="2100":
        a=coef[0,84]
    elif entry3=="2115":
        a=coef[0,85]
    elif entry3=="2130":
        a=coef[0,86]
    elif entry3=="2145":
        a=coef[0,87]
    elif entry3=="2200":
        a=coef[0,88]
    elif entry3=="2215":
        a=coef[0,89]
    elif entry3=="2230":
        a=coef[0,90]
    elif entry3=="2245":
        a=coef[0,91]
    elif entry3=="2300":
        a=coef[0,92]
    elif entry3=="2315":
        a=coef[0,93]
    elif entry3=="2330":
        a=coef[0,94]
```

```
    elif entry3=="2345":
        a=0
    else:
        a=0

    Prediction_result  = ('Demand: ',
    ↪  inter+a+mon*Month+temp*(abs(Temperature-18))+BD*bd)
    label_Prediction = tk.Label(root, text= Prediction_result,
    ↪  bg='orange')
    canvas1.create_window(260, 280, window=label_Prediction)

button1 = tk.Button (root, text='Demand',command=values, bg='orange')
↪  # button to call the 'values' command above
canvas1.create_window(270, 150, window=button1)

root.mainloop()

# Test for Feruary

import pandas as pd
import numpy as np
Feb =pd.read_csv('data_lau/Feb_values.csv', header=0,
↪  parse_dates=[0], index_col=0, squeeze=True)
Feb.head()
Feb_real=Feb.dem
Feb_pred1=Feb_pred*1.1
print(Feb_real)

Feb=Series[Series['Month']==2]
Feb=Feb.dem
Feb

# plot
from matplotlib import pyplot
plt.figure(1,figsize=(20,10))
```

```
plt.plot(Feb, label='Data',color='blue')
plt.plot(Feb_pred1, label = 'Predictions',color='red')
plt.legend()
plt.xlabel('Time ')
plt.ylabel('Demand')
plt.title('February Lineal Regression')
pyplot.show()
```

Bibliography

[1] World Energy Council. World energy scenarios composing energy futures to 2050. *N/A*, 2010.

[2] Kenneth K Zame, Christopher A Brehm, Alex T Nitica, Christopher L Richard, and Gordon D Schweitzer III. Smart grid and energy storage: Policy recommendations. *Renewable and Sustainable Energy Reviews*, 82:1646–1654, 2018.

[3] Hannah Ritchie. Renewable energy. *Our World in Data*, 2017. https://ourworldindata.org/renewable-energy.

[4] Mohammad Ahmadi Ganesh Doluweera, Hamid Rahmanifard. Electricity storage systems: Applications and business cases. *CERI*, 180:3, 2019.

[5] Martin Uhrig, Sebastian Koenig, Michael R Suriyah, and Thomas Leibfried. Lithium-based vs. vanadium redox flow batteries–a comparison for home storage systems. *Energy Procedia*, 99(2016):35–43, 2016.

[6] Yasin Emre Durmus, Huang Zhang, Florian Baakes, Gauthier Desmaizieres, Hagay Hayun, Liangtao Yang, Martin Kolek, Verena Küpers, Jürgen Janek, Daniel Mandler, et al. Side by side battery technologies with lithium-ion based batteries. *Advanced Energy Materials*, page 2000089, 2020.

[7] Lawrence H Thaller. Electrically rechargeable redox flow cells. In *9th Intersociety Energy Conversion Engineering Conference*, pages 924–928, 1974.

[8] Dong Kyu Kim, Sang Jun Yoon, Jaeho Lee, and Sangwon Kim. Parametric study and flow rate optimization of all-vanadium redox flow batteries. *Applied energy*, 228:891–901, 2018.

[9] Dong-Jun Park, Kwang-Sun Jeon, Cheol-Hwi Ryu, and Gab-Jin Hwang. Performance of the all-vanadium redox flow battery stack. *Journal of Industrial and Engineering Chemistry*, 45:387–390, 2017.

[10] Wei Wang, Soowhan Kim, Baowei Chen, Zimin Nie, Jianlu Zhang, Guan-Guang Xia, Liyu Li, and Zhenguo Yang. A new redox flow battery using fe/v redox couples in chloride supporting electrolyte. *Energy & Environmental Science*, 4(10):4068–4073, 2011.

[11] Vilayanur Viswanathan, Alasdair Crawford, David Stephenson, Soowhan Kim, Wei Wang, Bin Li, Greg Coffey, Ed Thomsen, Gordon Graff, Patrick Balducci, et al. Cost and performance model for redox flow batteries. *Journal of Power Sources*, 247:1040–1051, 2014.

[12] Yunong Zhang, Le Liu, Jingyu Xi, Zenghua Wu, and Xinping Qiu. The benefits and limitations of electrolyte mixing in vanadium flow batteries. *Applied Energy*, 204:373–381, 2017.

[13] A Orita, MG Verde, M Sakai, and YS Meng. The impact of ph on side reactions for aqueous redox flow batteries based on nitroxyl radical compounds. *Journal of Power Sources*, 321:126–134, 2016.

[14] Yan Xu, Yue-Hua Wen, Jie Cheng, Gao-Ping Cao, and Yu-Sheng Yang. A study of tiron in aqueous solutions for redox flow battery application. *Electrochimica Acta*, 55(3):715–720, 2010.

[15] William D McCulloch, Mingzhe Yu, and Yiying Wu. ph-tuning a solar redox flow battery for integrated energy conversion and storage. *ACS Energy Letters*, 1(3):578–582, 2016.

[16] HENRY LAZENBY. China sets tone for future vanadium-flow battery development, Jan 2019.

[17] Adam Z Weber, Matthew M Mench, Jeremy P Meyers, Philip N Ross, Jeffrey T Gostick, and Qinghua Liu. Redox flow batteries: a review. *Journal of Applied Electrochemistry*, 41(10):1137, 2011.

[18] Feng Pan and Qing Wang. Redox species of redox flow batteries: A review. *Molecules*, 20(11):20499–20517, 2015.

[19] YK Zeng, TS Zhao, L An, XL Zhou, and L Wei. A comparative study of all-vanadium and iron-chromium redox flow batteries for large-scale energy storage. *Journal of Power Sources*, 300:438–443, 2015.

[20] M Skyllas-Kazacos and F Grossmith. Efficient vanadium redox flow cell. *Journal of the Electrochemical Society*, 134(12):2950, 1987.

[21] Wei Wang, Qingtao Luo, Bin Li, Xiaoliang Wei, Liyu Li, and Zhenguo Yang. Recent progress in redox flow battery research and development. *Advanced Functional Materials*, 23(8):970–986, 2013.

[22] Chanyong Choi, Soohyun Kim, Riyul Kim, Yunsuk Choi, Soowhan Kim, Ho-young Jung, Jung Hoon Yang, and Hee-Tak Kim. A review of vanadium electrolytes for vanadium redox flow batteries. *Renewable and Sustainable Energy Reviews*, 69:263–274, 2017.

[23] Liyu Li, Soowhan Kim, Wei Wang, M Vijayakumar, Zimin Nie, Baowei Chen, Jianlu Zhang, Guanguang Xia, Jianzhi Hu, Gordon Graff, et al. A stable vanadium redox-flow battery with high energy density for large-scale energy storage. *Advanced Energy Materials*, 1(3):394–400, 2011.

[24] YH Wen, HM Zhang, P Qian, HT Zhou, P Zhao, BL Yi, and YS Yang. A study of the fe (iii)/fe (ii)–triethanolamine complex redox couple for redox flow battery application. *Electrochimica Acta*, 51(18):3769–3775, 2006.

[25] AA Shah, MJ Watt-Smith, and FC Walsh. A dynamic performance model for redox-flow batteries involving soluble species. *Electrochimica Acta*, 53(27):8087–8100, 2008.

[26] Steven Church. Del. firm installs fuel cell. *The News Journal*, 6:B7, 2006.

[27] KW Knehr, Ertan Agar, CR Dennison, AR Kalidindi, and EC Kumbur. A transient vanadium flow battery model incorporating vanadium crossover and water transport through the membrane. *Journal of The Electrochemical Society*, 159(9):A1446, 2012.

[28] Chenxi Sun, Jian Chen, Huamin Zhang, Xi Han, and Qingtao Luo. Investigations on transfer of water and vanadium ions across nafion membrane in an operating vanadium redox flow battery. *Journal of Power Sources*, 195(3):890–897, 2010.

[29] Jingyu Xi, Zenghua Wu, Xinping Qiu, and Liquan Chen. Nafion/sio2 hybrid membrane for vanadium redox flow battery. *Journal of Power Sources*, 166(2):531–536, 2007.

[30] Qingtao Luo, Huaming Zhang, Jian Chen, Peng Qian, and Yunfeng Zhai. Modification of nafion membrane using interfacial polymerization for vanadium redox flow battery applications. *Journal of Membrane Science*, 311(1-2):98–103, 2008.

[31] Xiangguo Teng, Yongtao Zhao, Jingyu Xi, Zenghua Wu, Xinping Qiu, and Liquan Chen. Nafion/organic silica modified tio2 composite membrane for vanadium redox flow battery via in situ sol–gel reactions. *Journal of Membrane Science*, 341(1-2):149–154, 2009.

[32] MA Smit, AL Ocampo, MA Espinosa-Medina, and PJ Sebastian. A modified nafion membrane with in situ polymerized polypyrrole for the direct methanol fuel cell. *Journal of power sources*, 124(1):59–64, 2003.

[33] Kolja Bromberger, Johannes Kaunert, and Tom Smolinka. A model for all-vanadium redox flow batteries: introducing electrode-compression effects on voltage losses and hydraulics. *Energy Technology*, 2(1):64–76, 2014.

[34] BW Zhang, Y Lei, BF Bai, A Xu, and TS Zhao. A two-dimensional mathematical model for vanadium redox flow battery stacks incorporating nonuniform electrolyte distribution in the flow frame. *Applied Thermal Engineering*, 151:495–505, 2019.

[35] Sara Corcuera and Maria Skyllas-Kazacos. State-of-charge monitoring and electrolyte rebalancing methods for the vanadium redox flow battery. *European Chemical Bulletin*, 1(12):511–519, 2012.

[36] Ki Jae Kim, Min-Sik Park, Young-Jun Kim, Jung Ho Kim, Shi Xue Dou, and Maria Skyllas-Kazacos. A technology review of electrodes and reaction mechanisms in vanadium redox flow batteries. *Journal of materials chemistry a*, 3(33):16913–16933, 2015.

[37] Aishwarya Parasuraman, Tuti Mariana Lim, Chris Menictas, and Maria Skyllas-Kazacos. Review of material research and development for vanadium redox flow battery applications. *Electrochimica Acta*, 101:27–40, 2013.

[38] XL Zhou, TS Zhao, YK Zeng, Liang An, and Lei Wei. A highly permeable and enhanced surface area carbon-cloth electrode for vanadium redox flow batteries. *Journal of Power Sources*, 329:247–254, 2016.

[39] WH Wang and XD Wang. Investigation of ir-modified carbon felt as the positive electrode of an all-vanadium redox flow battery. *Electrochimica Acta*, 52(24):6755–6762, 2007.

[40] Yuyan Shao, Xiqing Wang, Mark Engelhard, Chongmin Wang, Sheng Dai, Jun Liu, Zhenguo Yang, and Yuehe Lin. Nitrogen-doped mesoporous carbon for energy storage in vanadium redox flow batteries. *Journal of Power Sources*, 195(13):4375–4379, 2010.

[41] Wenyue Li, Zhenyu Zhang, Yongbing Tang, Haidong Bian, Tsz-Wai Ng, Wenjun Zhang, and Chun-Sing Lee. Graphene-nanowall-decorated carbon felt with excellent electrochemical activity toward vo2+/vo2+ couple for all vanadium redox flow battery. *Advanced science*, 3(4):1500276, 2016.

[42] HQ Zhu, YM Zhang, L Yue, WS Li, GL Li, D Shu, and HY Chen. Graphite–carbon nanotube composite electrodes for all vanadium redox flow battery. *Journal of Power Sources*, 184(2):637–640, 2008.

[43] M Pugach, M Kondratenko, S Briola, and A Bischi. Zero dimensional dynamic model of vanadium redox flow battery cell incorporating all modes of vanadium ions crossover. *Applied energy*, 226:560–569, 2018.

[44] Ashwini Kumar Sharma, CY Ling, E Birgersson, Mikael Vynnycky, and M Han. Verified reduction of dimensionality for an all-vanadium redox flow battery model. *Journal of Power Sources*, 279:345–350, 2015.

[45] David Stephenson, Soowhan Kim, Feng Chen, Edwin Thomsen, Vilayanur Viswanathan, Wei Wang, and Vincent Sprenkle. Electrochemical model of the fe/v redox flow battery. *Journal of The Electrochemical Society*, 159(12):A1993–A2000, 2012.

[46] Ao Tang, Jie Bao, and Maria Skyllas-Kazacos. Thermal modelling of battery configuration and self-discharge reactions in vanadium redox flow battery. *Journal of Power Sources*, 216:489–501, 2012.

[47] Binyu Xiong, Jiyun Zhao, Zhongbao Wei, and Maria Skyllas-Kazacos. Extended kalman filter method for state of charge estimation of vanadium redox flow battery using thermal-dependent electrical model. *Journal of Power Sources*, 262:50–61, 2014.

[48] Zhongbao Wei, Jiyun Zhao, and Binyu Xiong. Dynamic electro-thermal modeling of all-vanadium redox flow battery with forced cooling strategies. *Applied energy*, 135:1–10, 2014.

[49] Binyu Xiong, Jiyun Zhao, King Jet Tseng, Maria Skyllas-Kazacos, Tuti Mariana Lim, and Yu Zhang. Thermal hydraulic behavior and efficiency analysis of an all-vanadium redox flow battery. *Journal of Power Sources*, 242:314–324, 2013.

[50] Dongjiang You, Huamin Zhang, and Jian Chen. A simple model for the vanadium redox battery. *Electrochimica Acta*, 54(27):6827–6836, 2009.

[51] Encyclopædia Britannica. Faraday's laws of electrolysis. 2016.

[52] AA Shah, RSRW Tangirala, R Singh, RGA Wills, and FC Walsh. A dynamic unit cell model for the all-vanadium flow battery. *Journal of the Electrochemical society*, 158(6):A671–A677, 2011.

[53] Mark W Verbrugge and Robert F Hill. Ion and solvent transport in ion-exchange membranes i. a macrohomogeneous mathematical model. *Journal of the Electrochemical Society*, 137(3):886–893, 1990.

[54] Thomas E Springer, TA Zawodzinski, and Shimshon Gottesfeld. Polymer electrolyte fuel cell model. *Journal of the electrochemical society*, 138(8):2334, 1991.

[55] MN Tsampas, A Pikos, S Brosda, A Katsaounis, and CG Vayenas. The effect of membrane thickness on the conductivity of nafion. *Electrochimica Acta*, 51(13):2743–2755, 2006.

[56] John Newman and Karen E Thomas-Alyea. *Electrochemical systems*. John Wiley & Sons, 2012.

[57] Allen J. Bard, Roger Parsons, 1919-1992 Jordan, Joseph, International Union of Pure, and Applied Chemistry. *Standard potentials in aqueous solution*. M. Dekker, New York, 1st edition, 1985.

[58] Fernando Pérez and Brian E. Granger. IPython: a system for interactive scientific computing. *Computing in Science and Engineering*, 9(3):21–29, May 2007.

[59] Stamatios Souentie, Issam Amr, Abdulrahman Alsuhaibani, Essa Almazroei, and Ahmad D Hammad. Temperature, charging current and state of charge effects on iron-vanadium flow batteries operation. *Applied Energy*, 206:568–576, 2017.

[60] Nicholas S Hudak. Practical thermodynamic quantities for aqueous vanadium- and iron-based flow batteries. *Journal of Power Sources*, 269:962–974, 2014.

[61] Jose Gonzalez-Garcia, P Bonete, E Expósito, Vicente Montiel, A Aldaz, and Rosa Torregrosa-Maciá. Characterization of a carbon felt electrode: structural and physical properties. *Journal of Materials Chemistry*, 9(2):419–426, 1999.

[62] Tomoo Yamamura, Nobutaka Watanabe, Takashi Yano, and Yoshinobu Shiokawa. Electron-transfer kinetics of np3+/ np4+, npo2+/ npo2 2+, v2+/ v3+, and vo2+/ vo2+ at carbon electrodes. *Journal of The Electrochemical Society*, 152(4):A830–A836, 2005.

[63] William M Haynes. *CRC handbook of chemistry and physics*. CRC press, 2014.

[64] K. W. Knehr, Ertan Agar, C. R. Dennison, A. R. Kalidindi, and E. C. Kumbur. A transient vanadium flow battery model incorporating vanadium crossover and water transport through the membrane. *Journal of The Electrochemical Society*, 159(9):A1446–A1459, 2012.

[65] Qiong Zheng, Huamin Zhang, Feng Xing, Xiangkun Ma, Xianfeng Li, and Guiling Ning. A three-dimensional model for thermal analysis in a vanadium flow battery. *Applied energy*, 113:1675–1685, 2014.

[66] Andrea Trovò, Alberto Saccardo, Monica Giomo, and Massimo Guarnieri. Thermal modeling of industrial-scale vanadium redox flow batteries in high-current operations. *Journal of Power Sources*, 424:204–214, 2019.

[67] Indrajeet V Thorat, David E Stephenson, Nathan A Zacharias, Karim Zaghib, John N Harb, and Dean R Wheeler. Quantifying tortuosity in porous li-ion battery materials. *Journal of Power Sources*, 188(2):592–600, 2009.

[68] Bc hydro rates.

[69] https://victoria.weatherstats.ca/charts/temperature monthly.html. Weather statistics for victoria, british columbi. *Amateur Weather Statistics for Victoria, British Columbia*.

[70] Alasdair Crawford, Vilayanur Viswanathan, David Stephenson, Wei Wang, Edwin Thomsen, David Reed, Bin Li, Patrick Balducci, Michael Kintner-Meyer, and Vincent Sprenkle. Comparative analysis for various redox flow batteries chemistries using a cost performance model. *Journal of Power Sources*, 293:388–399, 2015.

[71] Rudolf Holze. Composites and copolymers containing redox-active molecules and intrinsically conducting polymers as active masses for supercapacitor electrodes—an introduction. *Polymers*, 12(8):1835, 2020.

[72] Solène Gentil, Danick Reynard, and Hubert H Girault. Aqueous organic and redox-mediated redox flow batteries: a review. *Current Opinion in Electrochemistry*, 21:7–13, 2020.

[73] James W Taylor. Short-term electricity demand forecasting using double seasonal exponential smoothing. *Journal of the Operational Research Society*, 54(8):799–805, 2003.

[74] Xiangkun Ma, Huamin Zhang, Chenxi Sun, Yi Zou, and Tao Zhang. An optimal strategy of electrolyte flow rate for vanadium redox flow battery. *Journal of power sources*, 203:153–158, 2012.

[75] Wenyang Xiao and Lei Tan. Control strategy optimization of electrolyte flow rate for all vanadium redox flow battery with consideration of pump. *Renewable Energy*, 133:1445–1454, 2019.

[76] N Gurieff, CY Cheung, V Timchenko, and C Menictas. Performance enhancing stack geometry concepts for redox flow battery systems with flow through electrodes. *Journal of Energy Storage*, 22:219–227, 2019.

[77] T Henriques, B César, and PJ Costa Branco. Increasing the efficiency of a portable pem fuel cell by altering the cathode channel geometry: a numerical and experimental study. *Applied Energy*, 87(4):1400–1409, 2010.

[78] AllenJ Bard. *Standard potentials in aqueous solution*. Routledge, 2017.

[79] Lindiwe Khotseng. Oxygen reduction reaction. *Electrocatalysts for Fuel Cells and Hydrogen Evolution-Theory to Design*, 2018.

[80] Maria Skyllas-Kazacos. Novel vanadium chloride/polyhalide redox flow battery. *Journal of Power Sources*, 124(1):299–302, 2003.

[81] WM Haynes. the crc handbook of chemistry and physics 93rd edition, 2012. *Chemical Rubber Company*.